

EUROPEAN ORGANISATION FOR NUCLEAR RESEARCH (CERN)



JHEP 09 (2017) 084
DOI: [10.1007/JHEP09\(2017\)084](https://doi.org/10.1007/JHEP09(2017)084)



CERN-EP-2017-108
4th September 2019

Search for supersymmetry in final states with two same-sign or three leptons and jets using 36 fb^{-1} of $\sqrt{s} = 13 \text{ TeV}$ pp collision data with the ATLAS detector

The ATLAS Collaboration

A search for strongly produced supersymmetric particles using signatures involving multiple energetic jets and either two isolated same-sign leptons (e or μ), or at least three isolated leptons, is presented. The analysis relies on the identification of b -jets and high missing transverse momentum to achieve good sensitivity. A data sample of proton–proton collisions at $\sqrt{s} = 13 \text{ TeV}$ recorded with the ATLAS detector at the Large Hadron Collider in 2015 and 2016, corresponding to a total integrated luminosity of 36.1 fb^{-1} , is used for the search. No significant excess over the Standard Model prediction is observed. The results are interpreted in several simplified supersymmetric models featuring R -parity conservation or R -parity violation, extending the exclusion limits from previous searches. In models considering gluino pair production, gluino masses are excluded up to 1.87 TeV at 95% confidence level. When bottom squarks are pair-produced and decay to a chargino and a top quark, models with bottom squark masses below 700 GeV and light neutralinos are excluded at 95% confidence level. In addition, model-independent limits are set on a possible contribution of new phenomena to the signal region yields.

1 Introduction

Supersymmetry (SUSY) [1–6] is one of the best-motivated extensions of the Standard Model (SM). A general review can be found in Ref. [7]. In its minimal realization (the MSSM) [8, 9] it predicts a new bosonic (fermionic) partner for each fundamental SM fermion (boson), as well as an additional Higgs doublet. If R -parity [10] is conserved (RPC) the lightest supersymmetric particle (LSP) is stable and can be the lightest neutralino¹ $\tilde{\chi}_1^0$. In many models, the LSP can be a dark-matter candidate [11, 12] and produce signatures with large missing transverse momentum. If instead R -parity is violated (RPV), the LSP decay can generate events with high jet and lepton multiplicity. Both RPC and RPV scenarios can produce the final-state signatures considered in this article.

In order to address the SM hierarchy problem with SUSY models [13–16], TeV-scale masses are required [17, 18] for the partners of the gluons (gluinos \tilde{g}) and of the top quarks (top squarks \tilde{t}_L and \tilde{t}_R), due to the large top Yukawa coupling.² The latter also favours significant \tilde{t}_L – \tilde{t}_R mixing, so that the mass eigenstate \tilde{t}_1 is lighter than all the other squarks in many scenarios [19, 20]. Bottom squarks (\tilde{b}_1) may also be light, being bound to top squarks by $SU(2)_L$ invariance. This leads to potentially large production cross-sections for gluino pairs ($\tilde{g}\tilde{g}$), top–antitop squark pairs ($\tilde{t}_1\tilde{t}_1^*$) and bottom–antibottom squark pairs ($\tilde{b}_1\tilde{b}_1^*$) at the Large Hadron Collider (LHC) [21]. Production of isolated leptons may arise in the cascade decays of those superpartners to SM quarks and neutralinos $\tilde{\chi}_1^0$, via intermediate neutralinos $\tilde{\chi}_{2,3,4}^0$ or charginos $\tilde{\chi}_{1,2}^\pm$ that in turn lead to W , Z or Higgs bosons, or to lepton superpartners (sleptons, $\tilde{\ell}$). Light third-generation squarks would also enhance gluino decays to top or bottom quarks relative to the generic decays involving light-flavour squarks, favouring the production of heavy-flavour quarks and, in the case of top quarks, additional isolated leptons.

This article presents a search for SUSY in final states with two leptons (electrons or muons) of the same electric charge, referred to as same-sign (SS) leptons, or three leptons (3L), jets and in some cases also missing transverse momentum, whose magnitude is referred to as E_T^{miss} . Only prompt decays of SUSY particles are considered. It is an extension of an earlier search performed by the ATLAS experiment [22] with $\sqrt{s} = 13$ TeV data [23], and uses the data collected in proton–proton (pp) collisions during 2015 and 2016. Similar searches for SUSY in this topology were also performed by the CMS experiment at $\sqrt{s} = 13$ TeV [24–26]. While the same-sign or three-lepton signatures are present in many scenarios of physics beyond the SM (BSM), SM processes leading to such final states have very small cross-sections. Compared to other BSM searches, analyses based on these signatures therefore allow the use of looser kinematic requirements (for example, on E_T^{miss} or on the momentum of jets and leptons), preserving sensitivity to scenarios with small mass differences between the produced gluinos/squarks and the LSP, or in which R -parity is not conserved. This sensitivity to a wide range of BSM physics processes is illustrated by the interpretation of the results in the context of twelve different SUSY simplified models [27–29] that may lead to same-sign or three-lepton signatures.

For RPC models, the first four scenarios studied focus on gluino pair production with decays into on-shell (Figure 1(a)) or off-shell (Figure 1(b)) top quarks, as well as on-shell light quarks. The latter are accompanied by a cascade decay involving a $\tilde{\chi}_1^\pm$ and a $\tilde{\chi}_2^0$ (Figure 1(c)) or a $\tilde{\chi}_2^0$ and light sleptons (Figure 1(d)). The other two RPC scenarios target the direct production of third-generation squark pairs with

¹ The SUSY partners of the Higgs and electroweak gauge bosons, the electroweakinos, mix to form the mass eigenstates known as charginos ($\tilde{\chi}_l^\pm$, $l = 1, 2$ ordered by increasing mass) and neutralinos ($\tilde{\chi}_m^0$, $m = 1, \dots, 4$ ordered by increasing mass).

² The partners of the left-handed (right-handed) quarks are labelled $\tilde{q}_{L(R)}$. In the case where there is significant L/R mixing (as is the case for third-generation squarks) the mass eigenstates of these squarks are labelled $\tilde{q}_{1,2}$ ordered by increasing mass.

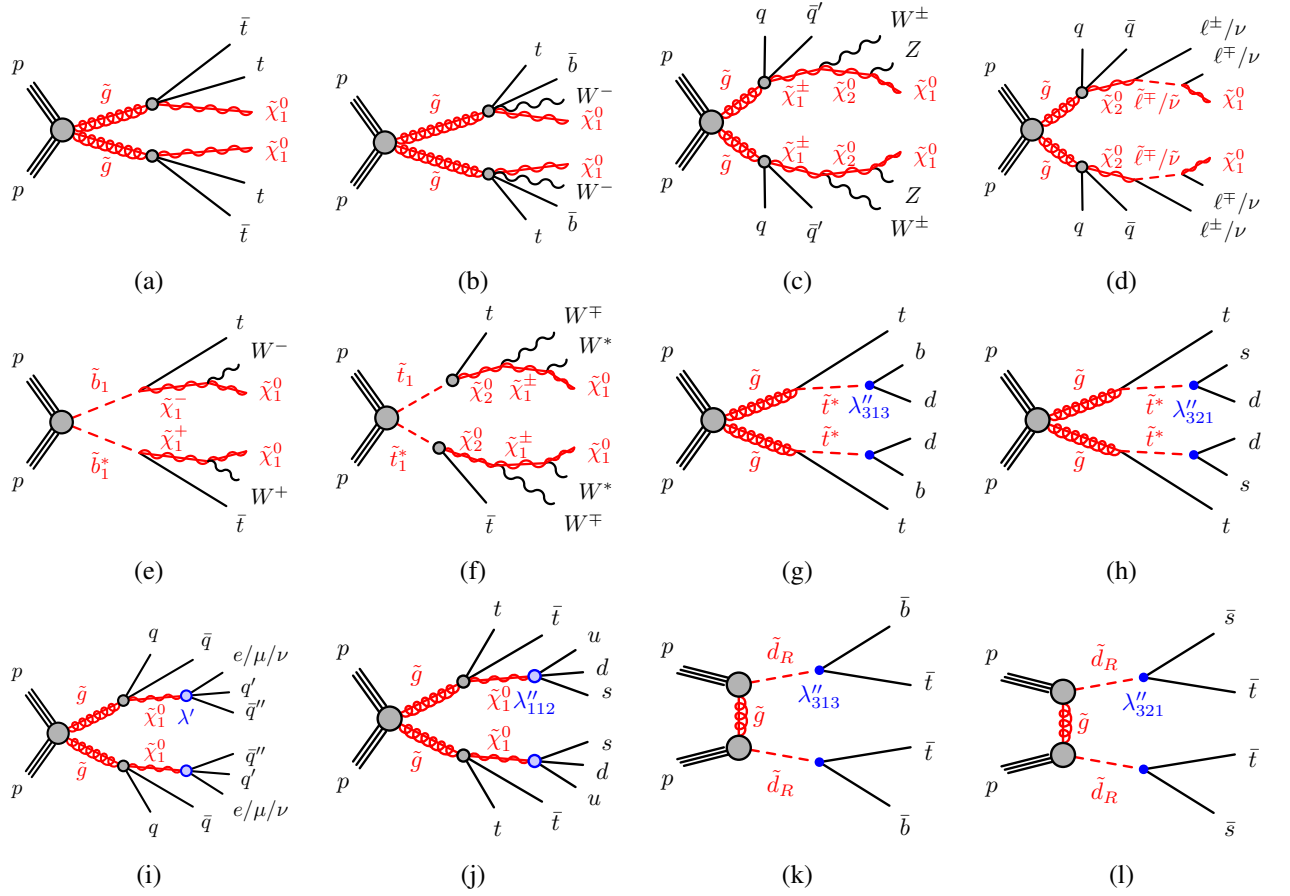


Figure 1: RPC SUSY processes featuring gluino ((a), (b), (c), (d)) or third-generation squark ((e), (f)) pair production studied in this analysis. RPV SUSY models considered are gluino pair production ((g), (h), (i), (j)) and t-channel production of down squark-rights ((k), (l)) which decay via baryon- or lepton-number violating couplings λ'' and λ' respectively. In the diagrams, $q \equiv u, d, c, s$ and $\ell \equiv e, \mu, \tau$. In Figure 1(d), $\tilde{t} \equiv \tilde{e}, \tilde{\mu}, \tilde{\tau}$ and $\tilde{\nu} \equiv \tilde{\nu}_e, \tilde{\nu}_\mu, \tilde{\nu}_\tau$. In Figure 1(f), the W^* labels indicate largely off-shell W bosons – the mass difference between $\tilde{\chi}_1^\pm$ and $\tilde{\chi}_1^0$ is around 1 GeV.

subsequent electroweakino-mediated decays (Figures 1(e) and 1(f)). The former is characterized by final states with bottom squark pairs decaying to $t\bar{t}WW\tilde{\chi}_1^0\tilde{\chi}_1^0$. The latter, addressed here by looking at a final state with three same-sign leptons, is a model that could explain the slight excess seen in same-sign lepton signatures during Run 1 [30]. Finally, a full SUSY model with low fine-tuning, the non-universal Higgs model with two extra parameters (NUHM2) [31, 32], is also considered. When the soft-SUSY-breaking electroweakino mass, $m_{1/2}$, is in the range 300–800 GeV, the model mainly involves gluino pair production with gluinos decaying predominantly to $t\bar{t}\tilde{\chi}_1^0$ and $t\bar{b}\tilde{\chi}_1^\pm$, giving rise to final states with two same-sign leptons and E_T^{miss} .

In the case of non-zero RPV couplings in the baryonic sector (λ''_{ijk}), as proposed in scenarios with minimal flavour violation [33–35], gluinos and squarks may decay directly to top quarks, leading to final states with same-sign leptons [36, 37] and b -quarks (Figures 1(g) and 1(h)). Although these figures illustrate decay modes mediated by non-zero λ''_{313} (resp. λ''_{321}) couplings, the exclusion limits set for these scenarios also hold for non-zero λ''_{323} (resp. λ''_{311} or λ''_{322}), as these couplings lead to experimentally indistinguishable

final states. Alternatively a gluino decaying to a neutralino LSP that further decays to SM particles via a non-zero RPV coupling in the leptonic sector, λ' , or in the baryonic sector λ'' , is also possible (Figures 1(i) and 1(j)). Lower E_T^{miss} is expected in these scenarios, as there is no stable LSP, and the E_T^{miss} originates from neutrinos produced in the $\tilde{\chi}_1^0$ and top quark decays. Pair production of same-sign down squark-right³ (Figures 1(k) and 1(l)) is also considered. In all of these scenarios, antisquarks decay into the charge-conjugate final states of those indicated for the corresponding squarks, and gluinos decay with equal probabilities into the given final state or its charge conjugate.

2 ATLAS detector

The ATLAS experiment [22] is a multipurpose particle detector with a forward-backward symmetric cylindrical geometry and nearly 4π coverage in solid angle.⁴ The interaction point is surrounded by an inner detector (ID) for tracking, a calorimeter system, and a muon spectrometer (MS). The ID provides precision tracking of charged particles with pseudorapidities $|\eta| < 2.5$ and is surrounded by a superconducting solenoid providing a 2 T axial magnetic field. It consists of silicon pixel and silicon micro-strip detectors inside a transition radiation tracker. One significant upgrade for the $\sqrt{s} = 13$ TeV running period is the presence of the insertable B-Layer [38], an additional pixel layer close to the interaction point, which provides high-resolution hits at small radius to improve the tracking and vertexing performance. In the pseudorapidity region $|\eta| < 2.5$, high-granularity lead/liquid-argon electromagnetic sampling calorimeters are used. A steel/scintillator tile calorimeter measures hadron energies for $|\eta| < 1.7$. The endcap and forward regions, spanning $1.5 < |\eta| < 4.9$, are instrumented with liquid-argon calorimeters for both the electromagnetic and hadronic measurements. The MS consists of three large superconducting toroids with eight coils each and a system of trigger and precision-tracking chambers, which provide triggering and tracking capabilities in the ranges $|\eta| < 2.4$ and $|\eta| < 2.7$, respectively. A two-level trigger system is used to select events [39]. The first-level trigger is implemented in hardware. This is followed by the software-based high-level trigger, which can run algorithms similar to those used in the offline reconstruction software, reducing the event rate to about 1 kHz.

3 Data set and simulated event samples

The data used in this analysis were collected during 2015 and 2016 with a peak instantaneous luminosity of $L = 1.4 \times 10^{34} \text{ cm}^{-2}\text{s}^{-1}$. The mean number of pp interactions per bunch crossing (pile-up) in the data set is 24. After the application of beam, detector and data-quality requirements, the integrated luminosity considered corresponds to 36.1 fb^{-1} . The uncertainty in the combined 2015+2016 integrated luminosity is 3.2%. It is derived, following a methodology similar to that detailed in Ref. [40], from a preliminary calibration of the luminosity scale using x - y beam-separation scans performed in August 2015 and May 2016.

³ These RPV baryon-number-violating couplings only apply to $SU(2)$ singlets.

⁴ ATLAS uses a right-handed coordinate system with its origin at the nominal interaction point (IP) in the centre of the detector and the z -axis along the beam pipe. The x -axis points from the IP to the centre of the LHC ring, and the y -axis points upward. Cylindrical coordinates (r, ϕ) are used in the transverse plane, ϕ being the azimuthal angle around the beam pipe. The pseudorapidity is defined in terms of the polar angle θ as $\eta = -\ln \tan(\theta/2)$. Rapidity is defined as $y = 0.5 \ln [(E + p_z)/(E - p_z)]$ where E denotes the energy and p_z is the component of the momentum along the beam direction. The transverse momentum p_T , the transverse energy E_T and the missing transverse momentum E_T^{miss} are defined in the x - y plane.

Monte Carlo (MC) simulated event samples are used to model the SUSY signals and to estimate the irreducible SM background with two same-sign and/or three “prompt” leptons. Prompt leptons are produced directly in the hard-scattering process, or in the subsequent decays of W , Z and H bosons or prompt τ leptons. The reducible background, mainly arising from $t\bar{t}$ production, is estimated from the data as described in Section 5.1. The MC samples were processed through a detailed ATLAS detector simulation [41] based on GEANT4 [42] or a fast simulation using a parameterization of the calorimeter response and GEANT4 for the ID and MS [43]. To simulate the effects of additional pp collisions in the same and nearby bunch crossings, inelastic interactions were generated using the soft strong-interaction processes of PYTHIA 8.186 [44] with a set of tuned parameters referred to as the A2 tune [45] and the MSTW2008LO parton distribution function (PDF) set [46]. These MC events were overlaid onto the simulated hard-scatter event and reweighted to match the pile-up conditions observed in the data. Table 1 presents, for all samples, the event generator, parton shower, cross-section normalization, PDF set and the set of tuned parameters for the modelling of the parton shower, hadronization and underlying event. In all MC samples, except those produced by the SHERPA event generator, the EvtGEN v1.2.0 program [47] was used to model the properties of bottom and charm hadron decays.

Physics process	Event generator	Parton shower	Cross-section normalization	PDF set	Set of tuned parameters
Signal RPC RPV except Fig. 1(j) RPV Fig. 1(j)	MG5_AMC@NLO 2.2.3 [48] MG5_AMC@NLO 2.2.3 HERWIG++ 2.7.1 [51]	PYTHIA 8.186 [44] PYTHIA 8.210 HERWIG++ 2.7.1	NLO+NLL or NLO-Prospino2 [52–57]	NNPDF2.3LO [49] NNPDF2.3LO CTEQ6L1 [58]	A14 [50] A14 UEEE5 [59]
$t\bar{t} + X$ $t\bar{t}W, t\bar{t}Z/\gamma^*$ $t\bar{t}H$ $4t$	MG5_AMC@NLO 2.2.2 MG5_AMC@NLO 2.3.2 MG5_AMC@NLO 2.2.2	PYTHIA 8.186 PYTHIA 8.186 PYTHIA 8.186	NLO [60] NLO [60] NLO [48]	NNPDF2.3LO NNPDF2.3LO NNPDF2.3LO	A14 A14 A14
Diboson ZZ, WZ Other (inc. $W^\pm W^\pm$)	SHERPA 2.2.1 [61] SHERPA 2.1.1	SHERPA 2.2.1 SHERPA 2.1.1	NLO [62] NLO [62]	NNPDF2.3LO CT10 [63]	SHERPA default SHERPA default
Rare $t\bar{t}WW, t\bar{t}WZ$ $t\bar{t}Z, t\bar{t}W, t\bar{t}t$ WH, ZH Triboson	MG5_AMC@NLO 2.2.2 MG5_AMC@NLO 2.2.2 MG5_AMC@NLO 2.2.2 SHERPA 2.1.1	PYTHIA 8.186 PYTHIA 8.186 PYTHIA 8.186 SHERPA 2.1.1	NLO [48] LO NLO [64] NLO [62]	NNPDF2.3LO NNPDF2.3LO NNPDF2.3LO CT10	A14 A14 A14 SHERPA default

Table 1: Simulated signal and background event samples: the corresponding event generator, parton shower, cross-section normalization, PDF set and set of tuned parameters are shown for each sample. Because of their very small contribution to the signal-region background estimate, $t\bar{t}WW$, $t\bar{t}WZ$, tZ , tWZ , $t\bar{t}t$, WH , ZH and triboson are summed and labelled “rare” in the following. NLO-Prospino2 refers to RPV down squark models of Figures 1(k) and 1(l), as well as the NUHM2 model.

The SUSY signals from Figure 1 are defined by an effective Lagrangian describing the interactions of a small number of new particles [27–29]. All SUSY particles not included in the decay of the pair-produced squarks and gluinos are effectively decoupled. These simplified models assume one production process and one decay channel with a 100% branching fraction. Apart from Figure 1(j), where events were generated with HERWIG++ [51], all simplified models were generated from leading-order (LO) matrix elements with up to two extra partons in the matrix element (only up to one for the $\tilde{g} \rightarrow q\bar{q}(\ell\ell/\nu\nu)\tilde{\chi}_1^0$ model) using MG5_AMC@NLO 2.2.3 [48] interfaced to PYTHIA 8 with the A14 tune [50] for the modelling of the parton shower, hadronization and underlying event. Jet-parton matching was realized following the CKKW-L prescription [65], with a matching scale set to one quarter of the pair-produced superpartner mass. All signal models were generated with prompt decays of the SUSY particles. Signal cross-sections were calculated at next-to-leading order (NLO) in the strong coupling constant, adding the resummation of soft-gluon emission at next-to-leading-logarithmic accuracy (NLO+NLL) [52–56], except for the RPV

models of Figures 1(k) and 1(l) and the NUHM2 model where NLO cross-sections were used [52, 66]. The nominal cross-sections and the uncertainties were taken from envelopes of cross-section predictions using different PDF sets and factorization and renormalization scales, as described in Refs. [21, 57]. Typical pair-production cross-sections are: 4.7 ± 1.2 fb for gluinos with a mass of 1.7 TeV, 28 ± 4 fb for bottom squarks with a mass of 800 GeV, and 15.0 ± 2.0 fb for down squark-rights with a mass of 800 GeV and a gluino mass of 2.0 TeV.

The two dominant irreducible background processes are $t\bar{t}V$ (with V being a W or Z/γ^* boson) and diboson production with final states of four charged leptons ℓ^5 , three charged leptons and one neutrino, or two same-sign charged leptons and two neutrinos. The MC simulation samples for these are described in Refs. [67] and [62], respectively. For diboson production, the matrix elements contain the doubly resonant diboson processes and all other diagrams with four or six electroweak vertices, such as $W^\pm W^\pm jj$, with one ($W^\pm W^\pm jj$) or two (WZ , ZZ) extra partons. NLO cross-sections for $t\bar{t}W$, $t\bar{t}Z/\gamma^*(\rightarrow \ell\ell)^6$ and leptonic diboson processes are respectively 0.60 pb [60], 0.12 pb and 6.0 pb [62]. The processes $t\bar{t}H$ and $4t$, with NLO cross-sections of 507.1 fb [60] and 9.2 fb [48] respectively, are also considered.

Other background processes, with small cross-sections and no significant contribution to any of the signal regions, are grouped into a category labelled “rare”. This category contains $t\bar{t}WW$ and $t\bar{t}WZ$ events generated with no extra parton in the matrix element, and tZ , tWZ , $t\bar{t}\bar{t}$, WH and ZH as well as triboson (WWW , WWZ , WZZ and ZZZ) production with fully leptonic decays, leading to up to six charged leptons. The processes WWW , WZZ and ZZZ were generated at NLO with additional LO matrix elements for up to two extra partons, while WWZ was generated at LO with up to two extra partons.

4 Event reconstruction and selection

Candidate events are required to have a reconstructed vertex [69] with at least two associated tracks with $p_T > 400$ MeV. The vertex with the largest $\sum p_T^2$ of the associated tracks is chosen as the primary vertex of the event.

For the data-driven background estimations, two categories of electrons and muons are used: “candidate” and “signal” with the latter being a subset of the “candidate” leptons satisfying tighter selection criteria. Electron candidates are reconstructed from energy depositions in the electromagnetic calorimeter which were matched to an ID track and are required to have $|\eta| < 2.47$, $p_T > 10$ GeV, and pass the “Loose” likelihood-based identification requirement [70]. Candidates within the transition region between the barrel and endcap electromagnetic calorimeters, $1.37 < |\eta| < 1.52$, are not considered. The track matched with the electron must have a significance of the transverse impact parameter d_0 with respect to the reconstructed primary vertex of $|d_0|/\sigma(d_0) < 5$. Muon candidates are reconstructed in the region $|\eta| < 2.5$ from muon spectrometer tracks matching ID tracks. All muon candidates must have $p_T > 10$ GeV and must pass the “Medium” identification requirements [71].

Jets are reconstructed with the anti- k_t algorithm [72] with radius parameter $R = 0.4$, using three-dimensional topological energy clusters in the calorimeter [73] as input. All jets must have $p_T > 20$ GeV and $|\eta| < 2.8$. For all jets the expected average energy contribution from pile-up is subtracted according to the jet

⁵ All lepton flavours are included here and τ leptons subsequently decay leptonically or hadronically.

⁶ This cross-section is computed using the configuration described in Refs. [48, 68].

area [74, 75]. Jets are then calibrated as described in Ref. [75]. In order to reduce the effects of pile-up, a significant fraction of the tracks in jets with $p_T < 60 \text{ GeV}$ and $|\eta| < 2.4$ must originate from the primary vertex, as defined by the jet vertex tagger (JVT) [76].

Identification of jets containing b -hadrons (b -tagging) is performed with the MV2c10 algorithm, a multivariate discriminant making use of track impact parameters and reconstructed secondary vertices [77, 78]. A requirement is chosen corresponding to a 70% average efficiency for tagging b -jets in simulated $t\bar{t}$ events. The rejection factors for light-quark/gluon jets, c -quark jets and $\tau \rightarrow \nu + \text{hadron}$ decays in simulated $t\bar{t}$ events are approximately 380, 12 and 54, respectively [78, 79]. Jets with $|\eta| < 2.5$ which satisfy the b -tagging and JVT requirements are identified as b -jets. Correction factors and uncertainties determined from data for the b -tagging efficiencies and mis-tag rates are applied to the simulated samples [78].

After the object identification, overlaps between the different objects are resolved. Any jet within a distance $\Delta R_y \equiv \sqrt{(\Delta y)^2 + (\Delta \phi)^2} = 0.2$ of a lepton candidate is discarded, unless the jet is b -tagged,⁷ in which case the lepton is discarded since it probably originated from a semileptonic b -hadron decay. Any remaining lepton within $\Delta R_y = \min\{0.4, 0.1 + 9.6 \text{ GeV}/p_T(\ell)\}$ of a jet is discarded. In the case of muons, the muon is retained and the jet is discarded if the jet has fewer than three associated tracks. This reduces inefficiencies for high-energy muons undergoing significant energy loss in the calorimeter.

Signal electrons must satisfy the ‘‘Medium’’ likelihood-based identification requirement [70]. In regions with large amounts of material in the tracker, an electron (positron) is more likely to emit a hard bremsstrahlung photon; if the photon subsequently converts to an asymmetric electron–positron pair, and the positron (electron) has high momentum and is reconstructed, the lepton charge can be misidentified (later referred to as ‘‘charge-flip’’). To reduce the impact of charge misidentification, signal electrons must satisfy $|\eta| < 2.0$. Furthermore, signal electrons that are likely to be reconstructed with an incorrect charge assignment are rejected using the electron cluster and track properties including the impact parameter, the curvature significance, the cluster width, and the quality of the matching between the cluster and its associated track, in terms of both energy and position. These variables, as well as the electron p_T and η , are combined into a single classifier using a boosted decision tree (BDT) algorithm. A selection requirement on the BDT output is chosen to achieve a rejection factor of 7–8 for electrons with a wrong charge assignment while selecting correctly measured electrons with an efficiency of 97%. Correction factors to account for differences in the selection efficiency between data and MC simulation are applied to the selected electrons in MC simulation. These correction factors are determined using $Z \rightarrow ee$ events [80].

Signal muons must fulfil the requirement $|d_0|/\sigma(d_0) < 3$. Tracks associated with the signal electrons or muons must have a longitudinal impact parameter z_0 with respect to the reconstructed primary vertex satisfying $|z_0 \sin \theta| < 0.5 \text{ mm}$. Isolation requirements are applied to both the signal electrons and muons. The scalar sum of the p_T of tracks within a variable-size cone around the lepton, excluding its own track, must be less than 6% of the lepton p_T .

The track isolation cone size for electrons (muons) $\Delta R_\eta \equiv \sqrt{(\Delta \eta)^2 + (\Delta \phi)^2}$ is given by the smaller of $\Delta R_\eta = 10 \text{ GeV}/p_T$ and $\Delta R_\eta = 0.2$ (0.3). In addition, in the case of electrons the calorimeter energy clusters in a cone of $\Delta R_\eta = 0.2$ around the electron (excluding the deposit from the electron itself) must be less than 6% of the electron p_T . Simulated events are corrected to account for differences in the lepton trigger, reconstruction, identification and isolation efficiencies between data and MC simulation.

The missing transverse momentum is defined as the negative vector sum of the transverse momenta of all identified candidate objects (electrons, photons [81], muons and jets) and an additional soft term. The

⁷ In this case the b -tagging operating point corresponding to an efficiency of 85% is used.

soft term is constructed from all tracks associated with the primary vertex but not with any physics object. In this way, the E_T^{miss} is adjusted for the best calibration of the jets and the other identified physics objects listed above, while maintaining approximate pile-up independence in the soft term [82, 83].

Events are selected using a combination of dilepton and E_T^{miss} triggers, the latter being used only for events with $E_T^{\text{miss}} > 250 \text{ GeV}$. The trigger-level requirements on E_T^{miss} and the leading and subleading lepton p_T are looser than those applied offline to ensure that trigger efficiencies are constant in the relevant phase space. The event selection requires at least two signal leptons with $p_T > 20 \text{ GeV}$ (apart from two signal regions where the lower bound on the subleading lepton p_T is 10 GeV).⁸ If the event contains exactly two signal leptons, they must have the same electric charge. In order to reject detector noise and non-collision backgrounds (including those from cosmic rays, beam-gas and beam-halo interactions), events are discarded if they contain any jet not satisfying basic quality criteria [84, 85].

To maximize the sensitivity to the signal models of Figure 1, 19 non-exclusive⁹ signal regions (SRs) are defined in Table 2. The SRs are named in the form $SNLMbX$, where S indicates if the signal region is targeting an RPC or RPV model, N indicates the number of leptons required, M the number of b -jets required, and X indicates the severity of the E_T^{miss} or m_{eff} requirements (Soft, Medium or Hard). All signal regions, except Rpv2L0b, allow any number of additional leptons in addition to a $e^\pm e^\pm$, $e^\pm \mu^\pm$ or $\mu^\pm \mu^\pm$ pair. Signal regions with a three lepton selection can either require any lepton charge combination (Rpc3L0bH, Rpc3L0bS) or that all three leptons have the same charge (Rpc3LSS1b). The other requirements used to define the SRs are the number of signal leptons ($N_{\text{leptons}}^{\text{signal}}$), number of b -jets with $p_T > 20 \text{ GeV}$ ($N_{b\text{-jets}}$), number of jets with p_T above 25, 40 or 50 GeV , regardless of their flavour (N_{jets}), E_T^{miss} , the effective mass (m_{eff}) and the charge of the signal leptons. The m_{eff} variable is defined as the scalar sum of the p_T of the signal leptons, jets and the E_T^{miss} . For SRs where the $Z + \text{jets}$ background is important (Rpc3LSS1b, Rpv2L0b and Rpv2L2bH), events in which the invariant mass of two same-sign electrons is close to the Z boson mass are vetoed. For SRs targeting the production of down squark pairs (Rpv2L1bS, Rpv2L2bS, Rpv2L1bM), only events with at least two negatively charged leptons are considered, as the down squarks decay exclusively to top antiquarks. Finally, SRs targeting signal scenarios with lepton p_T spectra softer than typical background processes impose an upper bound on the leptons' p_T . The last column of Table 2 indicates the targeted signal model. The Rpc3L1b and Rpc3L1bH SRs are not motivated by a particular signal model and can be seen as a natural extension of the Rpc3L0b SRs with the same kinematic selections but requiring at least one b -jet.

The values of acceptance times efficiency of the SR selections for the RPC SUSY signal models, with masses near the exclusion limit, typically range between 0.5% and 7% for models with a light $\tilde{\chi}_1^0$ and between 0.5 and 2% for models with a heavy $\tilde{\chi}_1^0$. For RPV SUSY signal models, these values are in the range 0.2–4%. To increase the signal efficiency for the SUSY models with low-energy leptons (Figure 1(b)), the p_T threshold of leptons is relaxed from 20 GeV to 10 GeV in the SR definition.

5 Background estimation

Two main sources of SM background can be distinguished in this analysis. The first category is the reducible background, which includes events containing electrons with mismeasured charge, mainly from

⁸ To ensure that the trigger efficiency is constant for selected events where the subleading lepton p_T lies between 10 and 20 GeV only the E_T^{miss} trigger is used in this case.

⁹ Each signal region partially overlaps with at least one other signal region.

Signal region	$N_{\text{leptons}}^{\text{signal}}$	$N_{b\text{-jets}}$	N_{jets}	p_T^{jet} [GeV]	E_T^{miss} [GeV]	m_{eff} [GeV]	$E_T^{\text{miss}}/m_{\text{eff}}$	Other	Targeted Signal
Rpc2L2bS	$\geq 2\text{SS}$	≥ 2	≥ 6	> 25	> 200	> 600	> 0.25	–	Fig. 1(a)
Rpc2L2bH	$\geq 2\text{SS}$	≥ 2	≥ 6	> 25	–	> 1800	> 0.15	–	Fig. 1(a), NUHM2
Rpc2Lsoft1b	$\geq 2\text{SS}$	≥ 1	≥ 6	> 25	> 100	–	> 0.3	$20, 10 < p_T^{\ell_1}, p_T^{\ell_2} < 100 \text{ GeV}$	Fig. 1(b)
Rpc2Lsoft2b	$\geq 2\text{SS}$	≥ 2	≥ 6	> 25	> 200	> 600	> 0.25	$20, 10 < p_T^{\ell_1}, p_T^{\ell_2} < 100 \text{ GeV}$	Fig. 1(b)
Rpc2L0bS	$\geq 2\text{SS}$	$= 0$	≥ 6	> 25	> 150	–	> 0.25	–	Fig. 1(c)
Rpc2L0bH	$\geq 2\text{SS}$	$= 0$	≥ 6	> 40	> 250	> 900	–	–	Fig. 1(c)
Rpc3L0bS	≥ 3	$= 0$	≥ 4	> 40	> 200	> 600	–	–	Fig. 1(d)
Rpc3L0bH	≥ 3	$= 0$	≥ 4	> 40	> 200	> 1600	–	–	Fig. 1(d)
Rpc3L1bS	≥ 3	≥ 1	≥ 4	> 40	> 200	> 600	–	–	Other
Rpc3L1bH	≥ 3	≥ 1	≥ 4	> 40	> 200	> 1600	–	–	Other
Rpc2L1bS	$\geq 2\text{SS}$	≥ 1	≥ 6	> 25	> 150	> 600	> 0.25	–	Fig. 1(e)
Rpc2L1bH	$\geq 2\text{SS}$	≥ 1	≥ 6	> 25	> 250	–	> 0.2	–	Fig. 1(e)
Rpc3LSS1b	$\geq \ell^\pm \ell^\pm \ell^\pm$	≥ 1	–	–	–	–	–	veto $81 < m_{e^\pm e^\pm} < 101 \text{ GeV}$	Fig. 1(f)
Rpv2L1bH	$\geq 2\text{SS}$	≥ 1	≥ 6	> 50	–	> 2200	–	–	Figs. 1(g), 1(h)
Rpv2L0b	$= 2\text{SS}$	$= 0$	≥ 6	> 40	–	> 1800	–	veto $81 < m_{e^\pm e^\pm} < 101 \text{ GeV}$	Fig. 1(i)
Rpv2L2bH	$\geq 2\text{SS}$	≥ 2	≥ 6	> 40	–	> 2000	–	veto $81 < m_{e^\pm e^\pm} < 101 \text{ GeV}$	Fig. 1(j)
Rpv2L2bS	$\geq \ell^- \ell^-$	≥ 2	≥ 3	> 50	–	> 1200	–	–	Fig. 1(k)
Rpv2L1bS	$\geq \ell^- \ell^-$	≥ 1	≥ 4	> 50	–	> 1200	–	–	Fig. 1(l)
Rpv2L1bM	$\geq \ell^- \ell^-$	≥ 1	≥ 4	> 50	–	> 1800	–	–	Fig. 1(l)

Table 2: Summary of the signal region definitions. Unless explicitly stated in the table, at least two signal leptons with $p_T > 20 \text{ GeV}$ and same charge (SS) are required in each signal region. Requirements are placed on the number of signal leptons ($N_{\text{leptons}}^{\text{signal}}$), the number of b -jets with $p_T > 20 \text{ GeV}$ ($N_{b\text{-jets}}$), the number of jets (N_{jets}) above a certain p_T threshold (p_T^{jet}), E_T^{miss} , m_{eff} and/or $E_T^{\text{miss}}/m_{\text{eff}}$. The last column indicates the targeted signal model. The Rpc3L1b and Rpc3L1bH SRs are not motivated by a particular signal model and can be seen as a natural extension of the Rpc3L0b SRs with the same kinematic selections but requiring at least one b -jet.

the production of top quark pairs, and events containing at least one fake or non-prompt (FNP) lepton. The FNP lepton mainly originates from heavy-flavour hadron decays in events containing top quarks, or W or Z bosons. Hadrons misidentified as leptons, electrons from photon conversions and leptons from pion or kaon decays in flight are other possible sources. Data-driven methods used for the estimation of this reducible background in the signal and validation regions are described in Section 5.1.

The second background category is the irreducible background from events with two same-sign prompt leptons or at least three prompt leptons and is estimated using the MC simulation samples. Since diboson and $t\bar{t}V$ events are the main irreducible backgrounds in the signal regions, dedicated validation regions (VR) with an enhanced contribution from these processes, and small signal contamination, are defined to verify the background predictions from the simulation (Section 5.2). Section 5.3 discusses the systematic uncertainties considered when performing the background estimation in the signal and validation regions.

5.1 Reducible background estimation methods

Charge misidentification is only relevant for electrons. The contribution of charge-flip events to the SR/VR is estimated using the data. The electron charge-flip probability is extracted in a $Z/\gamma^* \rightarrow ee$ data sample using a likelihood fit which takes as input the numbers of same-sign and opposite-sign electron pairs observed in a window of 10 GeV around the Z boson mass. The charge-flip probability is a free

parameter of the fit and is extracted as a function of the electron p_T and η . These probabilities are around 0.5% (1%) and 0.1% (0.2%) for the candidate and signal electrons for $|\eta| < 1.37$ ($|\eta| > 1.52$), respectively. The former is used only in the FNP lepton background estimation. The event yield of the charge-flip electron background in the signal or validation regions is obtained by multiplying the measured charge-flip probability with the number of events in data regions with the same kinematic requirements as the signal or validation regions but with opposite-sign lepton pairs.

Two data-driven methods are used to estimate the FNP lepton background, referred to as the “matrix method” and the “MC template method”. The estimates from these methods are combined to give the final estimate. These two methods are described below.

The first estimation of the FNP lepton background is performed with a matrix method similar to that described in Ref. [86]. Two types of lepton identification criteria are defined: “tight”, corresponding to the signal lepton criteria described in Section 4, and “loose”, corresponding to candidate leptons after object overlap removal and the charge-flip BDT selection described also in Section 4. The matrix method relates the number of events containing prompt or FNP leptons to the number of observed events with tight or loose-not-tight leptons using the probability for loose prompt or FNP leptons to satisfy the tight criteria. The probability for loose prompt leptons to satisfy the tight selection criteria (ε) is obtained using a $Z/\gamma^* \rightarrow \ell\ell$ data sample and is modelled as a function of the lepton p_T and η . The efficiencies for electrons (muons) rise from 60% (80%) at low p_T to almost 100% at p_T above 50 GeV – apart from endcap electrons, for which they reach only 95%. The probability for loose FNP leptons to satisfy the tight selection criteria (FNP lepton rate, f) is determined from data in SS control regions enriched in non-prompt leptons mostly originating from heavy-flavour hadron decays in single-lepton $t\bar{t}$ events. These regions contain events with at least one b -jet, one well-isolated muon (referred to as the “tag”), and an additional loose electron or muon which is used for the measurement. The rates f are measured as a function of p_T after subtracting the small contribution from prompt-lepton processes predicted by simulation and the data-driven estimation of events with electron charge-flip.¹⁰ For electrons, and muons with $|\eta| < 2.3$, f is constant at around 10% for $p_T < 30$ GeV (20% for muons with $|\eta| > 2.3$) and increases at higher p_T . With these values of ε and f , the method has been demonstrated to correctly estimate the FNP lepton background.

The second method for FNP lepton estimation is the MC template method described in details in Refs. [86, 87]. It relies on the correct modelling of the kinematic distributions of the FNP leptons and charge-flipped electron processes in $t\bar{t}$ and $V+jets$ samples. These samples were simulated with the Powheg-Box generator [88–91] and the parton shower and hadronization performed by either Pythia 6.428 [92] ($t\bar{t}$) or Pythia 8.186 ($V+jets$). The FNP leptons are classified in five categories, namely electrons and muons originating from b - and light-quark jets as well as electrons from photon conversions. Normalization factors for each of the five sources are adjusted to match the observed data in dedicated control regions. Events are selected with at least two same-sign signal leptons, $E_T^{\text{miss}} > 40$ GeV, two or more jets, and are required not to belong to the SRs. They are further split into regions with or without b -jets and with different lepton flavours of the same-sign lepton pair, giving a total of six control regions. The global normalization factors applied to the MC samples for estimating the reducible background in each SR vary from 1.2 ± 1.1 to 2.9 ± 2.0 , where the errors account for statistical uncertainties and uncertainties related to the choice of event generator (see Section 5.3).

Since the FNP lepton predictions from the MC template and matrix methods in the signal and validation regions are consistent with each other, a weighted average of the two results is used. With this approach,

¹⁰ For muons with $p_T < 20$ GeV, f is parameterized as a function of p_T and η .

the combined estimate is always dominated by systematic uncertainties, which is not always the case when only the matrix method is used due to small number of events in the control regions. To check the validity and robustness of the FNP lepton estimate, the distributions of several discriminating variables in data are compared with the predicted background after various requirements on the number of jets and b -jets. Examples of such distributions are shown in Figure 2, and illustrate that the data are described by the prediction within uncertainties. The apparent disagreement for m_{eff} above 1 TeV in Figure 2(d) is covered by the large theory uncertainty for the diboson background, which is not shown but amounts to about 30% for m_{eff} above 1 TeV.

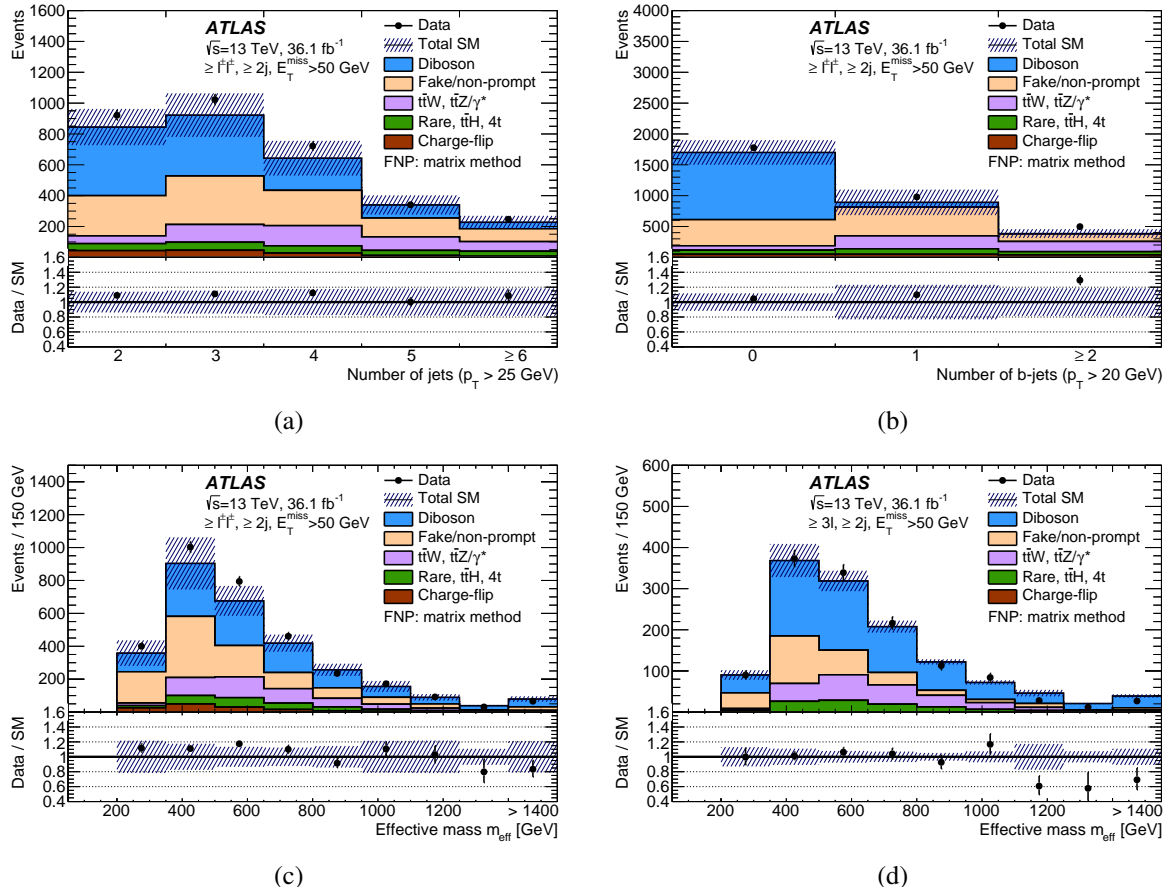


Figure 2: Distributions of (a) the number of jets, (b) the number of b -tagged jets and (c), (d) the effective mass. The distributions are made after requiring at least two jets ($p_T > 40 \text{ GeV}$) and $E_T^{\text{miss}} > 50 \text{ GeV}$, as well as at least two same-sign leptons (a, b, c) or three leptons (d). The uncertainty bands include the statistical uncertainties for the background prediction as well as the systematic uncertainties for fake- or non-prompt-lepton backgrounds (using the matrix method) and charge-flip electrons. Not included are theoretical uncertainties in the irreducible background contributions. The rare category is defined in the text.

5.2 Validation of irreducible background estimates

Dedicated validation regions are defined to verify the estimate of the $t\bar{t}V$, WZ and $W^\pm W^\pm$ background in the signal regions. The corresponding selections are summarized in Table 3. The overlap with the signal regions is resolved by removing events that are selected in the signal regions. The purity of the targeted

Validation Region	$N_{\text{leptons}}^{\text{signal}}$	$N_{b\text{-jets}}$	N_{jets}	$p_{\text{T}}^{\text{jet}}$ [GeV]	$E_{\text{T}}^{\text{miss}}$ [GeV]	m_{eff} [GeV]	Other
$t\bar{t}W$	$= 2SS$	≥ 1	$\geq 4 (e^\pm e^\pm, e^\pm \mu^\pm)$ $\geq 3 (\mu^\pm \mu^\pm)$	> 40 > 25	> 45	> 550	$p_{\text{T}}^{\ell_2} > 40 \text{ GeV}$ $\sum p_{\text{T}}^{b\text{-jet}} / \sum p_{\text{T}}^{\text{jet}} > 0.25$
$t\bar{t}Z$	≥ 3 $\geq 1 \text{ SFOS pair}$	≥ 1	≥ 3	> 35	—	> 450	$81 < m_{\text{SFOS}} < 101 \text{ GeV}$
$WZ4j$	$= 3$	$= 0$	≥ 4	> 25	—	> 450	$E_{\text{T}}^{\text{miss}} / \sum p_{\text{T}}^{\ell} < 0.7$
$WZ5j$	$= 3$	$= 0$	≥ 5	> 25	—	> 450	$E_{\text{T}}^{\text{miss}} / \sum p_{\text{T}}^{\ell} < 0.7$
$W^\pm W^\pm jj$	$= 2SS$	$= 0$	≥ 2	> 50	> 55	> 650	veto $81 < m_{e^\pm e^\pm} < 101 \text{ GeV}$ $p_{\text{T}}^{\ell_2} > 30 \text{ GeV}$ $\Delta R_\eta(\ell_{1,2}, j) > 0.7$ $\Delta R_\eta(\ell_1, \ell_2) > 1.3$
All VRs	Veto events belonging to any SR						

Table 3: Summary of the event selection in the validation regions (VRs). Requirements are placed on the number of signal leptons ($N_{\text{leptons}}^{\text{signal}}$), the number of b -jets with $p_{\text{T}} > 20 \text{ GeV}$ ($N_{b\text{-jets}}$) or the number of jets (N_{jets}) above a certain p_{T} threshold ($p_{\text{T}}^{\text{jet}}$). The two leading- p_{T} leptons are referred to as $\ell_{1,2}$ with decreasing p_{T} . Additional requirements are set on $E_{\text{T}}^{\text{miss}}$, m_{eff} , the invariant mass of the two leading electrons $m_{e^\pm e^\pm}$, the presence of SS leptons or a pair of same-flavour opposite-sign leptons (SFOS) and its invariant mass m_{SFOS} . A minimum angular separation between the leptons and the jets ($\Delta R_\eta(\ell_{1,2}, j)$) and between the two leptons ($\Delta R_\eta(\ell_1, \ell_2)$) is imposed in the $W^\pm W^\pm jj$ VR. For the two WZ VRs the selection also relies on the ratio of the $E_{\text{T}}^{\text{miss}}$ in the event to the sum of p_{T} of all signal leptons p_{T} ($E_{\text{T}}^{\text{miss}} / \sum p_{\text{T}}^{\ell}$). The ratio of the scalar sum of the p_{T} of all b -jets to that of all jets in the event ($\sum p_{\text{T}}^{b\text{-jet}} / \sum p_{\text{T}}^{\text{jet}}$) is used in the $t\bar{t}W$ VR selection.

background processes in these regions ranges from 35% to 65%. The expected signal contamination is generally below 5% for models near the limit of exclusion in $t\bar{t}Z$, WZ and $W^\pm W^\pm$ VRs and about 20% in the $t\bar{t}W$ VR. The observed yields, compared with the background predictions and uncertainties, are shown in Table 4. There is good agreement between data and the estimated background in all the validation regions.

5.3 Systematic uncertainties

Statistical uncertainties due to the number of data events in the loose and tight lepton control regions are considered in the FNP lepton background estimate. In the matrix method, the systematic uncertainties mainly come from potentially different compositions of b -jets, light-quark jets and photon conversions between the signal regions and the regions where the FNP lepton rates are measured. The uncertainty coming from the prompt-lepton contamination in the FNP lepton control regions is also considered. Overall, the uncertainty in the FNP lepton rate f amounts to 30% at low p_{T} , and can reach 85% for muons with $p_{\text{T}} > 40 \text{ GeV}$, and 50% for electrons with $p_{\text{T}} > 20 \text{ GeV}$; these values are driven respectively by the dependency of the isolation of non-prompt muons on the kinematic properties of the jets which emit them, and the uncertainty in the proportion of non-prompt electrons from heavy-flavoured hadron decays with respect to other sources of FNP electrons (mainly converted photons). The uncertainties in the prompt-lepton efficiency ε are much smaller. The uncertainties in the FNP lepton background estimated with the matrix method in each VR and SR are then evaluated by propagating the f and ε uncertainties. In the MC template method, the systematic uncertainty is obtained by changing the generator from PowHEG-Box to SHERPA and propagating uncertainties from the control region fit to the global normalization scale factors applied to the MC samples. The uncertainties in these scale factors are in the range 75–80%, depending

Validation Region	$t\bar{t}W$	$t\bar{t}Z$	$WZ4j$	$WZ5j$	$W^\pm W^\pm jj$
$t\bar{t}Z/\gamma^*$	6.2 ± 0.9	123 ± 17	17.8 ± 3.5	10.1 ± 2.3	1.06 ± 0.22
$t\bar{t}W$	19.0 ± 2.9	1.71 ± 0.27	1.30 ± 0.32	0.45 ± 0.14	4.1 ± 0.8
$t\bar{t}H$	5.8 ± 1.2	3.6 ± 1.8	1.8 ± 0.6	0.96 ± 0.34	0.69 ± 0.14
$4t$	1.02 ± 0.22	0.27 ± 0.14	0.04 ± 0.02	0.03 ± 0.02	0.03 ± 0.02
$W^\pm W^\pm$	0.5 ± 0.4	–	–	–	26 ± 14
WZ	1.4 ± 0.8	29 ± 17	200 ± 110	70 ± 40	27 ± 14
ZZ	0.04 ± 0.03	5.5 ± 3.1	22 ± 12	9 ± 5	0.53 ± 0.30
Rare	2.2 ± 0.5	26 ± 13	7.3 ± 2.1	3.0 ± 1.0	1.8 ± 0.5
Fake/non-prompt leptons	18 ± 16	22 ± 14	49 ± 31	17 ± 12	13 ± 10
Charge-flip electrons	3.4 ± 0.5	–	–	–	1.74 ± 0.22
Total SM background	57 ± 16	212 ± 35	300 ± 130	110 ± 50	77 ± 31
Observed	71	209	257	106	99

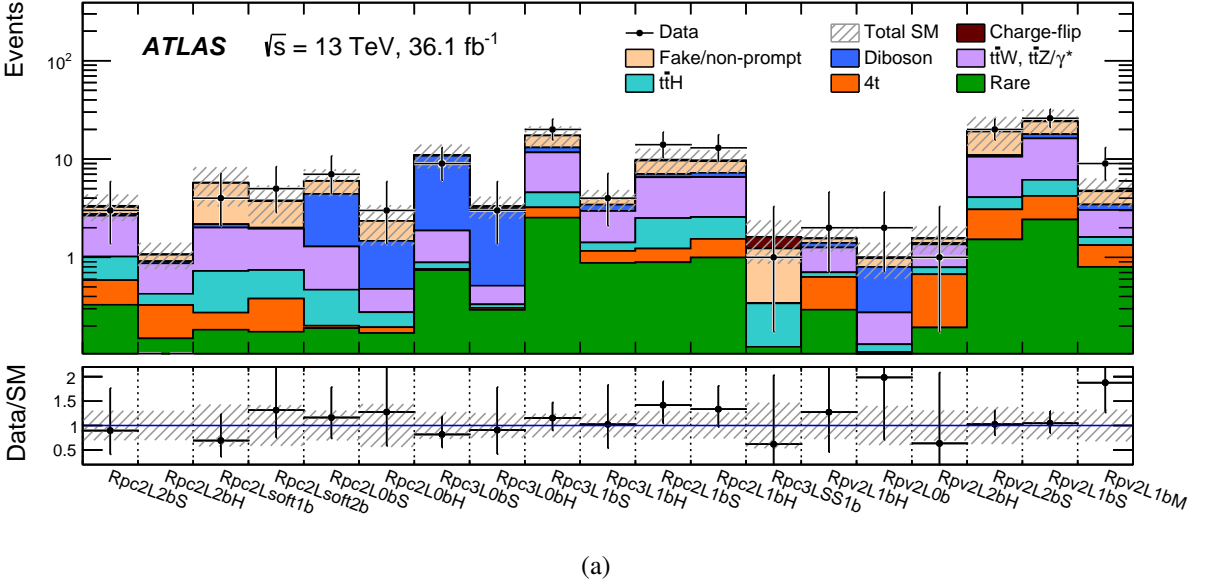
Table 4: The numbers of observed data and expected background events in the validation regions. The rare category is defined in the text. Background categories with yields shown as “–” do not contribute to a given region (e.g. charge flips in three-lepton regions) or their estimates are below 0.01 events. The displayed yields include all statistical and systematic uncertainties described in Section 5.3.

on the SRs. When combining the results of the MC template method and the matrix method to obtain the final estimate, systematic uncertainties are propagated assuming conservatively a full correlation between the two methods.

The uncertainty in the electron charge-flip probability mainly originates from the number of events in the regions used in the charge-flip probability measurement and the uncertainty related to the background subtraction from the Z boson’s mass peak. The relative error in the charge-flip rate is below 20% (30%) for signal (candidate) electrons with p_T above 20 GeV.

The systematic uncertainties related to the estimated background from same-sign prompt leptons arise from the experimental uncertainties (jet energy scale calibration, jet energy resolution and b -tagging efficiency) as well as theoretical modelling and theoretical cross-section uncertainties. The statistical uncertainty of the simulated event samples is also taken into account.

The cross-sections used to normalize the MC samples are varied according to the uncertainty in the cross-section calculation, which is 13% for $t\bar{t}W$, 12% for $t\bar{t}Z$ production [60], 6% for diboson production [62], 8% for $t\bar{t}H$ [60] and 30% for $4t$ [48]. Additional uncertainties are assigned to some of these backgrounds to account for the theoretical modelling of the kinematic distributions in the MC simulation. For $t\bar{t}W$ and $t\bar{t}Z$, the predictions from the MG5_AMC@NLO and SHERPA generators are compared, and the renormalization and factorization scales used to generate these samples are varied independently within a factor of two, leading to a 15–35% uncertainty in the expected SR yields for these processes. For diboson production, uncertainties are estimated by varying the QCD and matching scales, as well as the parton shower recoil scheme, leading to a 30–40% uncertainty for these processes after the SR selections. For $t\bar{t}H$, $4t$ and rare production processes, a 50% uncertainty in their total contribution is assigned.



(a)

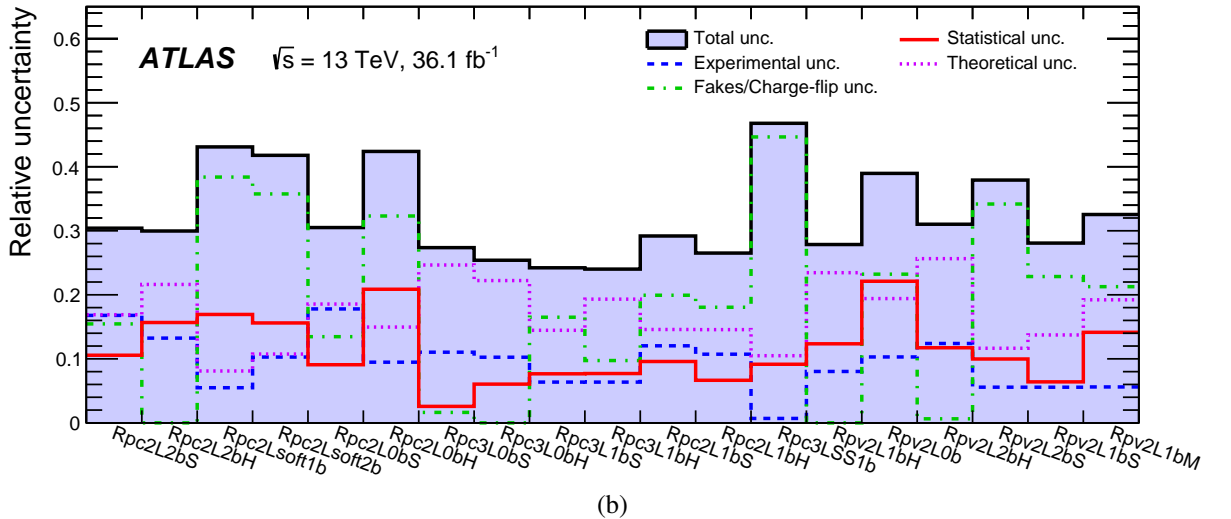


Figure 3: Comparison of (a) the observed and expected event yields in each signal region and (b) the relative uncertainties in the total background yield estimate. For the latter, “statistical uncertainty” corresponds to reducible and irreducible background statistical uncertainties. The background predictions correspond to those presented in Table 5 and the rare category is explained in the text.

6 Results and interpretation

Figure 3(a) shows the event yields for data and the expected background contributions in all signal regions. Detailed information about the yields can be found in Table 5. In all 19 SRs the number of observed data events is consistent with the expected background within the uncertainties. The contributions listed in the rare category are dominated by triboson, tWZ and $t\bar{t}WW$ production¹¹ : the triboson processes generally

¹¹ Contributions from WH , ZH , tZ and $t\bar{t}t$ production never represent more than 20% of the rare background.

dominate in the SRs with no b -jets, while tWZ and $t\bar{t}WW$ dominate in the SRs with one and two b -jets, respectively.

Figure 3(b) summarizes the contributions from the different sources of systematic uncertainty to the total SM background predictions in the signal regions. The uncertainties amount to 25–50% of the total background depending on the signal region, dominated by systematic uncertainties coming from the reducible background or the theory.

In the absence of any significant deviation from the SM predictions, upper limits on possible BSM contributions to the signal regions are derived, as well as exclusion limits on the masses of SUSY particles in the benchmark scenarios of Figure 1. The HistFitter framework [93], which utilizes a profile-likelihood-ratio test [94], is used to establish 95% confidence intervals using the CL_s prescription [95]. The likelihood is built as the product of a Poisson probability density function describing the observed number of events in the signal region and, to constrain the nuisance parameters associated with the systematic uncertainties, Gaussian distributions whose widths correspond to the sizes of these uncertainties; Poisson distributions are used instead for MC simulation statistical uncertainties. Correlations of a given nuisance parameter between the backgrounds and the signal are taken into account when relevant. The hypothesis tests are performed for each of the signal regions independently.

Table 5 presents 95% confidence level (CL) observed (expected) model-independent upper limits on the number of BSM events, S_{obs}^{95} (S_{exp}^{95}), that may contribute to the signal regions. Normalizing these by the integrated luminosity L of the data sample, they can be interpreted as upper limits on the visible BSM cross-section (σ_{vis}), defined as $\sigma_{\text{vis}} = \sigma_{\text{prod}} \times A \times \epsilon = S_{\text{obs}}^{95}/L$, where σ_{prod} is the production cross-section, A the acceptance and ϵ the reconstruction efficiency. The largest deviation of the data from the background prediction corresponds to an excess of 1.5 standard deviations in the Rpv2L1bM SR.

Exclusion limits at 95% CL are also set on the masses of the superpartners involved in the SUSY benchmark scenarios considered. Apart from the NUHM2 model, simplified models are used, corresponding to a single production mode and with 100% branching ratio to a specific decay chain, with the masses of the SUSY particles not involved in the process set to very high values. Figures 4, 5 and 6 show the exclusion limits in all the models considered in Figure 1 and the NUHM2 model. The assumptions about the decay chain considered for the different SUSY particles are stated above each figure. For each region of the signal parameter space, the SR with the best expected sensitivity is chosen.

For the RPC models, the limits set are compared with the existing limits set by other ATLAS SUSY searches [23, 96]. For the models shown in Figure 4, the mass limits on gluinos and bottom squarks are up to 400 GeV higher than the previous limits, reflecting the improvements in the signal region definitions as well as the increase in integrated luminosity. Gluinos with masses up to 1.75 TeV are excluded in scenarios with a light $\tilde{\chi}_1^0$ in Figure 4(a). This limit is extended to 1.87 TeV when $\tilde{\chi}_2^0$ and slepton masses are in-between the gluino and the $\tilde{\chi}_1^0$ masses (Figure 4(c)). More generally, gluino masses below 1.57 TeV and bottom squarks with masses below 700 GeV are excluded in models with a massless LSP. The “compressed” regions, where SUSY particle masses are close to each other, are also better covered and LSP masses up to 1200 and 250 GeV are excluded in the gluino and bottom squark pair-production models, respectively. Of particular interest is the observed exclusion of models producing gluino pairs with an off-shell top quark in the decay (Figure 1(b)), see Figure 4(a). In this case, models are excluded for mass differences between the gluino and neutralino of 205 GeV (only 35 GeV larger than the minimum mass difference for decays into two on-shell W bosons and two b -quarks) for a gluino mass below 0.9 TeV. The Rpc3LSS1b SR allows the exclusion of top squarks with masses below 700 GeV

Signal Region	Rpc2L2bS	Rpc2L2bH	Rpc2Lsoft1b	Rpc2Lsoft2b	Rpc2L0bS	Rpc2L0bH
$t\bar{t}W, t\bar{t}Z\gamma^*$	1.6 ± 0.4	0.44 ± 0.14	1.3 ± 0.4	1.21 ± 0.33	0.82 ± 0.31	0.20 ± 0.10
$t\bar{t}H$	0.43 ± 0.25	0.10 ± 0.06	0.45 ± 0.24	0.36 ± 0.21	0.27 ± 0.15	0.08 ± 0.07
$4t$	0.26 ± 0.13	0.18 ± 0.09	0.09 ± 0.05	0.21 ± 0.11	0.01 ± 0.01	0.02 ± 0.02
Diboson	0.10 ± 0.10	0.04 ± 0.02	0.17 ± 0.09	0.05 ± 0.03	3.1 ± 1.4	1.0 ± 0.5
Rare	0.33 ± 0.18	0.15 ± 0.09	0.18 ± 0.10	0.17 ± 0.10	0.19 ± 0.11	0.17 ± 0.10
Fake/non-prompt leptons	0.5 ± 0.6	0.15 ± 0.15	3.5 ± 2.4	1.7 ± 1.5	1.6 ± 1.0	0.9 ± 0.9
Charge-flip electrons	0.10 ± 0.01	0.02 ± 0.01	0.08 ± 0.02	0.08 ± 0.02	0.05 ± 0.01	0.01 ± 0.01
Total Background	3.3 ± 1.0	1.08 ± 0.32	5.8 ± 2.5	3.8 ± 1.6	6.0 ± 1.8	2.4 ± 1.0
Observed	3	0	4	5	7	3
S_{obs}^{95}	5.5	3.6	6.3	7.7	8.3	6.1
S_{exp}^{95}	$5.6_{-1.5}^{+2.2}$	$3.9_{-0.4}^{+1.4}$	$7.1_{-1.5}^{+2.5}$	$6.2_{-1.5}^{+2.6}$	$7.5_{-1.8}^{+2.6}$	$5.3_{-1.3}^{+2.1}$
$\sigma_{\text{vis}} [\text{fb}]$	0.15	0.10	0.17	0.21	0.23	0.17
$p_0 (Z)$	0.71 (-)	0.91 (-)	0.69 (-)	0.30 (0.5σ)	0.36 (0.4σ)	0.35 (0.4σ)

Signal Region	Rpc3L0bS	Rpc3L0bH	Rpc3L1bS	Rpc3L1bH	Rpc2L1bS	Rpc2L1bH	Rpc3LSS1b
$t\bar{t}W, t\bar{t}Z\gamma^*$	0.98 ± 0.25	0.18 ± 0.08	7.1 ± 1.1	1.54 ± 0.28	4.0 ± 1.0	4.0 ± 0.9	-
$t\bar{t}H$	0.12 ± 0.08	0.03 ± 0.02	1.4 ± 0.7	0.25 ± 0.14	1.3 ± 0.7	1.0 ± 0.6	0.22 ± 0.12
$4t$	0.02 ± 0.01	0.01 ± 0.01	0.7 ± 0.4	0.28 ± 0.15	0.34 ± 0.17	0.54 ± 0.28	-
Diboson	8.9 ± 2.9	2.6 ± 0.8	1.4 ± 0.5	0.48 ± 0.17	0.5 ± 0.3	0.7 ± 0.3	-
Rare	0.7 ± 0.4	0.29 ± 0.16	2.5 ± 1.3	0.9 ± 0.5	0.9 ± 0.5	1.0 ± 0.6	0.12 ± 0.07
Fake/non-prompt leptons	0.23 ± 0.23	0.15 ± 0.15	4.2 ± 3.1	0.5 ± 0.5	2.5 ± 2.2	2.3 ± 1.9	0.9 ± 0.7
Charge-flip electrons	-	-	-	-	0.25 ± 0.04	0.25 ± 0.05	0.39 ± 0.08
Total Background	11.0 ± 3.0	3.3 ± 0.8	17 ± 4	3.9 ± 0.9	9.8 ± 2.9	9.8 ± 2.6	1.6 ± 0.8
Observed	9	3	20	4	14	13	1
S_{obs}^{95}	8.3	5.4	14.7	6.1	13.7	12.4	3.9
S_{exp}^{95}	$9.3_{-2.3}^{+3.1}$	$5.5_{-1.5}^{+2.2}$	$12.6_{-3.4}^{+5.1}$	$5.9_{-1.8}^{+2.2}$	$10.0_{-2.6}^{+3.7}$	$9.7_{-2.6}^{+3.4}$	$4.0_{-0.3}^{+1.8}$
$\sigma_{\text{vis}} [\text{fb}]$	0.23	0.15	0.41	0.17	0.38	0.34	0.11
$p_0 (Z)$	0.72 (-)	0.85 (-)	0.32 (0.5σ)	0.46 (0.1σ)	0.17 (1.0σ)	0.21 (0.8σ)	0.56 (-)

Signal Region	Rpv2L1bH	Rpv2L0b	Rpv2L2bH	Rpv2L2bS	Rpv2L1bS	Rpv2L1bM
$t\bar{t}W, t\bar{t}Z\gamma^*$	0.56 ± 0.14	0.14 ± 0.08	0.56 ± 0.15	6.5 ± 1.3	10.1 ± 1.7	1.4 ± 0.5
$t\bar{t}H$	0.07 ± 0.05	0.02 ± 0.02	0.12 ± 0.07	1.0 ± 0.5	1.9 ± 1.0	0.28 ± 0.15
$4t$	0.34 ± 0.17	0.01 ± 0.01	0.48 ± 0.24	1.6 ± 0.8	1.8 ± 0.9	0.53 ± 0.27
Diboson	0.14 ± 0.06	0.52 ± 0.21	0.04 ± 0.02	0.42 ± 0.16	1.7 ± 0.6	0.42 ± 0.15
Rare	0.29 ± 0.17	0.10 ± 0.06	0.19 ± 0.13	1.5 ± 0.8	2.4 ± 1.2	0.8 ± 0.4
Fake/non-prompt leptons	0.15 ± 0.15	0.18 ± 0.31	0.15 ± 0.15	8 ± 7	6 ± 6	1.3 ± 1.2
Charge-flip electrons	0.02 ± 0.01	0.03 ± 0.02	0.03 ± 0.01	0.46 ± 0.08	0.74 ± 0.12	0.10 ± 0.02
Total Background	1.6 ± 0.4	1.0 ± 0.4	1.6 ± 0.5	19 ± 7	25 ± 7	4.8 ± 1.6
Observed	2	2	1	20	26	9
S_{obs}^{95}	4.8	5.2	3.9	17.5	18.1	11.4
S_{exp}^{95}	$4.1_{-0.4}^{+1.9}$	$4.0_{-0.3}^{+1.7}$	$4.1_{-0.4}^{+1.8}$	$16.8_{-4.2}^{+5.2}$	$17.2_{-4.2}^{+5.9}$	$7.3_{-1.8}^{+2.5}$
$\sigma_{\text{vis}} [\text{fb}]$	0.13	0.14	0.11	0.48	0.50	0.31
$p_0 (Z)$	0.33 (0.4σ)	0.19 (0.9σ)	0.55 (-)	0.48 (0.1σ)	0.44 (0.2σ)	0.07 (1.5σ)

Table 5: Numbers of events observed in the signal regions compared with the expected backgrounds. The rare category is defined in the text. Background categories with yields shown as a “-” do not contribute to a given region (e.g. charge flips in three-lepton regions) or their estimates are below 0.01. The 95% confidence level (CL) upper limits are shown on the observed and expected numbers of BSM events, S_{obs}^{95} and S_{exp}^{95} (as well as the $\pm 1\sigma$ excursions from the expected limit), respectively. The 95% CL upper limits on the visible cross-section (σ_{vis}) are also given. Finally, the p-values (p_0) give the probabilities to observe a deviation from the predicted background at least as large as that in the data. The number of equivalent Gaussian standard deviations (Z) is also shown when $p_0 < 0.5$.

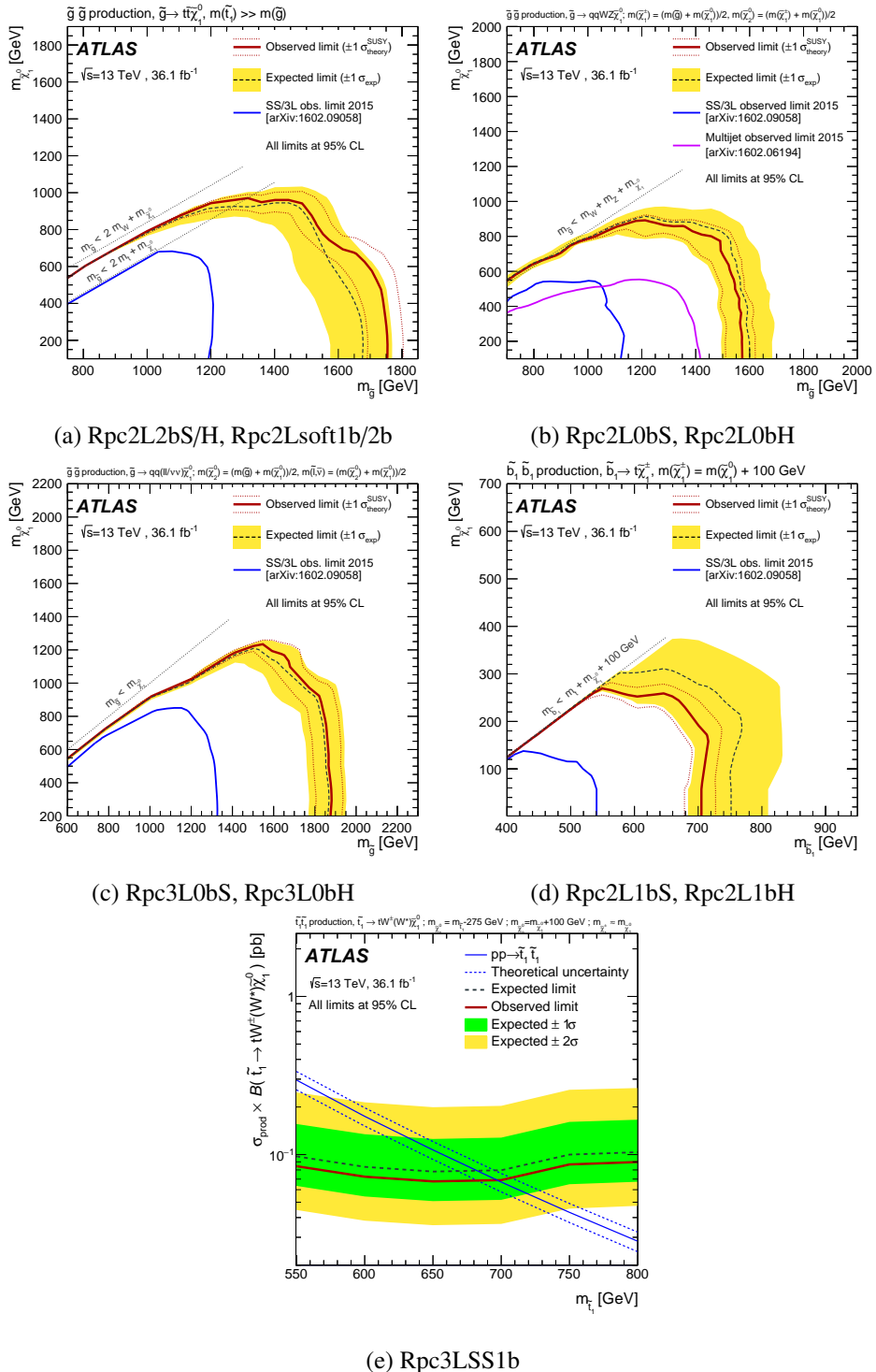


Figure 4: Observed and expected exclusion limits on the \tilde{g} , \tilde{b}_1 , \tilde{t}_1 and $\tilde{\chi}_1^0$ masses in the context of RPC SUSY scenarios with simplified mass spectra. The signal regions used to obtain the limits are specified in the subtitle of each scenario. All limits are computed at 95% CL. The dotted lines around the observed limit illustrate the change in the observed limit as the nominal signal cross-section is scaled up and down by the theoretical uncertainty. The contours of the band around the expected limit are the $\pm 1\sigma$ results ($\pm 2\sigma$ is also considered in Figure (e), including all uncertainties except the theoretical uncertainties in the signal cross-section. In Figures (a)–(d), the diagonal line indicates the kinematic limit for the decays in each specified scenario and results are compared with the observed limits obtained by previous ATLAS searches [23, 96].

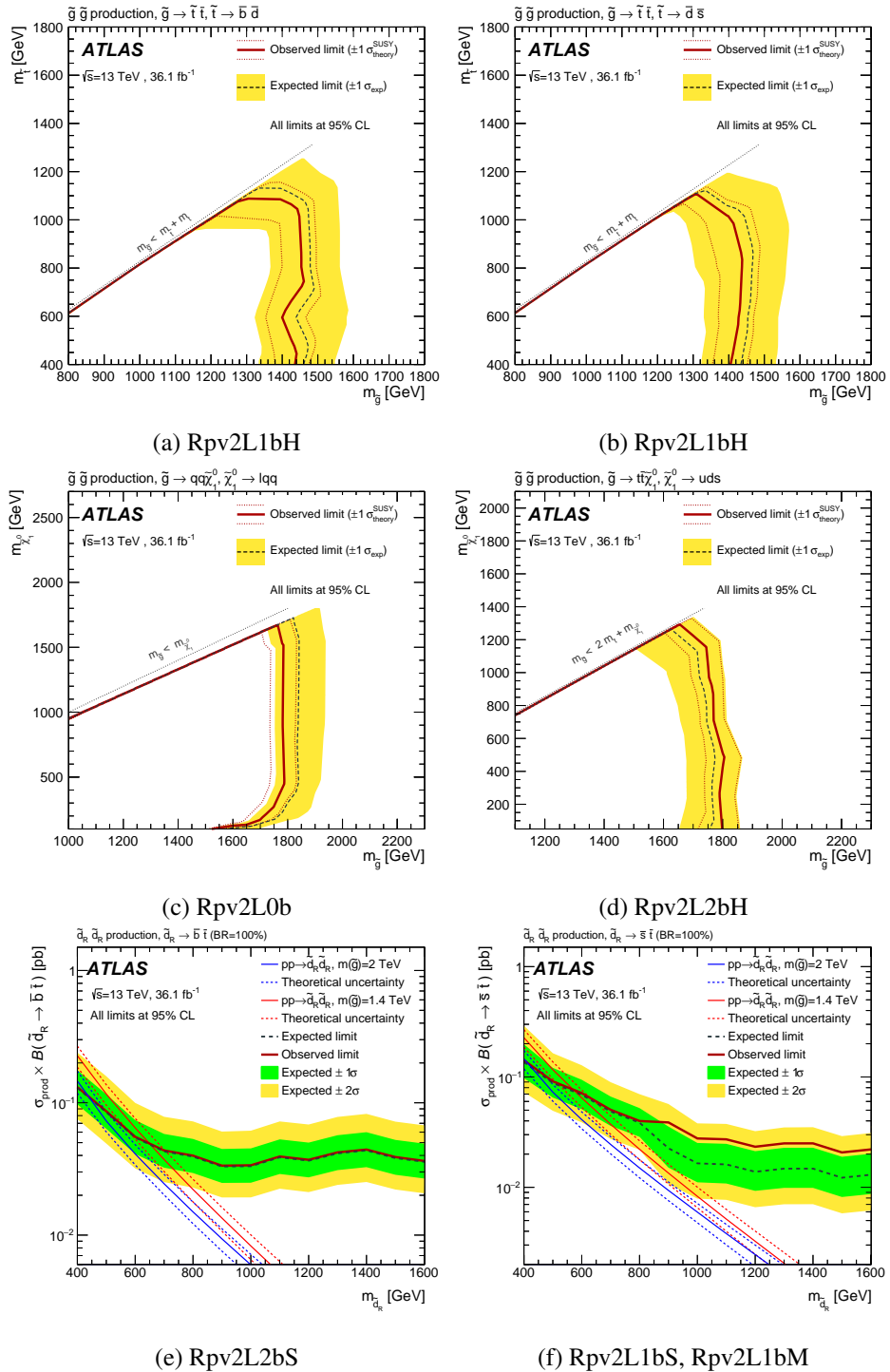


Figure 5: Observed and expected exclusion limits on the \tilde{g} , \tilde{t}_1 , \tilde{d}_R and $\tilde{\chi}_1^0$ masses in the context of RPV SUSY scenarios with simplified mass spectra featuring $\tilde{g}\tilde{g}$ or $\tilde{d}_R\tilde{d}_R$ pair production with exclusive decay modes. The signal regions used to obtain the limits are specified in the subtitle of each scenario. All limits are computed at 95% CL. The dotted lines around the observed limit illustrate the change in the observed limit as the nominal signal cross-section is scaled up and down by the theoretical uncertainty. The contours of the band around the expected limit are the $\pm 1\sigma$ results, including all uncertainties except theoretical uncertainties in the signal cross-section ($\pm 2\sigma$ is also considered in Figures 5(e) and 5(f)). In Figures 5(a)–5(d), the diagonal line indicates the kinematic limit for the decays in each specified scenario. For Figures 5(e) and 5(f), theoretical production cross-sections are shown for two different gluino masses in red (1.4 TeV) and blue (2.0 TeV).

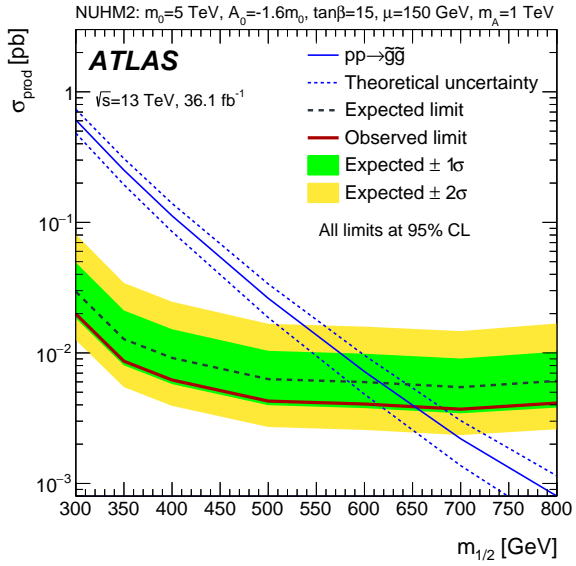


Figure 6: Observed and expected exclusion limits as a function of $m_{1/2}$ in the NUHM2 model [31, 32]. The signal region Rpc2L2bH is used to obtain the limits. The contours of the green (yellow) band around the expected limit are the $\pm 1\sigma$ ($\pm 2\sigma$) results, including all uncertainties. The limits are computed at 95% CL.

when the top squark decays to a top quark and a cascade of electroweakinos $\tilde{\chi}_2^0 \rightarrow \tilde{\chi}_1^\pm W^\mp \rightarrow W^* W^\mp \tilde{\chi}_1^0$ (see Figure 4(e) for the conditions on the sparticle masses).

For the RPV models with gluino pair production (Figures 5(a) – 5(d)), a generic exclusion of gluinos with masses below 1.3 TeV is obtained. Weaker exclusion limits, typically around 500 GeV, are obtained in models with pair production of \tilde{d}_R (Figures 5(e), 5(f)).

Finally, in the NUHM2 model with low fine-tuning, values of the parameter $m_{1/2}$ below 615 GeV are excluded, corresponding to gluino masses below 1500 GeV (Figure 6).

7 Conclusion

A search for supersymmetry in events with two same-sign leptons or at least three leptons, multiple jets, b -jets and large E_T^{miss} and/or large m_{eff} is presented. The analysis is performed with proton–proton collision data at $\sqrt{s} = 13$ TeV collected in 2015 and 2016 with the ATLAS detector at the Large Hadron Collider corresponding to an integrated luminosity of 36.1 fb^{-1} . With no significant excess over the Standard Model prediction observed, results are interpreted in the framework of simplified models featuring gluino and squark production in R -parity-conserving and R -parity-violating scenarios. Lower limits on particle masses are derived at 95% confidence level. In the $\tilde{g}\tilde{g}$ simplified RPC models considered, gluinos with masses up to 1.87 TeV are excluded in scenarios with a light $\tilde{\chi}_1^0$. RPC models with bottom squark masses below 700 GeV are also excluded in a $\tilde{b}_1\tilde{b}_1^*$ simplified model with $\tilde{b}_1 \rightarrow tW^-\tilde{\chi}_1^0$ and a light $\tilde{\chi}_1^0$. In RPV scenarios, masses of down squark-rights are probed up to $m_{\tilde{d}_R} \approx 500$ GeV. All models with gluino masses below 1.3 TeV are excluded, greatly extending the previous exclusion limits obtained within this search. Model-independent limits on the cross-section of a possible signal contribution to the signal regions are set.

Acknowledgements

We thank CERN for the very successful operation of the LHC, as well as the support staff from our institutions without whom ATLAS could not be operated efficiently.

We acknowledge the support of ANPCyT, Argentina; YerPhI, Armenia; ARC, Australia; BMWFW and FWF, Austria; ANAS, Azerbaijan; SSTC, Belarus; CNPq and FAPESP, Brazil; NSERC, NRC and CFI, Canada; CERN; CONICYT, Chile; CAS, MOST and NSFC, China; COLCIENCIAS, Colombia; MSMT CR, MPO CR and VSC CR, Czech Republic; DNRF and DNSRC, Denmark; IN2P3-CNRS, CEA-DSM/IRFU, France; SRNSF, Georgia; BMBF, HGF, and MPG, Germany; GSRT, Greece; RGC, Hong Kong SAR, China; ISF, I-CORE and Benoziyo Center, Israel; INFN, Italy; MEXT and JSPS, Japan; CNRST, Morocco; NWO, Netherlands; RCN, Norway; MNiSW and NCN, Poland; FCT, Portugal; MNE/IFA, Romania; MES of Russia and NRC KI, Russian Federation; JINR; MESTD, Serbia; MSSR, Slovakia; ARRS and MIZŠ, Slovenia; DST/NRF, South Africa; MINECO, Spain; SRC and Wallenberg Foundation, Sweden; SERI, SNSF and Cantons of Bern and Geneva, Switzerland; MOST, Taiwan; TAEK, Turkey; STFC, United Kingdom; DOE and NSF, United States of America. In addition, individual groups and members have received support from BCKDF, the Canada Council, CANARIE, CRC, Compute Canada, FQRNT, and the Ontario Innovation Trust, Canada; EPLANET, ERC, ERDF, FP7, Horizon 2020 and Marie Skłodowska-Curie Actions, European Union; Investissements d’Avenir Labex and Idex, ANR, Région Auvergne and Fondation Partager le Savoir, France; DFG and AvH Foundation, Germany; Herakleitos, Thales and Aristeia programmes co-financed by EU-ESF and the Greek NSRF; BSF, GIF and Minerva, Israel; BRF, Norway; CERCA Programme Generalitat de Catalunya, Generalitat Valenciana, Spain; the Royal Society and Leverhulme Trust, United Kingdom.

The crucial computing support from all WLCG partners is acknowledged gratefully, in particular from CERN, the ATLAS Tier-1 facilities at TRIUMF (Canada), NDGF (Denmark, Norway, Sweden), CC-IN2P3 (France), KIT/GridKA (Germany), INFN-CNAF (Italy), NL-T1 (Netherlands), PIC (Spain), ASGC (Taiwan), RAL (UK) and BNL (USA), the Tier-2 facilities worldwide and large non-WLCG resource providers. Major contributors of computing resources are listed in Ref. [97].

References

- [1] Yu. A. Gol’fand and E. P. Likhtman, *Extension of the algebra of Poincaré group generators and violation of P invariance*, JETP Lett. **13** (1971) 323, [*Pisma Zh. Eksp. Teor. Fiz.* **13** (1971) 452].
- [2] D. V. Volkov and V. P. Akulov, *Is the neutrino a Goldstone particle?*, Phys. Lett. B **46** (1973) 109.
- [3] J. Wess and B. Zumino, *Supergauge transformations in four dimensions*, Nucl. Phys. B **70** (1974) 39.
- [4] J. Wess and B. Zumino, *Supergauge invariant extension of quantum electrodynamics*, Nucl. Phys. B **78** (1974) 1.
- [5] S. Ferrara and B. Zumino, *Supergauge invariant Yang-Mills theories*, Nucl. Phys. B **79** (1974) 413.
- [6] A. Salam and J. Strathdee, *Super-symmetry and non-Abelian gauges*, Phys. Lett. B **51** (1974) 353.

- [7] S. P. Martin, *A Supersymmetry Primer*, *Adv. Ser. Direct. High Energy Phys.* **18** (1998) 1, arXiv: [hep-ph/9709356](#).
- [8] P. Fayet, *Supersymmetry and weak, electromagnetic and strong interactions*, *Phys. Lett. B* **64** (1976) 159.
- [9] P. Fayet, *Spontaneously broken supersymmetric theories of weak, electromagnetic and strong interactions*, *Phys. Lett. B* **69** (1977) 489.
- [10] G. R. Farrar and P. Fayet, *Phenomenology of the production, decay, and detection of new hadronic states associated with supersymmetry*, *Phys. Lett. B* **76** (1978) 575.
- [11] H. Goldberg, *Constraint on the Photino Mass from Cosmology*, *Phys. Rev. Lett.* **50** (1983) 1419, [Erratum: *Phys. Rev. Lett.* **103** (2009) 099905].
- [12] J. Ellis et al., *Supersymmetric relics from the Big Bang*, *Nucl. Phys. B* **238** (1984) 453.
- [13] N. Sakai, *Naturalness in Supersymmetric GUTS*, *Z. Phys. C* **11** (1981) 153.
- [14] S. Dimopoulos, S. Raby and F. Wilczek, *Supersymmetry and the scale of unification*, *Phys. Rev. D* **24** (1981) 1681.
- [15] L. E. Ibáñez and G. G. Ross, *Low-energy predictions in supersymmetric grand unified theories*, *Phys. Lett. B* **105** (1981) 439.
- [16] S. Dimopoulos and H. Georgi, *Softly broken supersymmetry and SU(5)*, *Nucl. Phys. B* **193** (1981) 150.
- [17] R. Barbieri and G. F. Giudice, *Upper bounds on supersymmetric particle masses*, *Nucl. Phys. B* **306** (1988) 63.
- [18] B. de Carlos and J. A. Casas, *One loop analysis of the electroweak breaking in supersymmetric models and the fine tuning problem*, *Phys. Lett. B* **309** (1993) 320, arXiv: [hep-ph/9303291](#).
- [19] K. Inoue, A. Kakuto, H. Komatsu and S. Takeshita, *Aspects of Grand Unified Models with Softly Broken Supersymmetry*, *Prog. Theor. Phys.* **68** (1982) 927, [Erratum: *Prog. Theor. Phys.* **70** (1983) 330].
- [20] J. Ellis and S. Rudaz, *Search for supersymmetry in toponium decays*, *Phys. Lett. B* **128** (1983) 248.
- [21] C. Borschensky et al., *Squark and gluino production cross sections in pp collisions at $\sqrt{s} = 13, 14, 33$ and 100 TeV*, *Eur. Phys. J. C* **74** (2014) 3174, arXiv: [1407.5066 \[hep-ph\]](#).
- [22] ATLAS Collaboration, *The ATLAS Experiment at the CERN Large Hadron Collider*, *JINST* **3** (2008) S08003.
- [23] ATLAS Collaboration, *Search for supersymmetry at $\sqrt{s} = 13$ TeV in final states with jets and two same-sign leptons or three leptons with the ATLAS detector*, *Eur. Phys. J. C* **76** (2016) 259, arXiv: [1602.09058 \[hep-ex\]](#).
- [24] CMS Collaboration, *Search for new physics in same-sign dilepton events in proton–proton collisions at $\sqrt{s} = 13$ TeV*, *Eur. Phys. J. C* **76** (2016) 439, arXiv: [1605.03171 \[hep-ex\]](#).
- [25] CMS Collaboration, *Search for supersymmetry with multiple charged leptons in proton–proton collisions at $\sqrt{s} = 13$ TeV*, arXiv: [1701.06940 \[hep-ex\]](#).

- [26] CMS Collaboration, *Search for physics beyond the standard model in events with two leptons of same sign, missing transverse momentum, and jets in proton–proton collisions at $\sqrt{s} = 13$ TeV*, arXiv: [1704.07323 \[hep-ex\]](#).
- [27] J. Alwall, M.-P. Le, M. Lisanti and J. G. Wacker, *Searching for directly decaying gluinos at the Tevatron*, *Phys. Lett. B* **666** (2008) 34, arXiv: [0803.0019 \[hep-ph\]](#).
- [28] J. Alwall, P. C. Schuster and N. Toro, *Simplified models for a first characterization of new physics at the LHC*, *Phys. Rev. D* **79** (2009) 075020, arXiv: [0810.3921 \[hep-ph\]](#).
- [29] D. Alves et al., *Simplified models for LHC new physics searches*, *J. Phys. G* **39** (2012) 105005, arXiv: [1105.2838 \[hep-ph\]](#).
- [30] P. Huang, A. Ismail, I. Low and C. E. M. Wagner, *Same-sign dilepton excesses and light top squarks*, *Phys. Rev. D* **92** (2015) 075035, arXiv: [1507.01601 \[hep-ph\]](#).
- [31] J. Ellis, T. Falk, K. A. Olive and Y. Santoso, *Exploration of the MSSM with non-universal Higgs masses*, *Nucl. Phys. B* **652** (2003) 259, arXiv: [hep-ph/0210205](#).
- [32] J. Ellis, K. A. Olive and Y. Santoso, *The MSSM parameter space with non-universal Higgs masses*, *Phys. Lett. B* **539** (2002) 107, arXiv: [hep-ph/0204192](#).
- [33] E. Nikolidakis and C. Smith, *Minimal flavor violation, seesaw, and R-parity*, *Phys. Rev. D* **77** (2008) 015021, arXiv: [0710.3129 \[hep-ph\]](#).
- [34] C. Smith, *Minimal flavor violation as an alternative to R-parity*, Proceedings of the 34th International Conference on High Energy Physics (2008), arXiv: [0809.3152 \[hep-ph\]](#).
- [35] C. Csáki, Y. Grossman and B. Heidenreich, *Minimal flavor violation supersymmetry: A natural theory for R-Parity violation*, *Phys. Rev. D* **85** (2012) 095009, arXiv: [1111.1239 \[hep-ph\]](#).
- [36] G. Durieux and C. Smith, *The same-sign top signature of R-parity violation*, *JHEP* **10** (2013) 068, arXiv: [1307.1355 \[hep-ph\]](#).
- [37] J. Berger, M. Perelstein, M. Saelim and P. Tanedo, *The same-sign dilepton signature of RPV/MFV SUSY*, *JHEP* **04** (2013) 077, arXiv: [1302.2146 \[hep-ph\]](#).
- [38] ATLAS Collaboration, *ATLAS Insertable B-Layer Technical Design Report*, ATLAS-TDR-19, 2010, URL: <https://cds.cern.ch/record/1291633>, *ATLAS Insertable B-Layer Technical Design Report Addendum*, ATLAS-TDR-19-ADD-1, 2012, URL: <https://cds.cern.ch/record/1451888>.
- [39] ATLAS Collaboration, *Performance of the ATLAS Trigger System in 2015*, *Eur. Phys. J. C* **77** (2017) 317, arXiv: [1611.09661 \[hep-ex\]](#).
- [40] ATLAS Collaboration, *Luminosity determination in pp collisions at $\sqrt{s} = 8$ TeV using the ATLAS detector at the LHC*, *Eur. Phys. J. C* **76** (2016) 653, arXiv: [1608.03953 \[hep-ex\]](#).

- [41] ATLAS Collaboration, *The ATLAS simulation infrastructure*, Eur. Phys. J. C **70** (2010) 823, arXiv: [1005.4568 \[physics.ins-det\]](#).
- [42] S. Agostinelli et al., GEANT4: A simulation toolkit, Nucl. Instrum. Meth. A **506** (2003) 250.
- [43] ATLAS Collaboration, *The simulation principle and performance of the ATLAS fast calorimeter simulation FastCaloSim*, ATL-PHYS-PUB-2010-013, 2010, URL: <https://cds.cern.ch/record/1300517>.
- [44] T. Sjöstrand, S. Mrenna and P. Skands, *A brief introduction to PYTHIA 8.1*, Comput. Phys. Commun. **178** (2008) 852, arXiv: [0710.3820 \[hep-ph\]](#).
- [45] ATLAS Collaboration, *Summary of ATLAS Pythia 8 tunes*, ATL-PHYS-PUB-2012-003, 2012, URL: <https://cds.cern.ch/record/1474107>.
- [46] A. D. Martin, W. J. Stirling, R. S. Thorne and G. Watt, *Parton distributions for the LHC*, Eur. Phys. J. C **63** (2009) 189, arXiv: [0901.0002 \[hep-ph\]](#).
- [47] D. J. Lange, *The EvtGen particle decay simulation package*, Nucl. Instrum. Meth. A **462** (2001) 152.
- [48] J. Alwall et al., *The automated computation of tree-level and next-to-leading order differential cross sections, and their matching to parton shower simulations*, JHEP **07** (2014) 079, arXiv: [1405.0301 \[hep-ph\]](#).
- [49] R. D. Ball et al., *Parton distributions with LHC data*, Nucl. Phys. B **867** (2013) 244, arXiv: [1207.1303 \[hep-ph\]](#).
- [50] ATLAS Collaboration, *ATLAS Pythia 8 tunes to 7 TeV data*, ATL-PHYS-PUB-2014-021, 2014, URL: <https://cds.cern.ch/record/1966419>.
- [51] G. Corcella et al., *HERWIG 6: an event generator for hadron emission reactions with interfering gluons (including supersymmetric processes)*, JHEP **01** (2001) 010, arXiv: [hep-ph/0011363](#).
- [52] W. Beenakker, R. Höpker, M. Spira and P. Zerwas, *Squark and gluino production at hadron colliders*, Nucl. Phys. B **492** (1997) 51, arXiv: [hep-ph/9610490](#).
- [53] A. Kulesza and L. Motyka, *Threshold Resummation for Squark-Antisquark and Gluino-Pair Production at the LHC*, Phys. Rev. Lett. **102** (2009) 111802, arXiv: [0807.2405 \[hep-ph\]](#).
- [54] A. Kulesza and L. Motyka, *Soft gluon resummation for the production of gluino-gluino and squark-antisquark pairs at the LHC*, Phys. Rev. D **80** (2009) 095004, arXiv: [0905.4749 \[hep-ph\]](#).
- [55] W. Beenakker et al., *Soft-gluon resummation for squark and gluino hadroproduction*, JHEP **12** (2009) 041, arXiv: [0909.4418 \[hep-ph\]](#).
- [56] W. Beenakker et al., *Squark and gluino hadroproduction*, Int. J. Mod. Phys. A **26** (2011) 2637, arXiv: [1105.1110 \[hep-ph\]](#).
- [57] M. Krämer et al., *Supersymmetry production cross sections in pp collisions at $\sqrt{s} = 7 \text{ TeV}$* , (2012), arXiv: [1206.2892 \[hep-ph\]](#).
- [58] J. Pumplin et al., *New Generation of Parton Distributions with Uncertainties from Global QCD Analysis*, JHEP **07** (2002) 012, arXiv: [hep-ph/0201195](#).

- [59] S. Gieseke, C. Röhr and A. Siodmok, *Colour reconnections in Herwig++*, *Eur. Phys. J. C* **72** (2012) 2225, arXiv: [1206.0041 \[hep-ph\]](#).
- [60] D. de Florian et al., *Handbook of LHC Higgs cross sections: 4. Deciphering the nature of the Higgs sector*, (2016), arXiv: [1610.07922 \[hep-ph\]](#).
- [61] T. Gleisberg et al., *Event generation with SHERPA 1.1*, *JHEP* **02** (2009) 007, arXiv: [0811.4622 \[hep-ph\]](#).
- [62] ATLAS Collaboration, *Multi-boson simulation for 13 TeV ATLAS analyses*, ATL-PHYS-PUB-2016-002, 2016, URL: <https://cds.cern.ch/record/2119986>.
- [63] H.-L. Lai et al., *New parton distributions for collider physics*, *Phys. Rev. D* **82** (2010) 074024, arXiv: [1007.2241 \[hep-ph\]](#).
- [64] D. de Florian et al., *Handbook of LHC Higgs cross sections: 2. Differential distributions*, (2012), arXiv: [1201.3084 \[hep-ph\]](#).
- [65] L. Lönnblad and S. Prestel, *Matching tree-level matrix elements with interleaved showers*, *JHEP* **03** (2012) 019, arXiv: [1109.4829 \[hep-ph\]](#).
- [66] W. Beenakker, R. Höpker and M. Spira, *PROSPINO: A Program for the production of supersymmetric particles in next-to-leading order QCD*, (1996), arXiv: [hep-ph/9611232](#).
- [67] ATLAS Collaboration, *Modelling of the $t\bar{t}H$ and $t\bar{t}V(V = W, Z)$ processes for $\sqrt{s} = 13$ TeV ATLAS analyses*, ATL-PHYS-PUB-2016-005, 2016, URL: <https://cds.cern.ch/record/2120826>.
- [68] S. Frixione et al., *Electroweak and QCD corrections to top-pair hadroproduction in association with heavy bosons*, *JHEP* **06** (2015) 184, arXiv: [1504.03446 \[hep-ph\]](#).
- [69] ATLAS Collaboration, *Vertex Reconstruction Performance of the ATLAS Detector at $\sqrt{s} = 13$ TeV*, ATL-PHYS-PUB-2015-026, 2015, URL: <https://cds.cern.ch/record/2037717>.
- [70] ATLAS Collaboration, *Electron efficiency measurements with the ATLAS detector using the 2015 LHC proton–proton collision data*, ATLAS-CONF-2016-024, 2016, URL: <https://cds.cern.ch/record/2157687>.
- [71] ATLAS Collaboration, *Muon reconstruction performance of the ATLAS detector in proton–proton collision data at $\sqrt{s} = 13$ TeV*, *Eur. Phys. J. C* **76** (2016) 292, arXiv: [1603.05598 \[hep-ex\]](#).
- [72] M. Cacciari, G. P. Salam and G. Soyez, *The anti- k_t jet clustering algorithm*, *JHEP* **04** (2008) 063, arXiv: [0802.1189 \[hep-ph\]](#).
- [73] ATLAS Collaboration, *Topological cell clustering in the ATLAS calorimeters and its performance in LHC Run 1*, (2016), arXiv: [1603.02934 \[hep-ex\]](#).
- [74] M. Cacciari and G. P. Salam, *Pileup subtraction using jet areas*, *Phys. Lett. B* **659** (2008) 119, arXiv: [0707.1378 \[hep-ph\]](#).
- [75] ATLAS Collaboration, *Jet energy scale measurements and their systematic uncertainties in proton–proton collisions at $\sqrt{s} = 13$ TeV with the ATLAS detector*, arXiv: [1703.09665 \[hep-ex\]](#).

- [76] ATLAS Collaboration, *Tagging and suppression of pileup jets with the ATLAS detector*, ATLAS-CONF-2014-018, 2014, URL: <https://cds.cern.ch/record/1700870>.
- [77] ATLAS Collaboration, *Performance of b-jet identification in the ATLAS experiment*, JINST **11** (2016) P04008, arXiv: [1512.01094 \[hep-ex\]](https://arxiv.org/abs/1512.01094).
- [78] ATLAS Collaboration, *Expected performance of the ATLAS b-tagging algorithms in Run-2*, ATL-PHYS-PUB-2015-022, 2015, URL: <https://cds.cern.ch/record/2037697>.
- [79] ATLAS Collaboration, *Optimisation of the ATLAS b-tagging performance for the 2016 LHC Run*, ATL-PHYS-PUB-2016-012, 2016, URL: <https://cds.cern.ch/record/2160731>.
- [80] ATLAS Collaboration, *Electron efficiency measurements with the ATLAS detector using 2012 LHC proton–proton collision data*, Eur. Phys. J. C **77** (2017) 195, arXiv: [1612.01456 \[hep-ex\]](https://arxiv.org/abs/1612.01456).
- [81] ATLAS Collaboration, *Measurement of the photon identification efficiencies with the ATLAS detector using LHC Run-1 data*, Eur. Phys. J. C **76** (2016) 666, arXiv: [1606.01813 \[hep-ex\]](https://arxiv.org/abs/1606.01813).
- [82] ATLAS Collaboration, *Performance of missing transverse momentum reconstruction with the ATLAS detector in the first proton–proton collisions at $\sqrt{s} = 13$ TeV*, ATL-PHYS-PUB-2015-027, 2015, URL: <https://cds.cern.ch/record/2037904>.
- [83] ATLAS Collaboration, *Expected performance of missing transverse momentum reconstruction for the ATLAS detector at $\sqrt{s} = 13$ TeV*, ATL-PHYS-PUB-2015-023, 2015, URL: <https://cds.cern.ch/record/2037700>.
- [84] ATLAS Collaboration, *Characterisation and mitigation of beam-induced backgrounds observed in the ATLAS detector during the 2011 proton–proton run*, JINST **8** (2013) P07004, arXiv: [1303.0223 \[hep-ex\]](https://arxiv.org/abs/1303.0223).
- [85] ATLAS Collaboration, *Jet energy measurement and its systematic uncertainty in proton–proton collisions at $\sqrt{s} = 7$ TeV with the ATLAS detector*, Eur. Phys. J. C **75** (2015) 17, arXiv: [1406.0076 \[hep-ex\]](https://arxiv.org/abs/1406.0076).
- [86] ATLAS Collaboration, *Search for supersymmetry at $\sqrt{s}=8$ TeV in final states with jets and two same-sign leptons or three leptons with the ATLAS detector*, JHEP **06** (2014) 035, arXiv: [1404.2500 \[hep-ex\]](https://arxiv.org/abs/1404.2500).
- [87] ATLAS Collaboration, *Search for supersymmetry using events with three leptons, multiple jets, and missing transverse momentum in 13.0 fb^{-1} of pp collisions with the ATLAS detector at $\sqrt{s} = 8$ TeV*, ATLAS-CONF-2012-151, 2012, URL: <https://cds.cern.ch/record/1493490>.
- [88] P. Nason, *A new method for combining NLO QCD with shower Monte Carlo algorithms*, JHEP **11** (2004) 040, arXiv: [hep-ph/0409146](https://arxiv.org/abs/hep-ph/0409146).
- [89] S. Frixione, P. Nason and C. Oleari, *Matching NLO QCD computations with parton shower simulations: the POWHEG method*, JHEP **11** (2007) 070, arXiv: [0709.2092 \[hep-ph\]](https://arxiv.org/abs/0709.2092).
- [90] S. Alioli, P. Nason, C. Oleari and E. Re, *A general framework for implementing NLO calculations in shower Monte Carlo programs: the POWHEG BOX*, JHEP **06** (2010) 043, arXiv: [1002.2581 \[hep-ph\]](https://arxiv.org/abs/1002.2581).
- [91] J. M. Campbell, R. K. Ellis, P. Nason and E. Re, *Top-pair production and decay at NLO matched with parton showers*, JHEP **04** (2015) 114, arXiv: [1412.1828 \[hep-ph\]](https://arxiv.org/abs/1412.1828).

- [92] T. Sjöstrand, S. Mrenna and P. Skands, *PYTHIA 6.4 physics and manual*, JHEP **05** (2006) 026, arXiv: [hep-ph/0603175](#).
- [93] M. Baak et al., *HistFitter software framework for statistical data analysis*, Eur. Phys. J. C **75** (2015) 153, arXiv: [1410.1280 \[hep-ex\]](#).
- [94] G. Cowan, K. Cranmer, E. Gross and O. Vitells, *Asymptotic formulae for likelihood-based tests of new physics*, Eur. Phys. J. C **71** (2011) 1554, [Erratum: Eur. Phys. J. C **73** (2013) 2501], arXiv: [1007.1727 \[physics.data-an\]](#).
- [95] A. L. Read, *Presentation of search results: The CL_s technique*, J. Phys. G **28** (2002) 2693.
- [96] ATLAS Collaboration, *Search for new phenomena in final states with large jet multiplicities and missing transverse momentum with ATLAS using $\sqrt{s} = 13$ TeV proton–proton collisions*, Phys. Lett. B **757** (2016) 334, arXiv: [1602.06194 \[hep-ex\]](#).
- [97] ATLAS Collaboration, *ATLAS computing acknowledgements 2016–2017*, ATL-GEN-PUB-2016-002, 2016, URL: <https://cds.cern.ch/record/2202407>.

The ATLAS Collaboration

M. Aaboud^{137d}, G. Aad⁸⁸, B. Abbott¹¹⁵, O. Abdinov^{12,*}, B. Abeloos¹¹⁹, S.H. Abidi¹⁶¹, O.S. AbouZeid¹³⁹, N.L. Abraham¹⁵¹, H. Abramowicz¹⁵⁵, H. Abreu¹⁵⁴, R. Abreu¹¹⁸, Y. Abulaiti^{148a,148b}, B.S. Acharya^{167a,167b,a}, S. Adachi¹⁵⁷, L. Adamczyk^{41a}, J. Adelman¹¹⁰, M. Adersberger¹⁰², T. Adye¹³³, A.A. Affolder¹³⁹, Y. Afik¹⁵⁴, T. Agatonovic-Jovin¹⁴, C. Agheorghiesei^{28c}, J.A. Aguilar-Saavedra^{128a,128f}, S.P. Ahlen²⁴, F. Ahmadov^{68,b}, G. Aielli^{135a,135b}, S. Akatsuka⁷¹, H. Akerstedt^{148a,148b}, T.P.A. Åkesson⁸⁴, E. Akilli⁵², A.V. Akimov⁹⁸, G.L. Alberghi^{22a,22b}, J. Albert¹⁷², P. Albicocco⁵⁰, M.J. Alconada Verzini⁷⁴, S.C. Alderweireldt¹⁰⁸, M. Aleksa³², I.N. Aleksandrov⁶⁸, C. Alexa^{28b}, G. Alexander¹⁵⁵, T. Alexopoulos¹⁰, M. Alhroob¹¹⁵, B. Ali¹³⁰, M. Aliev^{76a,76b}, G. Alimonti^{94a}, J. Alison³³, S.P. Alkire³⁸, B.M.M. Allbrooke¹⁵¹, B.W. Allen¹¹⁸, P.P. Allport¹⁹, A. Aloisio^{106a,106b}, A. Alonso³⁹, F. Alonso⁷⁴, C. Alpigiani¹⁴⁰, A.A. Alshehri⁵⁶, M.I. Alstaty⁸⁸, B. Alvarez Gonzalez³², D. Álvarez Piqueras¹⁷⁰, M.G. Alvaggi^{106a,106b}, B.T. Amadio¹⁶, Y. Amaral Coutinho^{26a}, C. Amelung²⁵, D. Amidei⁹², S.P. Amor Dos Santos^{128a,128c}, S. Amoroso³², G. Amundsen²⁵, C. Anastopoulos¹⁴¹, L.S. Ancu⁵², N. Andari¹⁹, T. Andeen¹¹, C.F. Anders^{60b}, J.K. Anders⁷⁷, K.J. Anderson³³, A. Andreazza^{94a,94b}, V. Andrei^{60a}, S. Angelidakis³⁷, I. Angelozzi¹⁰⁹, A. Angerami³⁸, A.V. Anisenkov^{111,c}, N. Anjos¹³, A. Annovi^{126a,126b}, C. Antel^{60a}, M. Antonelli⁵⁰, A. Antonov^{100,*}, D.J. Antrim¹⁶⁶, F. Anulli^{134a}, M. Aoki⁶⁹, L. Aperio Bella³², G. Arabidze⁹³, Y. Arai⁶⁹, J.P. Araque^{128a}, V. Araujo Ferraz^{26a}, A.T.H. Arce⁴⁸, R.E. Ardell⁸⁰, F.A. Arduh⁷⁴, J-F. Arguin⁹⁷, S. Argyropoulos⁶⁶, M. Arik^{20a}, A.J. Armbruster³², L.J. Armitage⁷⁹, O. Arnaez¹⁶¹, H. Arnold⁵¹, M. Arratia³⁰, O. Arslan²³, A. Artamonov^{99,*}, G. Artoni¹²², S. Artz⁸⁶, S. Asai¹⁵⁷, N. Asbah⁴⁵, A. Ashkenazi¹⁵⁵, L. Asquith¹⁵¹, K. Assamagan²⁷, R. Astalos^{146a}, M. Atkinson¹⁶⁹, N.B. Atlay¹⁴³, K. Augsten¹³⁰, G. Avolio³², B. Axen¹⁶, M.K. Ayoub¹¹⁹, G. Azuelos^{97,d}, A.E. Baas^{60a}, M.J. Baca¹⁹, H. Bachacou¹³⁸, K. Bachas^{76a,76b}, M. Backes¹²², P. Bagnaia^{134a,134b}, M. Bahmani⁴², H. Bahrasemani¹⁴⁴, J.T. Baines¹³³, M. Bajic³⁹, O.K. Baker¹⁷⁹, E.M. Baldin^{111,c}, P. Balek¹⁷⁵, F. Balli¹³⁸, W.K. Balunas¹²⁴, E. Banas⁴², A. Bandyopadhyay²³, Sw. Banerjee^{176,e}, A.A.E. Bannoura¹⁷⁸, L. Barak¹⁵⁵, E.L. Barberio⁹¹, D. Barberis^{53a,53b}, M. Barbero⁸⁸, T. Barillari¹⁰³, M-S Barisits³², J.T. Barkeloo¹¹⁸, T. Barklow¹⁴⁵, N. Barlow³⁰, S.L. Barnes^{36c}, B.M. Barnett¹³³, R.M. Barnett¹⁶, Z. Barnovska-Blenessy^{36a}, A. Baroncelli^{136a}, G. Barone²⁵, A.J. Barr¹²², L. Barranco Navarro¹⁷⁰, F. Barreiro⁸⁵, J. Barreiro Guimarães da Costa^{35a}, R. Bartoldus¹⁴⁵, A.E. Barton⁷⁵, P. Bartos^{146a}, A. Basalaev¹²⁵, A. Bassalat^{119,f}, R.L. Bates⁵⁶, S.J. Batista¹⁶¹, J.R. Batley³⁰, M. Battaglia¹³⁹, M. Bauce^{134a,134b}, F. Bauer¹³⁸, H.S. Bawa^{145,g}, J.B. Beacham¹¹³, M.D. Beattie⁷⁵, T. Beau⁸³, P.H. Beauchemin¹⁶⁵, P. Bechtle²³, H.P. Beck^{18,h}, H.C. Beck⁵⁷, K. Becker¹²², M. Becker⁸⁶, C. Becot¹¹², A.J. Beddall^{20e}, A. Beddall^{20b}, V.A. Bednyakov⁶⁸, M. Bedognetti¹⁰⁹, C.P. Bee¹⁵⁰, T.A. Beermann³², M. Begalli^{26a}, M. Begel²⁷, J.K. Behr⁴⁵, A.S. Bell⁸¹, G. Bella¹⁵⁵, L. Bellagamba^{22a}, A. Bellerive³¹, M. Bellomo¹⁵⁴, K. Belotskiy¹⁰⁰, O. Beltramello³², N.L. Belyaev¹⁰⁰, O. Benary^{155,*}, D. Bencheikoun^{137a}, M. Bender¹⁰², K. Bendtz^{148a,148b}, N. Benekos¹⁰, Y. Benhammou¹⁵⁵, E. Benhar Noccioli¹⁷⁹, J. Benitez⁶⁶, D.P. Benjamin⁴⁸, M. Benoit⁵², J.R. Bensinger²⁵, S. Bentvelsen¹⁰⁹, L. Beresford¹²², M. Beretta⁵⁰, D. Berge¹⁰⁹, E. Bergeaas Kuutmann¹⁶⁸, N. Berger⁵, J. Beringer¹⁶, S. Berlendis⁵⁸, N.R. Bernard⁸⁹, G. Bernardi⁸³, C. Bernius¹⁴⁵, F.U. Bernlochner²³, T. Berry⁸⁰, P. Berta⁸⁶, C. Bertella^{35a}, G. Bertoli^{148a,148b}, F. Bertolucci^{126a,126b}, I.A. Bertram⁷⁵, C. Bertsche⁴⁵, D. Bertsche¹¹⁵, G.J. Besjes³⁹, O. Bessidskaia Bylund^{148a,148b}, M. Bessner⁴⁵, N. Besson¹³⁸, A. Bethani⁸⁷, S. Bethke¹⁰³, A.J. Bevan⁷⁹, J. Beyer¹⁰³, R.M. Bianchi¹²⁷, O. Biebel¹⁰², D. Biedermann¹⁷, R. Bielski⁸⁷, K. Bierwagen⁸⁶, N.V. Biesuz^{126a,126b}, M. Biglietti^{136a}, T.R.V. Billoud⁹⁷, H. Bilokon⁵⁰, M. Bindi⁵⁷, A. Bingul^{20b}, C. Bini^{134a,134b}, S. Biondi^{22a,22b}, T. Bisanz⁵⁷, C. Bittrich⁴⁷, D.M. Bjergaard⁴⁸, J.E. Black¹⁴⁵, K.M. Black²⁴, R.E. Blair⁶, T. Blazek^{146a}, I. Bloch⁴⁵, C. Blocker²⁵, A. Blue⁵⁶, W. Blum^{86,*},

U. Blumenschein⁷⁹, S. Blunier^{34a}, G.J. Bobbink¹⁰⁹, V.S. Bobrovnikov^{111,c}, S.S. Bocchetta⁸⁴, A. Bocci⁴⁸, C. Bock¹⁰², M. Boehler⁵¹, D. Boerner¹⁷⁸, D. Bogavac¹⁰², A.G. Bogdanchikov¹¹¹, C. Bohm^{148a}, V. Boisvert⁸⁰, P. Bokan^{168,i}, T. Bold^{41a}, A.S. Boldyrev¹⁰¹, A.E. Bolz^{60b}, M. Bomben⁸³, M. Bona⁷⁹, M. Boonekamp¹³⁸, A. Borisov¹³², G. Borissov⁷⁵, J. Bortfeldt³², D. Bortoletto¹²², V. Bortolotto^{62a}, D. Boscherini^{22a}, M. Bosman¹³, J.D. Bossio Sola²⁹, J. Boudreau¹²⁷, J. Bouffard², E.V. Bouhova-Thacker⁷⁵, D. Boumediene³⁷, C. Bourdarios¹¹⁹, S.K. Boutle⁵⁶, A. Boveia¹¹³, J. Boyd³², I.R. Boyko⁶⁸, J. Bracinik¹⁹, A. Brandt⁸, G. Brandt⁵⁷, O. Brandt^{60a}, U. Bratzler¹⁵⁸, B. Brau⁸⁹, J.E. Brau¹¹⁸, W.D. Breaden Madden⁵⁶, K. Brendlinger⁴⁵, A.J. Brennan⁹¹, L. Brenner¹⁰⁹, R. Brenner¹⁶⁸, S. Bressler¹⁷⁵, D.L. Briglin¹⁹, T.M. Bristow⁴⁹, D. Britton⁵⁶, D. Britzger⁴⁵, F.M. Brochu³⁰, I. Brock²³, R. Brock⁹³, G. Brooijmans³⁸, T. Brooks⁸⁰, W.K. Brooks^{34b}, J. Brosamer¹⁶, E. Brost¹¹⁰, J.H. Broughton¹⁹, P.A. Bruckman de Renstrom⁴², D. Bruncko^{146b}, A. Bruni^{22a}, G. Bruni^{22a}, L.S. Bruni¹⁰⁹, BH Brunt³⁰, M. Bruschi^{22a}, N. Bruscino²³, P. Bryant³³, L. Bryngemark⁴⁵, T. Buanes¹⁵, Q. Buat¹⁴⁴, P. Buchholz¹⁴³, A.G. Buckley⁵⁶, I.A. Budagov⁶⁸, F. Buehrer⁵¹, M.K. Bugge¹²¹, O. Bulekov¹⁰⁰, D. Bullock⁸, T.J. Burch¹¹⁰, S. Burdin⁷⁷, C.D. Burgard⁵¹, A.M. Burger⁵, B. Burghgrave¹¹⁰, K. Burkhardt⁴², S. Burke¹³³, I. Burmeister⁴⁶, J.T.P. Burr¹²², E. Busato³⁷, D. Büscher⁵¹, V. Büscher⁸⁶, P. Bussey⁵⁶, J.M. Butler²⁴, C.M. Buttar⁵⁶, J.M. Butterworth⁸¹, P. Butti³², W. Buttlinger²⁷, A. Buzatu¹⁵³, A.R. Buzykaev^{111,c}, S. Cabrera Urbán¹⁷⁰, D. Caforio¹³⁰, V.M. Cairo^{40a,40b}, O. Cakir^{4a}, N. Calace⁵², P. Calafuria¹⁶, A. Calandri⁸⁸, G. Calderini⁸³, P. Calfayan⁶⁴, G. Callea^{40a,40b}, L.P. Caloba^{26a}, S. Calvente Lopez⁸⁵, D. Calvet³⁷, S. Calvet³⁷, T.P. Calvet⁸⁸, R. Camacho Toro³³, S. Camarda³², P. Camarri^{135a,135b}, D. Cameron¹²¹, R. Caminal Armadans¹⁶⁹, C. Camincher⁵⁸, S. Campana³², M. Campanelli⁸¹, A. Camplani^{94a,94b}, A. Campoverde¹⁴³, V. Canale^{106a,106b}, M. Cano Bret^{36c}, J. Cantero¹¹⁶, T. Cao¹⁵⁵, M.D.M. Capeans Garrido³², I. Caprini^{28b}, M. Caprini^{28b}, M. Capua^{40a,40b}, R.M. Carbone³⁸, R. Cardarelli^{135a}, F. Cardillo⁵¹, I. Carli¹³¹, T. Carli³², G. Carlino^{106a}, B.T. Carlson¹²⁷, L. Carminati^{94a,94b}, R.M.D. Carney^{148a,148b}, S. Caron¹⁰⁸, E. Carquin^{34b}, S. Carrá^{94a,94b}, G.D. Carrillo-Montoya³², D. Casadei¹⁹, M.P. Casado^{13,j}, M. Casolino¹³, D.W. Casper¹⁶⁶, R. Castelijn¹⁰⁹, V. Castillo Gimenez¹⁷⁰, N.F. Castro^{128a,k}, A. Catinaccio³², J.R. Catmore¹²¹, A. Cattai³², J. Caudron²³, V. Cavalieri¹⁶⁹, E. Cavallaro¹³, D. Cavalli^{94a}, M. Cavalli-Sforza¹³, V. Cavasinni^{126a,126b}, E. Celebi^{20d}, F. Ceradini^{136a,136b}, L. Cerdà Alberich¹⁷⁰, A.S. Cerqueira^{26b}, A. Cerri¹⁵¹, L. Cerrito^{135a,135b}, F. Cerutti¹⁶, A. Cervelli¹⁸, S.A. Cetin^{20d}, A. Chafaq^{137a}, D. Chakraborty¹¹⁰, S.K. Chan⁵⁹, W.S. Chan¹⁰⁹, Y.L. Chan^{62a}, P. Chang¹⁶⁹, J.D. Chapman³⁰, D.G. Charlton¹⁹, C.C. Chau³¹, C.A. Chavez Barajas¹⁵¹, S. Che¹¹³, S. Cheatham^{167a,167c}, A. Chegwidden⁹³, S. Chekanov⁶, S.V. Chekulaev^{163a}, G.A. Chelkov^{68,l}, M.A. Chelstowska³², C. Chen⁶⁷, H. Chen²⁷, J. Chen^{36a}, S. Chen^{35b}, S. Chen¹⁵⁷, X. Chen^{35c,m}, Y. Chen⁷⁰, H.C. Cheng⁹², H.J. Cheng^{35a,35d}, A. Cheplakov⁶⁸, E. Cheremushkina¹³², R. Cherkaooui El Moursli^{137e}, E. Cheu⁷, K. Cheung⁶³, L. Chevalier¹³⁸, V. Chiarella⁵⁰, G. Chiarelli^{126a,126b}, G. Chiodini^{76a}, A.S. Chisholm³², A. Chitan^{28b}, Y.H. Chiu¹⁷², M.V. Chizhov⁶⁸, K. Choi⁶⁴, A.R. Chomont³⁷, S. Chouridou¹⁵⁶, Y.S. Chow^{62a}, V. Christodoulou⁸¹, M.C. Chu^{62a}, J. Chudoba¹²⁹, A.J. Chuinard⁹⁰, J.J. Chwastowski⁴², L. Chytka¹¹⁷, A.K. Ciftci^{4a}, D. Cinca⁴⁶, V. Cindro⁷⁸, I.A. Cioara²³, C. Ciocca^{22a,22b}, A. Ciocio¹⁶, F. Cirotto^{106a,106b}, Z.H. Citron¹⁷⁵, M. Citterio^{94a}, M. Ciubancan^{28b}, A. Clark⁵², B.L. Clark⁵⁹, M.R. Clark³⁸, P.J. Clark⁴⁹, R.N. Clarke¹⁶, C. Clement^{148a,148b}, Y. Coadou⁸⁸, M. Cobal^{167a,167c}, A. Coccaro⁵², J. Cochran⁶⁷, L. Colasurdo¹⁰⁸, B. Cole³⁸, A.P. Colijn¹⁰⁹, J. Collot⁵⁸, T. Colombo¹⁶⁶, P. Conde Muiño^{128a,128b}, E. Coniavitis⁵¹, S.H. Connell^{147b}, I.A. Connelly⁸⁷, S. Constantinescu^{28b}, G. Conti³², F. Conventi^{106a,n}, M. Cooke¹⁶, A.M. Cooper-Sarkar¹²², F. Cormier¹⁷¹, K.J.R. Cormier¹⁶¹, M. Corradi^{134a,134b}, F. Corriveau^{90,o}, A. Cortes-Gonzalez³², G. Cortiana¹⁰³, G. Costa^{94a}, M.J. Costa¹⁷⁰, D. Costanzo¹⁴¹, G. Cottin³⁰, G. Cowan⁸⁰, B.E. Cox⁸⁷, K. Cranmer¹¹², S.J. Crawley⁵⁶, R.A. Creager¹²⁴, G. Cree³¹, S. Crépé-Renaudin⁵⁸, F. Crescioli⁸³, W.A. Cribbs^{148a,148b}, M. Cristinziani²³, V. Croft¹⁰⁸, G. Crosetti^{40a,40b}, A. Cueto⁸⁵, T. Cuhadar Donszelmann¹⁴¹, A.R. Cukierman¹⁴⁵, J. Cummings¹⁷⁹,

M. Curatolo⁵⁰, J. Cúth⁸⁶, S. Czekierda⁴², P. Czodrowski³², G. D'amen^{22a,22b}, S. D'Auria⁵⁶,
 L. D'eramo⁸³, M. D'Onofrio⁷⁷, M.J. Da Cunha Sargedas De Sousa^{128a,128b}, C. Da Via⁸⁷,
 W. Dabrowski^{41a}, T. Dado^{146a}, T. Dai⁹², O. Dale¹⁵, F. Dallaire⁹⁷, C. Dallapiccola⁸⁹, M. Dam³⁹,
 J.R. Dandoy¹²⁴, M.F. Daneri²⁹, N.P. Dang¹⁷⁶, A.C. Daniells¹⁹, N.S. Dann⁸⁷, M. Danninger¹⁷¹,
 M. Dano Hoffmann¹³⁸, V. Dao¹⁵⁰, G. Darbo^{53a}, S. Darmora⁸, J. Dassoulas³, A. Dattagupta¹¹⁸,
 T. Daubney⁴⁵, W. Davey²³, C. David⁴⁵, T. Davidek¹³¹, D.R. Davis⁴⁸, P. Davison⁸¹, E. Dawe⁹¹,
 I. Dawson¹⁴¹, K. De⁸, R. de Asmundis^{106a}, A. De Benedetti¹¹⁵, S. De Castro^{22a,22b}, S. De Cecco⁸³,
 N. De Groot¹⁰⁸, P. de Jong¹⁰⁹, H. De la Torre⁹³, F. De Lorenzi⁶⁷, A. De Maria⁵⁷, D. De Pedis^{134a},
 A. De Salvo^{134a}, U. De Sanctis^{135a,135b}, A. De Santo¹⁵¹, K. De Vasconcelos Corga⁸⁸,
 J.B. De Vivie De Regie¹¹⁹, R. Debbe²⁷, C. Debenedetti¹³⁹, D.V. Dedovich⁶⁸, N. Dehghanian³,
 I. Deigaard¹⁰⁹, M. Del Gaudio^{40a,40b}, J. Del Peso⁸⁵, D. Delgove¹¹⁹, F. Deliot¹³⁸, C.M. Delitzsch⁷,
 A. Dell'Acqua³², L. Dell'Asta²⁴, M. Dell'Orso^{126a,126b}, M. Della Pietra^{106a,106b}, D. della Volpe⁵²,
 M. Delmastro⁵, C. Delporte¹¹⁹, P.A. Delsart⁵⁸, D.A. DeMarco¹⁶¹, S. Demers¹⁷⁹, M. Demichev⁶⁸,
 A. Demilly⁸³, S.P. Denisov¹³², D. Denysiuk¹³⁸, D. Derendarz⁴², J.E. Derkaoui^{137d}, F. Derue⁸³,
 P. Dervan⁷⁷, K. Desch²³, C. Deterre⁴⁵, K. Dette¹⁶¹, M.R. Devesa²⁹, P.O. Deviveiros³², A. Dewhurst¹³³,
 S. Dhaliwal²⁵, F.A. Di Bello⁵², A. Di Ciaccio^{135a,135b}, L. Di Ciaccio⁵, W.K. Di Clemente¹²⁴,
 C. Di Donato^{106a,106b}, A. Di Girolamo³², B. Di Girolamo³², B. Di Micco^{136a,136b}, R. Di Nardo³²,
 K.F. Di Petrillo⁵⁹, A. Di Simone⁵¹, R. Di Sipio¹⁶¹, D. Di Valentino³¹, C. Diaconu⁸⁸, M. Diamond¹⁶¹,
 F.A. Dias³⁹, M.A. Diaz^{34a}, E.B. Diehl⁹², J. Dietrich¹⁷, S. Díez Cornell⁴⁵, A. Dimitrievska¹⁴,
 J. Dingfelder²³, P. Dita^{28b}, S. Dita^{28b}, F. Dittus³², F. Djama⁸⁸, T. Djobava^{54b}, J.I. Djuvsland^{60a},
 M.A.B. do Vale^{26c}, D. Dobos³², M. Dobre^{28b}, C. Doglioni⁸⁴, J. Dolejsi¹³¹, Z. Dolezal¹³¹,
 M. Donadelli^{26d}, S. Donati^{126a,126b}, P. Dondero^{123a,123b}, J. Donini³⁷, J. Dopke¹³³, A. Doria^{106a},
 M.T. Dova⁷⁴, A.T. Doyle⁵⁶, E. Drechsler⁵⁷, M. Dris¹⁰, Y. Du^{36b}, J. Duarte-Campderros¹⁵⁵,
 A. Dubreuil⁵², E. Duchovni¹⁷⁵, G. Duckeck¹⁰², A. Ducourthial⁸³, O.A. Ducu^{97,p}, D. Duda¹⁰⁹,
 A. Dudarev³², A.Chr. Dudder⁸⁶, E.M. Duffield¹⁶, L. Duflot¹¹⁹, M. Dührssen³², C. Dulsen¹⁷⁸,
 M. Dumancic¹⁷⁵, A.E. Dumitriu^{28b}, A.K. Duncan⁵⁶, M. Dunford^{60a}, H. Duran Yildiz^{4a}, M. Düren⁵⁵,
 A. Durglishvili^{54b}, D. Duschinger⁴⁷, B. Dutta⁴⁵, D. Duvnjak¹, M. Dyndal⁴⁵, B.S. Dziedzic⁴²,
 C. Eckardt⁴⁵, K.M. Ecker¹⁰³, R.C. Edgar⁹², T. Eifert³², G. Eigen¹⁵, K. Einsweiler¹⁶, T. Ekelof¹⁶⁸,
 M. El Kacimi^{137c}, R. El Kosseifi⁸⁸, V. Ellajosyula⁸⁸, M. Ellert¹⁶⁸, S. Elles⁵, F. Ellinghaus¹⁷⁸,
 A.A. Elliot¹⁷², N. Ellis³², J. Elmsheuser²⁷, M. Elsing³², D. Emeliyanov¹³³, Y. Enari¹⁵⁷, O.C. Endner⁸⁶,
 J.S. Ennis¹⁷³, J. Erdmann⁴⁶, A. Ereditato¹⁸, M. Ernst²⁷, S. Errede¹⁶⁹, M. Escalier¹¹⁹, C. Escobar¹⁷⁰,
 B. Esposito⁵⁰, O. Estrada Pastor¹⁷⁰, A.I. Etienne¹³⁸, E. Etzion¹⁵⁵, H. Evans⁶⁴, A. Ezhilov¹²⁵,
 M. Ezzi^{137e}, F. Fabbri^{22a,22b}, L. Fabbri^{22a,22b}, V. Fabiani¹⁰⁸, G. Facini⁸¹, R.M. Fakhrutdinov¹³²,
 S. Falciano^{134a}, R.J. Falla⁸¹, J. Faltova³², Y. Fang^{35a}, M. Fanti^{94a,94b}, A. Farbin⁸, A. Farilla^{136a},
 C. Farina¹²⁷, E.M. Farina^{123a,123b}, T. Farooque⁹³, S. Farrell¹⁶, S.M. Farrington¹⁷³, P. Farthouat³²,
 F. Fassi^{137e}, P. Fassnacht³², D. Fassouliotis⁹, M. Faucci Giannelli⁴⁹, A. Favareto^{53a,53b}, W.J. Fawcett¹²²,
 L. Fayard¹¹⁹, O.L. Fedin^{125,q}, W. Fedorko¹⁷¹, S. Feigl¹²¹, L. Feligioni⁸⁸, C. Feng^{36b}, E.J. Feng³²,
 H. Feng⁹², M.J. Fenton⁵⁶, A.B. Fenyuk¹³², L. Feremenga⁸, P. Fernandez Martinez¹⁷⁰,
 S. Fernandez Perez¹³, J. Ferrando⁴⁵, A. Ferrari¹⁶⁸, P. Ferrari¹⁰⁹, R. Ferrari^{123a}, D.E. Ferreira de Lima^{60b},
 A. Ferrer¹⁷⁰, D. Ferrere⁵², C. Ferretti⁹², F. Fiedler⁸⁶, A. Filipčič⁷⁸, M. Filipuzzi⁴⁵, F. Filthaut¹⁰⁸,
 M. Fincke-Keeler¹⁷², K.D. Finelli¹⁵², M.C.N. Fiolhais^{128a,128c,r}, L. Fiorini¹⁷⁰, A. Fischer², C. Fischer¹³,
 J. Fischer¹⁷⁸, W.C. Fisher⁹³, N. Flasche⁴⁵, I. Fleck¹⁴³, P. Fleischmann⁹², R.R.M. Fletcher¹²⁴,
 T. Flick¹⁷⁸, B.M. Flier¹⁰², L.R. Flores Castillo^{62a}, M.J. Flowerdew¹⁰³, G.T. Forcolin⁸⁷, A. Formica¹³⁸,
 F.A. Förster¹³, A. Forti⁸⁷, A.G. Foster¹⁹, D. Fournier¹¹⁹, H. Fox⁷⁵, S. Fracchia¹⁴¹, P. Francavilla⁸³,
 M. Franchini^{22a,22b}, S. Franchino^{60a}, D. Francis³², L. Franconi¹²¹, M. Franklin⁵⁹, M. Frate¹⁶⁶,
 M. Fraternali^{123a,123b}, D. Freeborn⁸¹, S.M. Fressard-Batraneanu³², B. Freund⁹⁷, D. Froidevaux³²,
 J.A. Frost¹²², C. Fukunaga¹⁵⁸, T. Fusayasu¹⁰⁴, J. Fuster¹⁷⁰, C. Gabaldon⁵⁸, O. Gabizon¹⁵⁴,

A. Gabrielli^{22a,22b}, A. Gabrielli¹⁶, G.P. Gach^{41a}, S. Gadatsch³², S. Gadomski⁸⁰, G. Gagliardi^{53a,53b}, L.G. Gagnon⁹⁷, C. Galea¹⁰⁸, B. Galhardo^{128a,128c}, E.J. Gallas¹²², B.J. Gallop¹³³, P. Gallus¹³⁰, G. Galster³⁹, K.K. Gan¹¹³, S. Ganguly³⁷, Y. Gao⁷⁷, Y.S. Gao^{145,g}, F.M. Garay Walls^{34a}, C. García¹⁷⁰, J.E. García Navarro¹⁷⁰, J.A. García Pascual^{35a}, M. Garcia-Sciveres¹⁶, R.W. Gardner³³, N. Garelli¹⁴⁵, V. Garonne¹²¹, A. Gascon Bravo⁴⁵, K. Gasnikova⁴⁵, C. Gatti⁵⁰, A. Gaudiello^{53a,53b}, G. Gaudio^{123a}, I.L. Gavrilenko⁹⁸, C. Gay¹⁷¹, G. Gaycken²³, E.N. Gazis¹⁰, C.N.P. Gee¹³³, J. Geisen⁵⁷, M. Geisen⁸⁶, M.P. Geisler^{60a}, K. Gellerstedt^{148a,148b}, C. Gemme^{53a}, M.H. Genest⁵⁸, C. Geng⁹², S. Gentile^{134a,134b}, C. Gentsos¹⁵⁶, S. George⁸⁰, D. Gerbaudo¹³, A. Gershon¹⁵⁵, G. Geßner⁴⁶, S. Ghasemi¹⁴³, M. Ghneimat²³, B. Giacobbe^{22a}, S. Giagu^{134a,134b}, N. Giangiacomi^{22a,22b}, P. Giannetti^{126a,126b}, S.M. Gibson⁸⁰, M. Gignac¹⁷¹, M. Gilchriese¹⁶, D. Gillberg³¹, G. Gilles¹⁷⁸, D.M. Gingrich^{3,d}, M.P. Giordani^{167a,167c}, F.M. Giorgi^{22a}, P.F. Giraud¹³⁸, P. Giromini⁵⁹, G. Giugliarelli^{167a,167c}, D. Giugni^{94a}, F. Giuli¹²², C. Giuliani¹⁰³, M. Giuliani^{60b}, B.K. Gjelsten¹²¹, S. Gkaitatzis¹⁵⁶, I. Gkialas^{9,s}, E.L. Gkougkousis¹³, P. Gkountoumis¹⁰, L.K. Gladilin¹⁰¹, C. Glasman⁸⁵, J. Glatzer¹³, P.C.F. Glaysher⁴⁵, A. Glazov⁴⁵, M. Goblirsch-Kolb²⁵, J. Godlewski⁴², S. Goldfarb⁹¹, T. Golling⁵², D. Golubkov¹³², A. Gomes^{128a,128b,128d}, R. Gonçalo^{128a}, R. Goncalves Gama^{26a}, J. Goncalves Pinto Firmino Da Costa¹³⁸, G. Gonella⁵¹, L. Gonella¹⁹, A. Gongadze⁶⁸, S. González de la Hoz¹⁷⁰, S. Gonzalez-Sevilla⁵², L. Goossens³², P.A. Gorbounov⁹⁹, H.A. Gordon²⁷, I. Gorelov¹⁰⁷, B. Gorini³², E. Gorini^{76a,76b}, A. Gorišek⁷⁸, A.T. Goshaw⁴⁸, C. Gössling⁴⁶, M.I. Gostkin⁶⁸, C.A. Gottardo²³, C.R. Goudet¹¹⁹, D. Goujdami^{137c}, A.G. Goussiou¹⁴⁰, N. Govender^{147b,t}, E. Gozani¹⁵⁴, L. Graber⁵⁷, I. Grabowska-Bold^{41a}, P.O.J. Gradin¹⁶⁸, J. Gramling¹⁶⁶, E. Gramstad¹²¹, S. Grancagnolo¹⁷, V. Gratchev¹²⁵, P.M. Gravila^{28f}, C. Gray⁵⁶, H.M. Gray¹⁶, Z.D. Greenwood^{82,u}, C. Grefe²³, K. Gregersen⁸¹, I.M. Gregor⁴⁵, P. Grenier¹⁴⁵, K. Grevtsov⁵, J. Griffiths⁸, A.A. Grillo¹³⁹, K. Grimm⁷⁵, S. Grinstein^{13,v}, Ph. Gris³⁷, J.-F. Grivaz¹¹⁹, S. Groh⁸⁶, E. Gross¹⁷⁵, J. Grosse-Knetter⁵⁷, G.C. Grossi⁸², Z.J. Grout⁸¹, A. Grummer¹⁰⁷, L. Guan⁹², W. Guan¹⁷⁶, J. Guenther⁶⁵, F. Guescini^{163a}, D. Guest¹⁶⁶, O. Gueta¹⁵⁵, B. Gui¹¹³, E. Guido^{53a,53b}, T. Guillemin⁵, S. Guindon³², U. Gul⁵⁶, C. Gumpert³², J. Guo^{36c}, W. Guo⁹², Y. Guo^{36a,w}, R. Gupta⁴³, S. Gupta¹²², G. Gustavino¹¹⁵, B.J. Gutelman¹⁵⁴, P. Gutierrez¹¹⁵, N.G. Gutierrez Ortiz⁸¹, C. Gutschow⁸¹, C. Guyot¹³⁸, M.P. Guzik^{41a}, C. Gwenlan¹²², C.B. Gwilliam⁷⁷, A. Haas¹¹², C. Haber¹⁶, H.K. Hadavand⁸, N. Haddad^{137e}, A. Hadef⁸⁸, S. Hageböck²³, M. Hagihara¹⁶⁴, H. Hakobyan^{180,*}, M. Haleem⁴⁵, J. Haley¹¹⁶, G. Halladjian⁹³, G.D. Hallewell⁸⁸, K. Hamacher¹⁷⁸, P. Hamal¹¹⁷, K. Hamano¹⁷², A. Hamilton^{147a}, G.N. Hamity¹⁴¹, P.G. Hamnett⁴⁵, L. Han^{36a}, S. Han^{35a,35d}, K. Hanagaki^{69,x}, K. Hanawa¹⁵⁷, M. Hance¹³⁹, B. Haney¹²⁴, P. Hanke^{60a}, J.B. Hansen³⁹, J.D. Hansen³⁹, M.C. Hansen²³, P.H. Hansen³⁹, K. Hara¹⁶⁴, A.S. Hard¹⁷⁶, T. Harenberg¹⁷⁸, F. Hariri¹¹⁹, S. Harkusha⁹⁵, R.D. Harrington⁴⁹, P.F. Harrison¹⁷³, N.M. Hartmann¹⁰², Y. Hasegawa¹⁴², A. Hasib⁴⁹, S. Hassani¹³⁸, S. Haug¹⁸, R. Hauser⁹³, L. Hauswald⁴⁷, L.B. Havener³⁸, M. Havranek¹³⁰, C.M. Hawkes¹⁹, R.J. Hawkings³², D. Hayakawa¹⁵⁹, D. Hayden⁹³, C.P. Hays¹²², J.M. Hays⁷⁹, H.S. Hayward⁷⁷, S.J. Haywood¹³³, S.J. Head¹⁹, T. Heck⁸⁶, V. Hedberg⁸⁴, L. Heelan⁸, S. Heer²³, K.K. Heidegger⁵¹, S. Heim⁴⁵, T. Heim¹⁶, B. Heinemann^{45,y}, J.J. Heinrich¹⁰², L. Heinrich¹¹², C. Heinz⁵⁵, J. Hejbal¹²⁹, L. Helary³², A. Held¹⁷¹, S. Hellman^{148a,148b}, C. Helsens³², R.C.W. Henderson⁷⁵, Y. Heng¹⁷⁶, S. Henkelmann¹⁷¹, A.M. Henriques Correia³², S. Henrot-Versille¹¹⁹, G.H. Herbert¹⁷, H. Herde²⁵, V. Herget¹⁷⁷, Y. Hernández Jiménez^{147c}, H. Herr⁸⁶, G. Herten⁵¹, R. Hertenberger¹⁰², L. Hervas³², T.C. Herwig¹²⁴, G.G. Hesketh⁸¹, N.P. Hessey^{163a}, J.W. Hetherly⁴³, S. Higashino⁶⁹, E. Higón-Rodríguez¹⁷⁰, K. Hildebrand³³, E. Hill¹⁷², J.C. Hill³⁰, K.H. Hiller⁴⁵, S.J. Hillier¹⁹, M. Hils⁴⁷, I. Hinchliffe¹⁶, M. Hirose⁵¹, D. Hirschbuehl¹⁷⁸, B. Hiti⁷⁸, O. Hladík¹²⁹, X. Hoad⁴⁹, J. Hobbs¹⁵⁰, N. Hod^{163a}, M.C. Hodgkinson¹⁴¹, P. Hodgson¹⁴¹, A. Hoecker³², M.R. Hoeferkamp¹⁰⁷, F. Hoenig¹⁰², D. Hohn²³, T.R. Holmes³³, M. Homann⁴⁶, S. Honda¹⁶⁴, T. Honda⁶⁹, T.M. Hong¹²⁷, B.H. Hooberman¹⁶⁹, W.H. Hopkins¹¹⁸, Y. Horii¹⁰⁵, A.J. Horton¹⁴⁴, J.-Y. Hostachy⁵⁸, S. Hou¹⁵³, A. Hoummada^{137a}, J. Howarth⁸⁷, J. Hoya⁷⁴, M. Hrabovsky¹¹⁷, J. Hrdinka³², I. Hristova¹⁷, J. Hrivnac¹¹⁹, T. Hryvn'ova⁵,

A. Hrynevich⁹⁶, P.J. Hsu⁶³, S.-C. Hsu¹⁴⁰, Q. Hu^{36a}, S. Hu^{36c}, Y. Huang^{35a}, Z. Hubacek¹³⁰, F. Hubaut⁸⁸,
 F. Huegging²³, T.B. Huffman¹²², E.W. Hughes³⁸, G. Hughes⁷⁵, M. Huhtinen³², P. Huo¹⁵⁰,
 N. Huseynov^{68,b}, J. Huston⁹³, J. Huth⁵⁹, G. Iacobucci⁵², G. Iakovidis²⁷, I. Ibragimov¹⁴³,
 L. Iconomidou-Fayard¹¹⁹, Z. Idrissi^{137e}, P. Iengo³², O. Igonkina^{109,z}, T. Iizawa¹⁷⁴, Y. Ikegami⁶⁹,
 M. Ikeno⁶⁹, Y. Ilchenko^{11,aa}, D. Iliadis¹⁵⁶, N. Ilic¹⁴⁵, G. Introzzi^{123a,123b}, P. Ioannou^{9,*}, M. Iodice^{136a},
 K. Iordanidou³⁸, V. Ippolito⁵⁹, M.F. Isacson¹⁶⁸, N. Ishijima¹²⁰, M. Ishino¹⁵⁷, M. Ishitsuka¹⁵⁹,
 C. Issever¹²², S. Isti^{20a}, F. Ito¹⁶⁴, J.M. Iturbe Ponce^{62a}, R. Iuppa^{162a,162b}, H. Iwasaki⁶⁹, J.M. Izen⁴⁴,
 V. Izzo^{106a}, S. Jabbar³, P. Jackson¹, R.M. Jacobs²³, V. Jain², K.B. Jakobi⁸⁶, K. Jakobs⁵¹, S. Jakobsen⁶⁵,
 T. Jakoubek¹²⁹, D.O. Jamin¹¹⁶, D.K. Jana⁸², R. Jansky⁵², J. Janssen²³, M. Janus⁵⁷, P.A. Janus^{41a},
 G. Jarlskog⁸⁴, N. Javadov^{68,b}, T. Javůrek⁵¹, M. Javurkova⁵¹, F. Jeanneau¹³⁸, L. Jeanty¹⁶, J. Jejelava^{54a,ab},
 A. Jelinskas¹⁷³, P. Jenni^{51,ac}, C. Jeske¹⁷³, S. Jézéquel⁵, H. Ji¹⁷⁶, J. Jia¹⁵⁰, H. Jiang⁶⁷, Y. Jiang^{36a},
 Z. Jiang¹⁴⁵, S. Jiggins⁸¹, J. Jimenez Pena¹⁷⁰, S. Jin^{35a}, A. Jinaru^{28b}, O. Jinnouchi¹⁵⁹, H. Jivan^{147c},
 P. Johansson¹⁴¹, K.A. Johns⁷, C.A. Johnson⁶⁴, W.J. Johnson¹⁴⁰, K. Jon-And^{148a,148b}, R.W.L. Jones⁷⁵,
 S.D. Jones¹⁵¹, S. Jones⁷, T.J. Jones⁷⁷, J. Jongmanns^{60a}, P.M. Jorge^{128a,128b}, J. Jovicevic^{163a}, X. Ju¹⁷⁶,
 A. Juste Rozas^{13,v}, M.K. Köhler¹⁷⁵, A. Kaczmarska⁴², M. Kado¹¹⁹, H. Kagan¹¹³, M. Kagan¹⁴⁵,
 S.J. Kahn⁸⁸, T. Kaji¹⁷⁴, E. Kajomovitz⁴⁸, C.W. Kalderon⁸⁴, A. Kaluza⁸⁶, S. Kama⁴³,
 A. Kamenshchikov¹³², N. Kanaya¹⁵⁷, L. Kanjir⁷⁸, V.A. Kantserov¹⁰⁰, J. Kanzaki⁶⁹, B. Kaplan¹¹²,
 L.S. Kaplan¹⁷⁶, D. Kar^{147c}, K. Karakostas¹⁰, N. Karastathis¹⁰, M.J. Kareem⁵⁷, E. Karentzos¹⁰,
 S.N. Karpov⁶⁸, Z.M. Karpova⁶⁸, K. Karthik¹¹², V. Kartvelishvili⁷⁵, A.N. Karyukhin¹³², K. Kasahara¹⁶⁴,
 L. Kashif¹⁷⁶, R.D. Kass¹¹³, A. Kastanas¹⁴⁹, Y. Kataoka¹⁵⁷, C. Kato¹⁵⁷, A. Katre⁵², J. Katzy⁴⁵,
 K. Kawade⁷⁰, K. Kawagoe⁷³, T. Kawamoto¹⁵⁷, G. Kawamura⁵⁷, E.F. Kay⁷⁷, V.F. Kazanin^{111,c},
 R. Keeler¹⁷², R. Kehoe⁴³, J.S. Keller³¹, E. Kellermann⁸⁴, J.J. Kempster⁸⁰, J Kendrick¹⁹,
 H. Keoshkerian¹⁶¹, O. Kepka¹²⁹, B.P. Kerševan⁷⁸, S. Kersten¹⁷⁸, R.A. Keyes⁹⁰, M. Khader¹⁶⁹,
 F. Khalil-zada¹², A. Khanov¹¹⁶, A.G. Kharlamov^{111,c}, T. Kharlamova^{111,c}, A. Khodinov¹⁶⁰, T.J. Khoo⁵²,
 V. Khovanskiy^{99,*}, E. Khramov⁶⁸, J. Khubua^{54b,ad}, S. Kido⁷⁰, C.R. Kilby⁸⁰, H.Y. Kim⁸, S.H. Kim¹⁶⁴,
 Y.K. Kim³³, N. Kimura¹⁵⁶, O.M. Kind¹⁷, B.T. King⁷⁷, D. Kirchmeier⁴⁷, J. Kirk¹³³, A.E. Kiryunin¹⁰³,
 T. Kishimoto¹⁵⁷, D. Kisielewska^{41a}, V. Kitali⁴⁵, O. Kivernyk⁵, E. Kladiva^{146b},
 T. Klapdor-Kleingrothaus⁵¹, M.H. Klein⁹², M. Klein⁷⁷, U. Klein⁷⁷, K. Kleinknecht⁸⁶, P. Klimek¹¹⁰,
 A. Klimentov²⁷, R. Klingenberg⁴⁶, T. Klingl²³, T. Klioutchnikova³², E.-E. Kluge^{60a}, P. Kluit¹⁰⁹,
 S. Kluth¹⁰³, E. Kneringer⁶⁵, E.B.F.G. Knoops⁸⁸, A. Knue¹⁰³, A. Kobayashi¹⁵⁷, D. Kobayashi¹⁵⁹,
 T. Kobayashi¹⁵⁷, M. Kobel⁴⁷, M. Kocian¹⁴⁵, P. Kodys¹³¹, T. Koffas³¹, E. Koffeman¹⁰⁹, N.M. Köhler¹⁰³,
 T. Koi¹⁴⁵, M. Kolb^{60b}, I. Koletsou⁵, A.A. Komar^{98,*}, T. Kondo⁶⁹, N. Kondrashova^{36c}, K. Köneke⁵¹,
 A.C. König¹⁰⁸, T. Kono^{69,ae}, R. Konoplich^{112,af}, N. Konstantinidis⁸¹, R. Kopeliansky⁶⁴, S. Koperny^{41a},
 A.K. Kopp⁵¹, K. Korcyl⁴², K. Kordas¹⁵⁶, A. Korn⁸¹, A.A. Korol^{111,c}, I. Korolkov¹³, E.V. Korolkova¹⁴¹,
 O. Kortner¹⁰³, S. Kortner¹⁰³, T. Kosek¹³¹, V.V. Kostyukhin²³, A. Kotwal⁴⁸, A. Koulouris¹⁰,
 A. Kourkoumeli-Charalampidi^{123a,123b}, C. Kourkoumelis⁹, E. Kourlitis¹⁴¹, V. Kouskoura²⁷,
 A.B. Kowalewska⁴², R. Kowalewski¹⁷², T.Z. Kowalski^{41a}, C. Kozakai¹⁵⁷, W. Kozanecki¹³⁸,
 A.S. Kozhin¹³², V.A. Kramarenko¹⁰¹, G. Kramberger⁷⁸, D. Krasnopoltev¹⁰⁰, M.W. Krasny⁸³,
 A. Krasznahorkay³², D. Krauss¹⁰³, J.A. Kremer^{41a}, J. Kretzschmar⁷⁷, K. Kreutzfeldt⁵⁵, P. Krieger¹⁶¹,
 K. Krizka¹⁶, K. Kroeninger⁴⁶, H. Kroha¹⁰³, J. Kroll¹²⁹, J. Kroll¹²⁴, J. Kroseberg²³, J. Krstic¹⁴,
 U. Kruchonak⁶⁸, H. Krüger²³, N. Krumnack⁶⁷, M.C. Kruse⁴⁸, T. Kubota⁹¹, H. Kucuk⁸¹, S. Kuday^{4b},
 J.T. Kuechler¹⁷⁸, S. Kuehn³², A. Kugel^{60a}, F. Kuger¹⁷⁷, T. Kuhl⁴⁵, V. Kukhtin⁶⁸, R. Kukla⁸⁸,
 Y. Kulchitsky⁹⁵, S. Kuleshov^{34b}, Y.P. Kulinich¹⁶⁹, M. Kuna^{134a,134b}, T. Kunigo⁷¹, A. Kupco¹²⁹,
 T. Kupfer⁴⁶, O. Kuprash¹⁵⁵, H. Kurashige⁷⁰, L.L. Kurchaninov^{163a}, Y.A. Kurochkin⁹⁵, M.G. Kurth^{35a,35d},
 V. Kus¹²⁹, E.S. Kuwertz¹⁷², M. Kuze¹⁵⁹, J. Kvita¹¹⁷, T. Kwan¹⁷², D. Kyriazopoulos¹⁴¹, A. La Rosa¹⁰³,
 J.L. La Rosa Navarro^{26d}, L. La Rotonda^{40a,40b}, F. La Ruffa^{40a,40b}, C. Lacasta¹⁷⁰, F. Lacava^{134a,134b},
 J. Lacey⁴⁵, D.P.J. Lack⁸⁷, H. Lacker¹⁷, D. Lacour⁸³, E. Ladygin⁶⁸, R. Lafaye⁵, B. Laforge⁸³,

T. Lagouri¹⁷⁹, S. Lai⁵⁷, S. Lammers⁶⁴, W. Lampl⁷, E. Lançon²⁷, U. Landgraf⁵¹, M.P.J. Landon⁷⁹,
 M.C. Lanfermann⁵², V.S. Lang⁴⁵, J.C. Lange¹³, R.J. Langenberg³², A.J. Lankford¹⁶⁶, F. Lanni²⁷,
 K. Lantzsch²³, A. Lanza^{123a}, A. Lapertosa^{53a,53b}, S. Laplace⁸³, J.F. Laporte¹³⁸, T. Lari^{94a},
 F. Lasagni Manghi^{22a,22b}, M. Lassnig³², T.S. Lau^{62a}, P. Laurelli⁵⁰, W. Lavrijsen¹⁶, A.T. Law¹³⁹,
 P. Laycock⁷⁷, T. Lazovich⁵⁹, M. Lazzaroni^{94a,94b}, B. Le⁹¹, O. Le Dortz⁸³, E. Le Guirriec⁸⁸,
 E.P. Le Quilleuc¹³⁸, M. LeBlanc¹⁷², T. LeCompte⁶, F. Ledroit-Guillon⁵⁸, C.A. Lee²⁷, G.R. Lee^{133,ag},
 S.C. Lee¹⁵³, L. Lee⁵⁹, B. Lefebvre⁹⁰, G. Lefebvre⁸³, M. Lefebvre¹⁷², F. Legger¹⁰², C. Leggett¹⁶,
 G. Lehmann Miotto³², X. Lei⁷, W.A. Leight⁴⁵, M.A.L. Leite^{26d}, R. Leitner¹³¹, D. Lellouch¹⁷⁵,
 B. Lemmer⁵⁷, K.J.C. Leney⁸¹, T. Lenz²³, B. Lenzi³², R. Leone⁷, S. Leone^{126a,126b}, C. Leonidopoulos⁴⁹,
 G. Lerner¹⁵¹, C. Leroy⁹⁷, A.A.J. Lesage¹³⁸, C.G. Lester³⁰, M. Levchenko¹²⁵, J. Levêque⁵, D. Levin⁹²,
 L.J. Levinson¹⁷⁵, M. Levy¹⁹, D. Lewis⁷⁹, B. Li^{36a,w}, Changqiao Li^{36a}, H. Li¹⁵⁰, L. Li^{36c}, Q. Li^{35a,35d},
 Q. Li^{36a}, S. Li⁴⁸, X. Li^{36c}, Y. Li¹⁴³, Z. Liang^{35a}, B. Liberti^{135a}, A. Liblong¹⁶¹, K. Lie^{62c}, J. Liebal²³,
 W. Liebig¹⁵, A. Limosani¹⁵², S.C. Lin¹⁸², T.H. Lin⁸⁶, R.A. Linck⁶⁴, B.E. Lindquist¹⁵⁰, A.E. Lioni⁵²,
 E. Lipeles¹²⁴, A. Lipniacka¹⁵, M. Lisovyi^{60b}, T.M. Liss^{169,ah}, A. Lister¹⁷¹, A.M. Litke¹³⁹, B. Liu⁶⁷,
 H. Liu⁹², H. Liu²⁷, J.K.K. Liu¹²², J. Liu^{36b}, J.B. Liu^{36a}, K. Liu⁸⁸, L. Liu¹⁶⁹, M. Liu^{36a}, Y. Liu^{35a,35d},
 Y.L. Liu^{36a}, Y. Liu^{36a}, M. Livan^{123a,123b}, A. Lleres⁵⁸, J. Llorente Merino^{35a}, S.L. Lloyd⁷⁹, C.Y. Lo^{62b},
 F. Lo Sterzo¹⁵³, E.M. Lobodzinska⁴⁵, P. Loch⁷, F.K. Loebinger⁸⁷, A. Loesle⁵¹, K.M. Loew²⁵,
 A. Loginov^{179,*}, T. Lohse¹⁷, K. Lohwasser¹⁴¹, M. Lokajicek¹²⁹, B.A. Long²⁴, J.D. Long¹⁶⁹,
 R.E. Long⁷⁵, L. Longo^{76a,76b}, K.A.Looper¹¹³, J.A. Lopez^{34b}, D. Lopez Mateos⁵⁹, I. Lopez Paz¹³,
 A. Lopez Solis⁸³, J. Lorenz¹⁰², N. Lorenzo Martinez⁵, M. Losada²¹, P.J. Lösel¹⁰², X. Lou^{35a},
 A. Lounis¹¹⁹, J. Love⁶, P.A. Love⁷⁵, H. Lu^{62a}, N. Lu⁹², Y.J. Lu⁶³, H.J. Lubatti¹⁴⁰, C. Luci^{134a,134b},
 A. Lucotte⁵⁸, C. Luedtke⁵¹, F. Luehring⁶⁴, W. Lukas⁶⁵, L. Luminari^{134a}, O. Lundberg^{148a,148b},
 B. Lund-Jensen¹⁴⁹, M.S. Lutz⁸⁹, P.M. Luzi⁸³, D. Lynn²⁷, R. Lysak¹²⁹, E. Lytken⁸⁴, F. Lyu^{35a},
 V. Lyubushkin⁶⁸, H. Ma²⁷, L.L. Ma^{36b}, Y. Ma^{36b}, G. Maccarrone⁵⁰, A. Macchiolo¹⁰³,
 C.M. Macdonald¹⁴¹, B. Maček⁷⁸, J. Machado Miguens^{124,128b}, D. Madaffari¹⁷⁰, R. Madar³⁷,
 W.F. Mader⁴⁷, A. Madsen⁴⁵, J. Maeda⁷⁰, S. Maeland¹⁵, T. Maeno²⁷, A.S. Maevskiy¹⁰¹, V. Magerl⁵¹,
 J. Mahlstedt¹⁰⁹, C. Maiani¹¹⁹, C. Maidantchik^{26a}, A.A. Maier¹⁰³, T. Maier¹⁰², A. Maio^{128a,128b,128d},
 O. Majersky^{146a}, S. Majewski¹¹⁸, Y. Makida⁶⁹, N. Makovec¹¹⁹, B. Malaescu⁸³, Pa. Malecki⁴²,
 V.P. Maleev¹²⁵, F. Malek⁵⁸, U. Mallik⁶⁶, D. Malon⁶, C. Malone³⁰, S. Maltezos¹⁰, S. Malyukov³²,
 J. Mamuzic¹⁷⁰, G. Mancini⁵⁰, I. Mandić⁷⁸, J. Maneira^{128a,128b}, L. Manhaes de Andrade Filho^{26b},
 J. Manjarres Ramos⁴⁷, K.H. Mankinen⁸⁴, A. Mann¹⁰², A. Manousos³², B. Mansoulie¹³⁸,
 J.D. Mansour^{35a}, R. Mantifel⁹⁰, M. Mantoani⁵⁷, S. Manzoni^{94a,94b}, L. Mapelli³², G. Marceca²⁹,
 L. March⁵², L. Marchese¹²², G. Marchiori⁸³, M. Marcisovsky¹²⁹, M. Marjanovic³⁷, D.E. Marley⁹²,
 F. Marroquim^{26a}, S.P. Marsden⁸⁷, Z. Marshall¹⁶, M.U.F Martensson¹⁶⁸, S. Marti-Garcia¹⁷⁰,
 C.B. Martin¹¹³, T.A. Martin¹⁷³, V.J. Martin⁴⁹, B. Martin dit Latour¹⁵, M. Martinez^{13,v},
 V.I. Martinez Outschoorn¹⁶⁹, S. Martin-Haugh¹³³, V.S. Martoiu^{28b}, A.C. Martyniuk⁸¹, A. Marzin³²,
 L. Masetti⁸⁶, T. Mashimo¹⁵⁷, R. Mashinistov⁹⁸, J. Masik⁸⁷, A.L. Maslennikov^{111,c}, L. Massa^{135a,135b},
 P. Mastrandrea⁵, A. Mastroberardino^{40a,40b}, T. Masubuchi¹⁵⁷, P. Mättig¹⁷⁸, J. Maurer^{28b}, S.J. Maxfield⁷⁷,
 D.A. Maximov^{111,c}, R. Mazini¹⁵³, I. Maznas¹⁵⁶, S.M. Mazza^{94a,94b}, N.C. Mc Fadden¹⁰⁷,
 G. Mc Goldrick¹⁶¹, S.P. Mc Kee⁹², A. McCarn⁹², R.L. McCarthy¹⁵⁰, T.G. McCarthy¹⁰³,
 L.I. McClymont⁸¹, E.F. McDonald⁹¹, J.A. McFayden³², G. Mchedlidze⁵⁷, S.J. McMahon¹³³,
 P.C. McNamara⁹¹, C.J. McNicol¹⁷³, R.A. McPherson^{172,o}, S. Meehan¹⁴⁰, T.J. Megy⁵¹, S. Mehlhase¹⁰²,
 A. Mehta⁷⁷, T. Meideck⁵⁸, K. Meier^{60a}, B. Meirose⁴⁴, D. Melini^{170,ai}, B.R. Mellado Garcia^{147c},
 J.D. Mellenthin⁵⁷, M. Melo^{146a}, F. Meloni¹⁸, A. Melzer²³, S.B. Menary⁸⁷, L. Meng⁷⁷, X.T. Meng⁹²,
 A. Mengarelli^{22a,22b}, S. Menke¹⁰³, E. Meoni^{40a,40b}, S. Mergelmeyer¹⁷, C. Merlassino¹⁸, P. Mermod⁵²,
 L. Merola^{106a,106b}, C. Meroni^{94a}, F.S. Merritt³³, A. Messina^{134a,134b}, J. Metcalfe⁶, A.S. Mete¹⁶⁶,
 C. Meyer¹²⁴, J.-P. Meyer¹³⁸, J. Meyer¹⁰⁹, H. Meyer Zu Theenhausen^{60a}, F. Miano¹⁵¹, R.P. Middleton¹³³,

S. Miglioranzi^{53a,53b}, L. Mijović⁴⁹, G. Mikenberg¹⁷⁵, M. Mikestikova¹²⁹, M. Mikuž⁷⁸, M. Milesi⁹¹,
 A. Milic¹⁶¹, D.A. Millar⁷⁹, D.W. Miller³³, C. Mills⁴⁹, A. Milov¹⁷⁵, D.A. Milstead^{148a,148b},
 A.A. Minaenko¹³², Y. Minami¹⁵⁷, I.A. Minashvili^{54b}, A.I. Mincer¹¹², B. Mindur^{41a}, M. Mineev⁶⁸,
 Y. Minegishi¹⁵⁷, Y. Ming¹⁷⁶, L.M. Mir¹³, K.P. Mistry¹²⁴, T. Mitani¹⁷⁴, J. Mitrevski¹⁰², V.A. Mitsou¹⁷⁰,
 A. Miucci¹⁸, P.S. Miyagawa¹⁴¹, A. Mizukami⁶⁹, J.U. Mjörnmark⁸⁴, T. Mkrtchyan¹⁸⁰,
 M. Mlynarikova¹³¹, T. Moa^{148a,148b}, K. Mochizuki⁹⁷, P. Mogg⁵¹, S. Mohapatra³⁸, S. Molander^{148a,148b},
 R. Moles-Valls²³, M.C. Mondragon⁹³, K. Mönig⁴⁵, J. Monk³⁹, E. Monnier⁸⁸, A. Montalbano¹⁵⁰,
 J. Montejo Berlingen³², F. Monticelli⁷⁴, S. Monzani^{94a,94b}, R.W. Moore³, N. Morange¹¹⁹, D. Moreno²¹,
 M. Moreno Llácer³², P. Morettini^{53a}, S. Morgenstern³², D. Mori¹⁴⁴, T. Mori¹⁵⁷, M. Morii⁵⁹,
 M. Morinaga¹⁷⁴, V. Morisbak¹²¹, A.K. Morley³², G. Mornacchi³², J.D. Morris⁷⁹, L. Morvaj¹⁵⁰,
 P. Moschovakos¹⁰, M. Mosidze^{54b}, H.J. Moss¹⁴¹, J. Moss^{145,aj}, K. Motohashi¹⁵⁹, R. Mount¹⁴⁵,
 E. Mountricha²⁷, E.J.W. Moyse⁸⁹, S. Muanza⁸⁸, F. Mueller¹⁰³, J. Mueller¹²⁷, R.S.P. Mueller¹⁰²,
 D. Muenstermann⁷⁵, P. Mullen⁵⁶, G.A. Mullier¹⁸, F.J. Munoz Sanchez⁸⁷, W.J. Murray^{173,133},
 H. Musheghyan³², M. Muškinja⁷⁸, A.G. Myagkov^{132,ak}, M. Myska¹³⁰, B.P. Nachman¹⁶,
 O. Nackenhorst⁵², K. Nagai¹²², R. Nagai^{69,ae}, K. Nagano⁶⁹, Y. Nagasaka⁶¹, K. Nagata¹⁶⁴, M. Nagel⁵¹,
 E. Nagy⁸⁸, A.M. Nairz³², Y. Nakahama¹⁰⁵, K. Nakamura⁶⁹, T. Nakamura¹⁵⁷, I. Nakano¹¹⁴,
 R.F. Naranjo Garcia⁴⁵, R. Narayan¹¹, D.I. Narrias Villar^{60a}, I. Naryshkin¹²⁵, T. Naumann⁴⁵,
 G. Navarro²¹, R. Nayyar⁷, H.A. Neal⁹², P.Yu. Nechaeva⁹⁸, T.J. Neep¹³⁸, A. Negri^{123a,123b}, M. Negrini^{22a},
 S. Nektarijevic¹⁰⁸, C. Nellist¹¹⁹, A. Nelson¹⁶⁶, M.E. Nelson¹²², S. Nemecek¹²⁹, P. Nemethy¹¹²,
 M. Nessi^{32,al}, M.S. Neubauer¹⁶⁹, M. Neumann¹⁷⁸, P.R. Newman¹⁹, T.Y. Ng^{62c}, T. Nguyen Manh⁹⁷,
 R.B. Nickerson¹²², R. Nicolaïdou¹³⁸, J. Nielsen¹³⁹, V. Nikolaenko^{132,ak}, I. Nikolic-Audit⁸³,
 K. Nikolopoulos¹⁹, J.K. Nilsen¹²¹, P. Nilsson²⁷, Y. Ninomiya¹⁵⁷, A. Nisati^{134a}, N. Nishu^{36c}, R. Nisius¹⁰³,
 I. Nitsche⁴⁶, T. Nitta¹⁷⁴, T. Nobe¹⁵⁷, Y. Noguchi⁷¹, M. Nomachi¹²⁰, I. Nomidis³¹, M.A. Nomura²⁷,
 T. Nooney⁷⁹, M. Nordberg³², N. Norjoharuddeen¹²², O. Novgorodova⁴⁷, M. Nozaki⁶⁹, L. Nozka¹¹⁷,
 K. Ntekas¹⁶⁶, E. Nurse⁸¹, F. Nuti⁹¹, K. O'connor²⁵, D.C. O'Neil¹⁴⁴, A.A. O'Rourke⁴⁵, V. O'Shea⁵⁶,
 F.G. Oakham^{31,d}, H. Oberlack¹⁰³, T. Obermann²³, J. Ocariz⁸³, A. Ochi⁷⁰, I. Ochoa³⁸,
 J.P. Ochoa-Ricoux^{34a}, S. Oda⁷³, S. Odaka⁶⁹, A. Oh⁸⁷, S.H. Oh⁴⁸, C.C. Ohm¹⁶, H. Ohman¹⁶⁸,
 H. Oide^{53a,53b}, H. Okawa¹⁶⁴, Y. Okumura¹⁵⁷, T. Okuyama⁶⁹, A. Olariu^{28b}, L.F. Oleiro Seabra^{128a},
 S.A. Olivares Pino^{34a}, D. Oliveira Damazio²⁷, A. Olszewski⁴², J. Olszowska⁴², A. Onofre^{128a,128e},
 K. Onogi¹⁰⁵, P.U.E. Onyisi^{11,aa}, H. Oppen¹²¹, M.J. Oreglia³³, Y. Oren¹⁵⁵, D. Orestano^{136a,136b},
 N. Orlando^{62b}, R.S. Orr¹⁶¹, B. Osculati^{53a,53b,*}, R. Ospanov^{36a}, G. Otero y Garzon²⁹, H. Otono⁷³,
 M. Ouchrif^{137d}, F. Ould-Saada¹²¹, A. Ouraou¹³⁸, K.P. Oussoren¹⁰⁹, Q. Ouyang^{35a}, M. Owen⁵⁶,
 R.E. Owen¹⁹, V.E. Ozcan^{20a}, N. Ozturk⁸, K. Pachal¹⁴⁴, A. Pacheco Pages¹³, L. Pacheco Rodriguez¹³⁸,
 C. Padilla Aranda¹³, S. Pagan Griso¹⁶, M. Paganini¹⁷⁹, F. Paige²⁷, G. Palacino⁶⁴, S. Palazzo^{40a,40b},
 S. Palestini³², M. Palka^{41b}, D. Pallin³⁷, E.St. Panagiotopoulou¹⁰, I. Panagoulias¹⁰, C.E. Pandini^{126a,126b},
 J.G. Panduro Vazquez⁸⁰, P. Pani³², S. Panitkin²⁷, D. Pantea^{28b}, L. Paolozzi⁵², Th.D. Papadopoulou¹⁰,
 K. Papageorgiou^{9,s}, A. Paramonov⁶, D. Paredes Hernandez¹⁷⁹, A.J. Parker⁷⁵, M.A. Parker³⁰,
 K.A. Parker⁴⁵, F. Parodi^{53a,53b}, J.A. Parsons³⁸, U. Parzefall⁵¹, V.R. Pascuzzi¹⁶¹, J.M. Pasner¹³⁹,
 E. Pasqualucci^{134a}, S. Passaggio^{53a}, Fr. Pastore⁸⁰, S. Pataraia⁸⁶, J.R. Pater⁸⁷, T. Pauly³², B. Pearson¹⁰³,
 S. Pedraza Lopez¹⁷⁰, R. Pedro^{128a,128b}, S.V. Peleganchuk^{111,c}, O. Penc¹²⁹, C. Peng^{35a,35d}, H. Peng^{36a},
 J. Penwell⁶⁴, B.S. Peralva^{26b}, M.M. Perego¹³⁸, D.V. Perepelitsa²⁷, F. Peri¹⁷, L. Perini^{94a,94b},
 H. Pernegger³², S. Perrella^{106a,106b}, R. Peschke⁴⁵, V.D. Peshekhanov^{68,*}, K. Peters⁴⁵, R.F.Y. Peters⁸⁷,
 B.A. Petersen³², T.C. Petersen³⁹, E. Petit⁵⁸, A. Petridis¹, C. Petridou¹⁵⁶, P. Petroff¹¹⁹, E. Petrolo^{134a},
 M. Petrov¹²², F. Petrucci^{136a,136b}, N.E. Pettersson⁸⁹, A. Peyaud¹³⁸, R. Pezoa^{34b}, F.H. Phillips⁹³,
 P.W. Phillips¹³³, G. Piacquadio¹⁵⁰, E. Pianori¹⁷³, A. Picazio⁸⁹, E. Piccaro⁷⁹, M.A. Pickering¹²²,
 R. Piegaia²⁹, J.E. Pilcher³³, A.D. Pilkington⁸⁷, A.W.J. Pin⁸⁷, M. Pinamonti^{135a,135b}, J.L. Pinfold³,
 H. Pirumov⁴⁵, M. Pitt¹⁷⁵, L. Plazak^{146a}, M.-A. Pleier²⁷, V. Pleskot⁸⁶, E. Plotnikova⁶⁸, D. Pluth⁶⁷,

P. Podberezko¹¹¹, R. Poettgen⁸⁴, R. Poggi^{123a,123b}, L. Poggioli¹¹⁹, I. Pogrebnyak⁹³, D. Pohl²³,
 G. Polesello^{123a}, A. Poley⁴⁵, A. Policicchio^{40a,40b}, R. Polifka³², A. Polini^{22a}, C.S. Pollard⁵⁶,
 V. Polychronakos²⁷, K. Pommès³², D. Ponomarenko¹⁰⁰, L. Pontecorvo^{134a}, G.A. Popeneciu^{28d},
 S. Pospisil¹³⁰, K. Potamianos¹⁶, I.N. Potrap⁶⁸, C.J. Potter³⁰, H. Potti¹¹, T. Poulsen⁸⁴, J. Poveda³²,
 M.E. Pozo Astigarraga³², P. Pralavorio⁸⁸, A. Pranko¹⁶, S. Prell⁶⁷, D. Price⁸⁷, M. Primavera^{76a},
 S. Prince⁹⁰, N. Proklova¹⁰⁰, K. Prokofiev^{62c}, F. Prokoshin^{34b}, S. Protopopescu²⁷, J. Proudfoot⁶,
 M. Przybycien^{41a}, A. Puri¹⁶⁹, P. Puzo¹¹⁹, J. Qian⁹², G. Qin⁵⁶, Y. Qin⁸⁷, A. Quadt⁵⁷,
 M. Queitsch-Maitland⁴⁵, D. Quilty⁵⁶, S. Raddum¹²¹, V. Radeka²⁷, V. Radescu¹²²,
 S.K. Radhakrishnan¹⁵⁰, P. Radloff¹¹⁸, P. Rados⁹¹, F. Ragusa^{94a,94b}, G. Rahal¹⁸¹, J.A. Raine⁸⁷,
 S. Rajagopalan²⁷, C. Rangel-Smith¹⁶⁸, T. Rashid¹¹⁹, S. Raspopov⁵, M.G. Ratti^{94a,94b}, D.M. Rauch⁴⁵,
 F. Rauscher¹⁰², S. Rave⁸⁶, I. Ravinovich¹⁷⁵, J.H. Rawling⁸⁷, M. Raymond³², A.L. Read¹²¹,
 N.P. Readoff⁵⁸, M. Reale^{76a,76b}, D.M. Rebuzzi^{123a,123b}, A. Redelbach¹⁷⁷, G. Redlinger²⁷, R. Reece¹³⁹,
 R.G. Reed^{147c}, K. Reeves⁴⁴, L. Rehnisch¹⁷, J. Reichert¹²⁴, A. Reiss⁸⁶, C. Rembser³², H. Ren^{35a,35d},
 M. Rescigno^{134a}, S. Resconi^{94a}, E.D. Ressegue¹²⁴, S. Rettie¹⁷¹, E. Reynolds¹⁹, O.L. Rezanova^{111,c},
 P. Reznicek¹³¹, R. Rezvani⁹⁷, R. Richter¹⁰³, S. Richter⁸¹, E. Richter-Was^{41b}, O. Ricken²³, M. Ridel⁸³,
 P. Rieck¹⁰³, C.J. Riegel¹⁷⁸, J. Rieger⁵⁷, O. Rifki¹¹⁵, M. Rijssenbeek¹⁵⁰, A. Rimoldi^{123a,123b},
 M. Rimoldi¹⁸, L. Rinaldi^{22a}, G. Ripellino¹⁴⁹, B. Ristic³², E. Ritsch³², I. Riu¹³, F. Rizatdinova¹¹⁶,
 E. Rizvi⁷⁹, C. Rizzi¹³, R.T. Roberts⁸⁷, S.H. Robertson^{90,o}, A. Robichaud-Veronneau⁹⁰, D. Robinson³⁰,
 J.E.M. Robinson⁴⁵, A. Robson⁵⁶, E. Rocco⁸⁶, C. Roda^{126a,126b}, Y. Rodina^{88,am}, S. Rodriguez Bosca¹⁷⁰,
 A. Rodriguez Perez¹³, D. Rodriguez Rodriguez¹⁷⁰, S. Roe³², C.S. Rogan⁵⁹, O. Røhne¹²¹, J. Roloff⁵⁹,
 A. Romaniouk¹⁰⁰, M. Romano^{22a,22b}, S.M. Romano Saez³⁷, E. Romero Adam¹⁷⁰, N. Rompotis⁷⁷,
 M. Ronzani⁵¹, L. Roos⁸³, S. Rosati^{134a}, K. Rosbach⁵¹, P. Rose¹³⁹, N.-A. Rosien⁵⁷, E. Rossi^{106a,106b},
 L.P. Rossi^{53a}, J.H.N. Rosten³⁰, R. Rosten¹⁴⁰, M. Rotaru^{28b}, J. Rothberg¹⁴⁰, D. Rousseau¹¹⁹,
 A. Rozanova⁸⁸, Y. Rozen¹⁵⁴, X. Ruan^{147c}, F. Rubbo¹⁴⁵, F. Rühr⁵¹, A. Ruiz-Martinez³¹, Z. Rurikova⁵¹,
 N.A. Rusakovich⁶⁸, H.L. Russell⁹⁰, J.P. Rutherford⁷, N. Ruthmann³², Y.F. Ryabov¹²⁵, M. Rybar¹⁶⁹,
 G. Rybkin¹¹⁹, S. Ryu⁶, A. Ryzhov¹³², G.F. Rzehorz⁵⁷, A.F. Saavedra¹⁵², G. Sabato¹⁰⁹, S. Sacerdoti²⁹,
 H.F-W. Sadrozinski¹³⁹, R. Sadykov⁶⁸, F. Safai Tehrani^{134a}, P. Saha¹¹⁰, M. Sahinsoy^{60a}, M. Saimpert⁴⁵,
 M. Saito¹⁵⁷, T. Saito¹⁵⁷, H. Sakamoto¹⁵⁷, Y. Sakurai¹⁷⁴, G. Salamanna^{136a,136b}, J.E. Salazar Loyola^{34b},
 D. Salek¹⁰⁹, P.H. Sales De Bruin¹⁶⁸, D. Salihagic¹⁰³, A. Salnikov¹⁴⁵, J. Salt¹⁷⁰, D. Salvatore^{40a,40b},
 F. Salvatore¹⁵¹, A. Salvucci^{62a,62b,62c}, A. Salzburger³², D. Sammel⁵¹, D. Sampsonidis¹⁵⁶,
 D. Sampsonidou¹⁵⁶, J. Sánchez¹⁷⁰, V. Sanchez Martinez¹⁷⁰, A. Sanchez Pineda^{167a,167c}, H. Sandaker¹²¹,
 R.L. Sandbach⁷⁹, C.O. Sander⁴⁵, M. Sandhoff¹⁷⁸, C. Sandoval²¹, D.P.C. Sankey¹³³, M. Sannino^{53a,53b},
 Y. Sano¹⁰⁵, A. Sansoni⁵⁰, C. Santoni³⁷, H. Santos^{128a}, I. Santoyo Castillo¹⁵¹, A. Sapronov⁶⁸,
 J.G. Saraiva^{128a,128d}, B. Sarrazin²³, O. Sasaki⁶⁹, K. Sato¹⁶⁴, E. Sauvan⁵, G. Savage⁸⁰, P. Savard^{161,d},
 N. Savic¹⁰³, C. Sawyer¹³³, L. Sawyer^{82,u}, J. Saxon³³, C. Sbarra^{22a}, A. Sbrizzi^{22a,22b}, T. Scanlon⁸¹,
 D.A. Scannicchio¹⁶⁶, J. Schaarschmidt¹⁴⁰, P. Schacht¹⁰³, B.M. Schachtner¹⁰², D. Schaefer³²,
 L. Schaefer¹²⁴, R. Schaefer⁴⁵, J. Schaeffer⁸⁶, S. Schaepe²³, S. Schaetzle^{60b}, U. Schäfer⁸⁶,
 A.C. Schaffer¹¹⁹, D. Schaile¹⁰², R.D. Schamberger¹⁵⁰, V.A. Schegelsky¹²⁵, D. Scheirich¹³¹,
 M. Schernau¹⁶⁶, C. Schiavi^{53a,53b}, S. Schier¹³⁹, L.K. Schildgen²³, C. Schillo⁵¹, M. Schioppa^{40a,40b},
 S. Schlenker³², K.R. Schmidt-Sommerfeld¹⁰³, K. Schmieden³², C. Schmitt⁸⁶, S. Schmitt⁴⁵,
 S. Schmitz⁸⁶, U. Schnoor⁵¹, L. Schoeffel¹³⁸, A. Schoening^{60b}, B.D. Schoenrock⁹³, E. Schopf²³,
 M. Schott⁸⁶, J.F.P. Schouwenberg¹⁰⁸, J. Schovancova³², S. Schramm⁵², N. Schuh⁸⁶, A. Schulte⁸⁶,
 M.J. Schultens²³, H.-C. Schultz-Coulon^{60a}, H. Schulz¹⁷, M. Schumacher⁵¹, B.A. Schumm¹³⁹,
 Ph. Schune¹³⁸, A. Schwartzman¹⁴⁵, T.A. Schwarz⁹², H. Schweiger⁸⁷, Ph. Schwemling¹³⁸,
 R. Schwienhorst⁹³, J. Schwindling¹³⁸, A. Sciandra²³, G. Sciolla²⁵, M. Scornajenghi^{40a,40b},
 F. Scuri^{126a,126b}, F. Scutti⁹¹, J. Searcy⁹², P. Seema²³, S.C. Seidel¹⁰⁷, A. Seiden¹³⁹, J.M. Seixas^{26a},
 G. Sekhniaidze^{106a}, K. Sekhon⁹², S.J. Sekula⁴³, N. Semprini-Cesari^{22a,22b}, S. Senkin³⁷, C. Serfon¹²¹,

L. Serin¹¹⁹, L. Serkin^{167a,167b}, M. Sessa^{136a,136b}, R. Seuster¹⁷², H. Severini¹¹⁵, T. Sfiligoj⁷⁸, F. Sforza¹⁶⁵, A. Sfyrla⁵², E. Shabalina⁵⁷, N.W. Shaikh^{148a,148b}, L.Y. Shan^{35a}, R. Shang¹⁶⁹, J.T. Shank²⁴, M. Shapiro¹⁶, P.B. Shatalov⁹⁹, K. Shaw^{167a,167b}, S.M. Shaw⁸⁷, A. Shcherbakova^{148a,148b}, C.Y. Shehu¹⁵¹, Y. Shen¹¹⁵, N. Sherafati³¹, P. Sherwood⁸¹, L. Shi^{153,an}, S. Shimizu⁷⁰, C.O. Shimmin¹⁷⁹, M. Shimojima¹⁰⁴, I.P.J. Shipsey¹²², S. Shirabe⁷³, M. Shiyakova^{68,ao}, J. Shlomi¹⁷⁵, A. Shmeleva⁹⁸, D. Shoaleh Saadi⁹⁷, M.J. Shochet³³, S. Shojaii^{94a,94b}, D.R. Shope¹¹⁵, S. Shrestha¹¹³, E. Shulga¹⁰⁰, M.A. Shupe⁷, P. Sicho¹²⁹, A.M. Sickles¹⁶⁹, P.E. Sidebo¹⁴⁹, E. Sideras Haddad^{147c}, O. Sidiropoulou¹⁷⁷, A. Sidoti^{22a,22b}, F. Siegert⁴⁷, Dj. Sijacki¹⁴, J. Silva^{128a,128d}, S.B. Silverstein^{148a}, V. Simak¹³⁰, L. Simic¹⁴, S. Simion¹¹⁹, E. Simioni⁸⁶, B. Simmons⁸¹, M. Simon⁸⁶, P. Sinervo¹⁶¹, N.B. Sinev¹¹⁸, M. Sioli^{22a,22b}, G. Siragusa¹⁷⁷, I. Siral⁹², S.Yu. Sivoklokov¹⁰¹, J. Sjölin^{148a,148b}, M.B. Skinner⁷⁵, P. Skubic¹¹⁵, M. Slater¹⁹, T. Slavicek¹³⁰, M. Slawinska⁴², K. Sliwa¹⁶⁵, R. Slovak¹³¹, V. Smakhtin¹⁷⁵, B.H. Smart⁵, J. Smiesko^{146a}, N. Smirnov¹⁰⁰, S.Yu. Smirnov¹⁰⁰, Y. Smirnov¹⁰⁰, L.N. Smirnova^{101,ap}, O. Smirnova⁸⁴, J.W. Smith⁵⁷, M.N.K. Smith³⁸, R.W. Smith³⁸, M. Smizanska⁷⁵, K. Smolek¹³⁰, A.A. Snesarev⁹⁸, I.M. Snyder¹¹⁸, S. Snyder²⁷, R. Sobie^{172,o}, F. Socher⁴⁷, A.M. Soffa¹⁶⁶, A. Soffer¹⁵⁵, A. Søgaard⁴⁹, D.A. Soh¹⁵³, G. Sokhrannyi⁷⁸, C.A. Solans Sanchez³², M. Solar¹³⁰, E.Yu. Soldatov¹⁰⁰, U. Soldevila¹⁷⁰, A.A. Solodkov¹³², A. Soloshenko⁶⁸, O.V. Solovyanov¹³², V. Solovyev¹²⁵, P. Sommer⁵¹, H. Son¹⁶⁵, A. Sopczak¹³⁰, D. Sosa^{60b}, C.L. Sotropoulou^{126a,126b}, R. Soualah^{167a,167c}, A.M. Soukharev^{111,c}, D. South⁴⁵, B.C. Sowden⁸⁰, S. Spagnolo^{76a,76b}, M. Spalla^{126a,126b}, M. Spangenberg¹⁷³, F. Spanò⁸⁰, D. Sperlich¹⁷, F. Spettel¹⁰³, T.M. Spieker^{60a}, R. Spighi^{22a}, G. Spigo³², L.A. Spiller⁹¹, M. Spousta¹³¹, R.D. St. Denis^{56,*}, A. Stabile^{94a}, R. Stamen^{60a}, S. Stamm¹⁷, E. Stanecka⁴², R.W. Stanek⁶, C. Stanescu^{136a}, M.M. Stanitzki⁴⁵, B.S. Stapf¹⁰⁹, S. Stappnes¹²¹, E.A. Starchenko¹³², G.H. Stark³³, J. Stark⁵⁸, S.H Stark³⁹, P. Staroba¹²⁹, P. Starovoitov^{60a}, S. Stärz³², R. Staszewski⁴², P. Steinberg²⁷, B. Stelzer¹⁴⁴, H.J. Stelzer³², O. Stelzer-Chilton^{163a}, H. Stenzel⁵⁵, G.A. Stewart⁵⁶, M.C. Stockton¹¹⁸, M. Stoebe⁹⁰, G. Stoica^{28b}, P. Stolte⁵⁷, S. Stonjek¹⁰³, A.R. Stradling⁸, A. Straessner⁴⁷, M.E. Stramaglia¹⁸, J. Strandberg¹⁴⁹, S. Strandberg^{148a,148b}, M. Strauss¹¹⁵, P. Strizenec^{146b}, R. Ströhmer¹⁷⁷, D.M. Strom¹¹⁸, R. Stroynowski⁴³, A. Strubig⁴⁹, S.A. Stucci²⁷, B. Stugu¹⁵, N.A. Styles⁴⁵, D. Su¹⁴⁵, J. Su¹²⁷, S. Suchek^{60a}, Y. Sugaya¹²⁰, M. Suk¹³⁰, V.V. Sulin⁹⁸, DMS Sultan^{162a,162b}, S. Sultansoy^{4c}, T. Sumida⁷¹, S. Sun⁵⁹, X. Sun³, K. Suruliz¹⁵¹, C.J.E. Suster¹⁵², M.R. Sutton¹⁵¹, S. Suzuki⁶⁹, M. Svatos¹²⁹, M. Swiatlowski³³, S.P. Swift², I. Sykora^{146a}, T. Sykora¹³¹, D. Ta⁵¹, K. Tackmann⁴⁵, J. Taenzer¹⁵⁵, A. Taffard¹⁶⁶, R. Tafirout^{163a}, E. Tahirovic⁷⁹, N. Taiblum¹⁵⁵, H. Takai²⁷, R. Takashima⁷², E.H. Takasugi¹⁰³, T. Takeshita¹⁴², Y. Takubo⁶⁹, M. Talby⁸⁸, A.A. Talyshев^{111,c}, J. Tanaka¹⁵⁷, M. Tanaka¹⁵⁹, R. Tanaka¹¹⁹, S. Tanaka⁶⁹, R. Tanioka⁷⁰, B.B. Tannenwald¹¹³, S. Tapia Araya^{34b}, S. Tapprogge⁸⁶, S. Tarem¹⁵⁴, G.F. Tartarelli^{94a}, P. Tas¹³¹, M. Tasevsky¹²⁹, T. Tashiro⁷¹, E. Tassi^{40a,40b}, A. Tavares Delgado^{128a,128b}, Y. Tayalati^{137e}, A.C. Taylor¹⁰⁷, A.J. Taylor⁴⁹, G.N. Taylor⁹¹, P.T.E. Taylor⁹¹, W. Taylor^{163b}, P. Teixeira-Dias⁸⁰, D. Temple¹⁴⁴, H. Ten Kate³², P.K. Teng¹⁵³, J.J. Teoh¹²⁰, F. Tepel¹⁷⁸, S. Terada⁶⁹, K. Terashi¹⁵⁷, J. Terron⁸⁵, S. Terzo¹³, M. Testa⁵⁰, R.J. Teuscher^{161,o}, T. Theveneaux-Pelzer⁸⁸, F. Thiele³⁹, J.P. Thomas¹⁹, J. Thomas-Wilsker⁸⁰, P.D. Thompson¹⁹, A.S. Thompson⁵⁶, L.A. Thomsen¹⁷⁹, E. Thomson¹²⁴, M.J. Tibbetts¹⁶, R.E. Ticse Torres⁸⁸, V.O. Tikhomirov^{98,ag}, Yu.A. Tikhonov^{111,c}, S. Timoshenko¹⁰⁰, P. Tipton¹⁷⁹, S. Tisserant⁸⁸, K. Todome¹⁵⁹, S. Todorova-Nova⁵, S. Todt⁴⁷, J. Tojo⁷³, S. Tokár^{146a}, K. Tokushuku⁶⁹, E. Tolley¹¹³, L. Tomlinson⁸⁷, M. Tomoto¹⁰⁵, L. Tompkins^{145,ar}, K. Toms¹⁰⁷, B. Tong⁵⁹, P. Tornambe⁵¹, E. Torrence¹¹⁸, H. Torres⁴⁷, E. Torró Pastor¹⁴⁰, J. Toth^{88,as}, F. Touchard⁸⁸, D.R. Tovey¹⁴¹, C.J. Treado¹¹², T. Trefzger¹⁷⁷, F. Tresoldi¹⁵¹, A. Tricoli²⁷, I.M. Trigger^{163a}, S. Trincaz-Duvold⁸³, M.F. Tripiana¹³, W. Trischuk¹⁶¹, B. Trocmé⁵⁸, A. Trofymov⁴⁵, C. Troncon^{94a}, M. Trottier-McDonald¹⁶, M. Trovatelli¹⁷², L. Truong^{147b}, M. Trzebinski⁴², A. Trzupek⁴², K.W. Tsang^{62a}, J.C.-L. Tseng¹²², P.V. Tsiareshka⁹⁵, G. Tsipolitis¹⁰, N. Tsirintanis⁹, S. Tsiskaridze¹³, V. Tsiskaridze⁵¹, E.G. Tskhadadze^{54a}, K.M. Tsui^{62a}, I.I. Tsukerman⁹⁹, V. Tsulaia¹⁶, S. Tsuno⁶⁹, D. Tsybychev¹⁵⁰, Y. Tu^{62b}, A. Tudorache^{28b}, V. Tudorache^{28b}, T.T. Tulbure^{28a}, A.N. Tuna⁵⁹,

S.A. Tupputi^{22a,22b}, S. Turchikhin⁶⁸, D. Turgeman¹⁷⁵, I. Turk Cakir^{4b,at}, R. Turra^{94a}, P.M. Tuts³⁸,
 G. Ucchielli^{22a,22b}, I. Ueda⁶⁹, M. Ughetto^{148a,148b}, F. Ukegawa¹⁶⁴, G. Unal³², A. Undrus²⁷, G. Unel¹⁶⁶,
 F.C. Ungaro⁹¹, Y. Unno⁶⁹, C. Unverdorben¹⁰², J. Urban^{146b}, P. Urquijo⁹¹, P. Urrejola⁸⁶, G. Usai⁸,
 J. Usui⁶⁹, L. Vacavant⁸⁸, V. Vacek¹³⁰, B. Vachon⁹⁰, K.O.H. Vadla¹²¹, A. Vaidya⁸¹, C. Valderanis¹⁰²,
 E. Valdes Santurio^{148a,148b}, M. Valente⁵², S. Valentini^{22a,22b}, A. Valero¹⁷⁰, L. Valéry¹³, S. Valkar¹³¹,
 A. Vallier⁵, J.A. Valls Ferrer¹⁷⁰, W. Van Den Wollenberg¹⁰⁹, H. van der Graaf¹⁰⁹, P. van Gemmeren⁶,
 J. Van Nieuwkoop¹⁴⁴, I. van Vulpen¹⁰⁹, M.C. van Woerden¹⁰⁹, M. Vanadia^{135a,135b}, W. Vandelli³²,
 A. Vaniachine¹⁶⁰, P. Vankov¹⁰⁹, G. Vardanyan¹⁸⁰, R. Vari^{134a}, E.W. Varnes⁷, C. Varni^{53a,53b}, T. Varol⁴³,
 D. Varouchas¹¹⁹, A. Vartapetian⁸, K.E. Varvell¹⁵², J.G. Vasquez¹⁷⁹, G.A. Vasquez^{34b}, F. Vazeille³⁷,
 T. Vazquez Schroeder⁹⁰, J. Veatch⁵⁷, V. Veeraraghavan⁷, L.M. Veloce¹⁶¹, F. Veloso^{128a,128c},
 S. Veneziano^{134a}, A. Ventura^{76a,76b}, M. Venturi¹⁷², N. Venturi³², A. Venturini²⁵, V. Vercesi^{123a},
 M. Verducci^{136a,136b}, W. Verkerke¹⁰⁹, A.T. Vermeulen¹⁰⁹, J.C. Vermeulen¹⁰⁹, M.C. Vetterli^{144,d},
 N. Viaux Maira^{34b}, O. Viazlo⁸⁴, I. Vichou^{169,*}, T. Vickey¹⁴¹, O.E. Vickey Boeriu¹⁴¹,
 G.H.A. Viehhauser¹²², S. Viel¹⁶, L. Vigani¹²², M. Villa^{22a,22b}, M. Villaplana Perez^{94a,94b}, E. Vilucchi⁵⁰,
 M.G. Vincter³¹, V.B. Vinogradov⁶⁸, A. Vishwakarma⁴⁵, C. Vittori^{22a,22b}, I. Vivarelli¹⁵¹, S. Vlachos¹⁰,
 M. Vogel¹⁷⁸, P. Vokac¹³⁰, G. Volpi¹³, H. von der Schmitt¹⁰³, E. von Toerne²³, V. Vorobel¹³¹,
 K. Vorobev¹⁰⁰, M. Vos¹⁷⁰, R. Voss³², J.H. Vossebeld⁷⁷, N. Vranjes¹⁴, M. Vranjes Milosavljevic¹⁴,
 V. Vrba¹³⁰, M. Vreeswijk¹⁰⁹, R. Vuillermet³², I. Vukotic³³, P. Wagner²³, W. Wagner¹⁷⁸,
 J. Wagner-Kuhr¹⁰², H. Wahlberg⁷⁴, S. Wahrmund⁴⁷, J. Walder⁷⁵, R. Walker¹⁰², W. Walkowiak¹⁴³,
 V. Wallangen^{148a,148b}, C. Wang^{35b}, C. Wang^{36b,au}, F. Wang¹⁷⁶, H. Wang¹⁶, H. Wang³, J. Wang⁴⁵,
 J. Wang¹⁵², Q. Wang¹¹⁵, R. Wang⁶, S.M. Wang¹⁵³, T. Wang³⁸, W. Wang^{153,au}, W. Wang^{36a,au},
 Z. Wang^{36c}, C. Wanotayaroj¹¹⁸, A. Warburton⁹⁰, C.P. Ward³⁰, D.R. Wardrope⁸¹, A. Washbrook⁴⁹,
 P.M. Watkins¹⁹, A.T. Watson¹⁹, M.F. Watson¹⁹, G. Watts¹⁴⁰, S. Watts⁸⁷, B.M. Waugh⁸¹, A.F. Webb¹¹,
 S. Webb⁸⁶, M.S. Weber¹⁸, S.W. Weber¹⁷⁷, S.A. Weber³¹, J.S. Webster⁶, A.R. Weidberg¹²², B. Weinert⁶⁴,
 J. Weingarten⁵⁷, M. Weirich⁸⁶, C. Weiser⁵¹, H. Weits¹⁰⁹, P.S. Wells³², T. Wenaus²⁷, T. Wengler³²,
 S. Wenig³², N. Wermes²³, M.D. Werner⁶⁷, P. Werner³², M. Wessels^{60a}, T.D. Weston¹⁸, K. Whalen¹¹⁸,
 N.L. Whallon¹⁴⁰, A.M. Wharton⁷⁵, A.S. White⁹², A. White⁸, M.J. White¹, R. White^{34b}, D. Whiteson¹⁶⁶,
 B.W. Whitmore⁷⁵, F.J. Wickens¹³³, W. Wiedenmann¹⁷⁶, M. Wielers¹³³, C. Wiglesworth³⁹,
 L.A.M. Wiik-Fuchs⁵¹, A. Wildauer¹⁰³, F. Wilk⁸⁷, H.G. Wilkens³², H.H. Williams¹²⁴, S. Williams¹⁰⁹,
 C. Willis⁹³, S. Willocq⁸⁹, J.A. Wilson¹⁹, I. Wingerter-Seez⁵, E. Winkels¹⁵¹, F. Winklmeier¹¹⁸,
 O.J. Winston¹⁵¹, B.T. Winter²³, M. Wittgen¹⁴⁵, M. Wobisch^{82,✉}, T.M.H. Wolf¹⁰⁹, R. Wolff⁸⁸,
 M.W. Wolter⁴², H. Wolters^{128a,128c}, V.W.S. Wong¹⁷¹, S.D. Worm¹⁹, B.K. Wosiek⁴², J. Wotschack³²,
 K.W. Wozniak⁴², M. Wu³³, S.L. Wu¹⁷⁶, X. Wu⁵², Y. Wu⁹², T.R. Wyatt⁸⁷, B.M. Wynne⁴⁹, S. Xella³⁹,
 Z. Xi⁹², L. Xia^{35c}, D. Xu^{35a}, L. Xu²⁷, T. Xu¹³⁸, B. Yabsley¹⁵², S. Yacoob^{147a}, D. Yamaguchi¹⁵⁹,
 Y. Yamaguchi¹⁵⁹, A. Yamamoto⁶⁹, S. Yamamoto¹⁵⁷, T. Yamanaka¹⁵⁷, F. Yamane⁷⁰, M. Yamatani¹⁵⁷,
 Y. Yamazaki⁷⁰, Z. Yan²⁴, H. Yang^{36c}, H. Yang¹⁶, Y. Yang¹⁵³, Z. Yang¹⁵, W.-M. Yao¹⁶, Y.C. Yap⁸³,
 Y. Yasu⁶⁹, E. Yatsenko⁵, K.H. Yau Wong²³, J. Ye⁴³, S. Ye²⁷, I. Yeletskikh⁶⁸, E. Yigitbasi²⁴,
 E. Yildirim⁸⁶, K. Yorita¹⁷⁴, K. Yoshihara¹²⁴, C. Young¹⁴⁵, C.J.S. Young³², J. Yu⁸, J. Yu⁶⁷, S.P.Y. Yuen²³,
 I. Yusuff^{30,ax}, B. Zabinski⁴², G. Zacharis¹⁰, R. Zaidan¹³, A.M. Zaitsev^{132,ak}, N. Zakharchuk⁴⁵,
 J. Zalieckas¹⁵, A. Zaman¹⁵⁰, S. Zambito⁵⁹, D. Zanzi⁹¹, C. Zeitnitz¹⁷⁸, G. Zemaityte¹²², A. Zemla^{41a},
 J.C. Zeng¹⁶⁹, Q. Zeng¹⁴⁵, O. Zenin¹³², T. Ženiš^{146a}, D. Zerwas¹¹⁹, D. Zhang⁹², F. Zhang¹⁷⁶,
 G. Zhang^{36a,au}, H. Zhang¹¹⁹, J. Zhang⁶, L. Zhang⁵¹, L. Zhang^{36a}, M. Zhang¹⁶⁹, P. Zhang^{35b}, R. Zhang²³,
 R. Zhang^{36a,au}, X. Zhang^{36b}, Y. Zhang^{35a,35d}, Z. Zhang¹¹⁹, X. Zhao⁴³, Y. Zhao^{36b,ay}, Z. Zhao^{36a},
 A. Zhemchugov⁶⁸, B. Zhou⁹², C. Zhou¹⁷⁶, L. Zhou⁴³, M. Zhou^{35a,35d}, M. Zhou¹⁵⁰, N. Zhou^{35c},
 C.G. Zhu^{36b}, H. Zhu^{35a}, J. Zhu⁹², Y. Zhu^{36a}, X. Zhuang^{35a}, K. Zhukov⁹⁸, A. Zibell¹⁷⁷, D. Ziemińska⁶⁴,
 N.I. Zimine⁶⁸, C. Zimmermann⁸⁶, S. Zimmermann⁵¹, Z. Zinonos¹⁰³, M. Zinser⁸⁶, M. Ziolkowski¹⁴³,
 L. Živković¹⁴, G. Zobernig¹⁷⁶, A. Zoccoli^{22a,22b}, R. Zou³³, M. zur Nedden¹⁷, L. Zwalski³².

- ¹ Department of Physics, University of Adelaide, Adelaide, Australia
² Physics Department, SUNY Albany, Albany NY, United States of America
³ Department of Physics, University of Alberta, Edmonton AB, Canada
⁴ ^(a) Department of Physics, Ankara University, Ankara; ^(b) Istanbul Aydin University, Istanbul; ^(c) Division of Physics, TOBB University of Economics and Technology, Ankara, Turkey
⁵ LAPP, CNRS/IN2P3 and Université Savoie Mont Blanc, Annecy-le-Vieux, France
⁶ High Energy Physics Division, Argonne National Laboratory, Argonne IL, United States of America
⁷ Department of Physics, University of Arizona, Tucson AZ, United States of America
⁸ Department of Physics, The University of Texas at Arlington, Arlington TX, United States of America
⁹ Physics Department, National and Kapodistrian University of Athens, Athens, Greece
¹⁰ Physics Department, National Technical University of Athens, Zografou, Greece
¹¹ Department of Physics, The University of Texas at Austin, Austin TX, United States of America
¹² Institute of Physics, Azerbaijan Academy of Sciences, Baku, Azerbaijan
¹³ Institut de Física d'Altes Energies (IFAE), The Barcelona Institute of Science and Technology, Barcelona, Spain
¹⁴ Institute of Physics, University of Belgrade, Belgrade, Serbia
¹⁵ Department for Physics and Technology, University of Bergen, Bergen, Norway
¹⁶ Physics Division, Lawrence Berkeley National Laboratory and University of California, Berkeley CA, United States of America
¹⁷ Department of Physics, Humboldt University, Berlin, Germany
¹⁸ Albert Einstein Center for Fundamental Physics and Laboratory for High Energy Physics, University of Bern, Bern, Switzerland
¹⁹ School of Physics and Astronomy, University of Birmingham, Birmingham, United Kingdom
²⁰ ^(a) Department of Physics, Bogazici University, Istanbul; ^(b) Department of Physics Engineering, Gaziantep University, Gaziantep; ^(d) Istanbul Bilgi University, Faculty of Engineering and Natural Sciences, Istanbul; ^(e) Bahcesehir University, Faculty of Engineering and Natural Sciences, Istanbul, Turkey
²¹ Centro de Investigaciones, Universidad Antonio Narino, Bogota, Colombia
²² ^(a) INFN Sezione di Bologna; ^(b) Dipartimento di Fisica e Astronomia, Università di Bologna, Bologna, Italy
²³ Physikalisches Institut, University of Bonn, Bonn, Germany
²⁴ Department of Physics, Boston University, Boston MA, United States of America
²⁵ Department of Physics, Brandeis University, Waltham MA, United States of America
²⁶ ^(a) Universidade Federal do Rio De Janeiro COPPE/EE/IF, Rio de Janeiro; ^(b) Electrical Circuits Department, Federal University of Juiz de Fora (UFJF), Juiz de Fora; ^(c) Federal University of Sao Joao del Rei (UFSJ), Sao Joao del Rei; ^(d) Instituto de Fisica, Universidade de Sao Paulo, Sao Paulo, Brazil
²⁷ Physics Department, Brookhaven National Laboratory, Upton NY, United States of America
²⁸ ^(a) Transilvania University of Brasov, Brasov; ^(b) Horia Hulubei National Institute of Physics and Nuclear Engineering, Bucharest; ^(c) Department of Physics, Alexandru Ioan Cuza University of Iasi, Iasi; ^(d) National Institute for Research and Development of Isotopic and Molecular Technologies, Physics Department, Cluj Napoca; ^(e) University Politehnica Bucharest, Bucharest; ^(f) West University in Timisoara, Timisoara, Romania
²⁹ Departamento de Física, Universidad de Buenos Aires, Buenos Aires, Argentina
³⁰ Cavendish Laboratory, University of Cambridge, Cambridge, United Kingdom
³¹ Department of Physics, Carleton University, Ottawa ON, Canada
³² CERN, Geneva, Switzerland
³³ Enrico Fermi Institute, University of Chicago, Chicago IL, United States of America

- ³⁴ ^(a) Departamento de Física, Pontificia Universidad Católica de Chile, Santiago; ^(b) Departamento de Física, Universidad Técnica Federico Santa María, Valparaíso, Chile
- ³⁵ ^(a) Institute of High Energy Physics, Chinese Academy of Sciences, Beijing; ^(b) Department of Physics, Nanjing University, Jiangsu; ^(c) Physics Department, Tsinghua University, Beijing 100084; ^(d) University of Chinese Academy of Science (UCAS), Beijing, China
- ³⁶ ^(a) Department of Modern Physics and State Key Laboratory of Particle Detection and Electronics, University of Science and Technology of China, Anhui; ^(b) School of Physics, Shandong University, Shandong; ^(c) Department of Physics and Astronomy, Key Laboratory for Particle Physics, Astrophysics and Cosmology, Ministry of Education; Shanghai Key Laboratory for Particle Physics and Cosmology, Shanghai Jiao Tong University, Shanghai(also at PKU-CHEP), China
- ³⁷ Université Clermont Auvergne, CNRS/IN2P3, LPC, Clermont-Ferrand, France
- ³⁸ Nevis Laboratory, Columbia University, Irvington NY, United States of America
- ³⁹ Niels Bohr Institute, University of Copenhagen, Kobenhavn, Denmark
- ⁴⁰ ^(a) INFN Gruppo Collegato di Cosenza, Laboratori Nazionali di Frascati; ^(b) Dipartimento di Fisica, Università della Calabria, Rende, Italy
- ⁴¹ ^(a) AGH University of Science and Technology, Faculty of Physics and Applied Computer Science, Krakow; ^(b) Marian Smoluchowski Institute of Physics, Jagiellonian University, Krakow, Poland
- ⁴² Institute of Nuclear Physics Polish Academy of Sciences, Krakow, Poland
- ⁴³ Physics Department, Southern Methodist University, Dallas TX, United States of America
- ⁴⁴ Physics Department, University of Texas at Dallas, Richardson TX, United States of America
- ⁴⁵ DESY, Hamburg and Zeuthen, Germany
- ⁴⁶ Lehrstuhl für Experimentelle Physik IV, Technische Universität Dortmund, Dortmund, Germany
- ⁴⁷ Institut für Kern- und Teilchenphysik, Technische Universität Dresden, Dresden, Germany
- ⁴⁸ Department of Physics, Duke University, Durham NC, United States of America
- ⁴⁹ SUPA - School of Physics and Astronomy, University of Edinburgh, Edinburgh, United Kingdom
- ⁵⁰ INFN e Laboratori Nazionali di Frascati, Frascati, Italy
- ⁵¹ Fakultät für Mathematik und Physik, Albert-Ludwigs-Universität, Freiburg, Germany
- ⁵² Departement de Physique Nucleaire et Corpusculaire, Université de Genève, Geneva, Switzerland
- ⁵³ ^(a) INFN Sezione di Genova; ^(b) Dipartimento di Fisica, Università di Genova, Genova, Italy
- ⁵⁴ ^(a) E. Andronikashvili Institute of Physics, Iv. Javakhishvili Tbilisi State University, Tbilisi; ^(b) High Energy Physics Institute, Tbilisi State University, Tbilisi, Georgia
- ⁵⁵ II Physikalischs Institut, Justus-Liebig-Universität Giessen, Giessen, Germany
- ⁵⁶ SUPA - School of Physics and Astronomy, University of Glasgow, Glasgow, United Kingdom
- ⁵⁷ II Physikalischs Institut, Georg-August-Universität, Göttingen, Germany
- ⁵⁸ Laboratoire de Physique Subatomique et de Cosmologie, Université Grenoble-Alpes, CNRS/IN2P3, Grenoble, France
- ⁵⁹ Laboratory for Particle Physics and Cosmology, Harvard University, Cambridge MA, United States of America
- ⁶⁰ ^(a) Kirchhoff-Institut für Physik, Ruprecht-Karls-Universität Heidelberg, Heidelberg; ^(b) Physikalischs Institut, Ruprecht-Karls-Universität Heidelberg, Heidelberg, Germany
- ⁶¹ Faculty of Applied Information Science, Hiroshima Institute of Technology, Hiroshima, Japan
- ⁶² ^(a) Department of Physics, The Chinese University of Hong Kong, Shatin, N.T., Hong Kong; ^(b) Department of Physics, The University of Hong Kong, Hong Kong; ^(c) Department of Physics and Institute for Advanced Study, The Hong Kong University of Science and Technology, Clear Water Bay, Kowloon, Hong Kong, China
- ⁶³ Department of Physics, National Tsing Hua University, Taiwan, Taiwan
- ⁶⁴ Department of Physics, Indiana University, Bloomington IN, United States of America

- ⁶⁵ Institut für Astro- und Teilchenphysik, Leopold-Franzens-Universität, Innsbruck, Austria
⁶⁶ University of Iowa, Iowa City IA, United States of America
⁶⁷ Department of Physics and Astronomy, Iowa State University, Ames IA, United States of America
⁶⁸ Joint Institute for Nuclear Research, JINR Dubna, Dubna, Russia
⁶⁹ KEK, High Energy Accelerator Research Organization, Tsukuba, Japan
⁷⁰ Graduate School of Science, Kobe University, Kobe, Japan
⁷¹ Faculty of Science, Kyoto University, Kyoto, Japan
⁷² Kyoto University of Education, Kyoto, Japan
⁷³ Research Center for Advanced Particle Physics and Department of Physics, Kyushu University, Fukuoka, Japan
⁷⁴ Instituto de Física La Plata, Universidad Nacional de La Plata and CONICET, La Plata, Argentina
⁷⁵ Physics Department, Lancaster University, Lancaster, United Kingdom
⁷⁶ ^(a) INFN Sezione di Lecce; ^(b) Dipartimento di Matematica e Fisica, Università del Salento, Lecce, Italy
⁷⁷ Oliver Lodge Laboratory, University of Liverpool, Liverpool, United Kingdom
⁷⁸ Department of Experimental Particle Physics, Jožef Stefan Institute and Department of Physics, University of Ljubljana, Ljubljana, Slovenia
⁷⁹ School of Physics and Astronomy, Queen Mary University of London, London, United Kingdom
⁸⁰ Department of Physics, Royal Holloway University of London, Surrey, United Kingdom
⁸¹ Department of Physics and Astronomy, University College London, London, United Kingdom
⁸² Louisiana Tech University, Ruston LA, United States of America
⁸³ Laboratoire de Physique Nucléaire et de Hautes Energies, UPMC and Université Paris-Diderot and CNRS/IN2P3, Paris, France
⁸⁴ Fysiska institutionen, Lunds universitet, Lund, Sweden
⁸⁵ Departamento de Fisica Teorica C-15, Universidad Autonoma de Madrid, Madrid, Spain
⁸⁶ Institut für Physik, Universität Mainz, Mainz, Germany
⁸⁷ School of Physics and Astronomy, University of Manchester, Manchester, United Kingdom
⁸⁸ CPPM, Aix-Marseille Université and CNRS/IN2P3, Marseille, France
⁸⁹ Department of Physics, University of Massachusetts, Amherst MA, United States of America
⁹⁰ Department of Physics, McGill University, Montreal QC, Canada
⁹¹ School of Physics, University of Melbourne, Victoria, Australia
⁹² Department of Physics, The University of Michigan, Ann Arbor MI, United States of America
⁹³ Department of Physics and Astronomy, Michigan State University, East Lansing MI, United States of America
⁹⁴ ^(a) INFN Sezione di Milano; ^(b) Dipartimento di Fisica, Università di Milano, Milano, Italy
⁹⁵ B.I. Stepanov Institute of Physics, National Academy of Sciences of Belarus, Minsk, Republic of Belarus
⁹⁶ Research Institute for Nuclear Problems of Byelorussian State University, Minsk, Republic of Belarus
⁹⁷ Group of Particle Physics, University of Montreal, Montreal QC, Canada
⁹⁸ P.N. Lebedev Physical Institute of the Russian Academy of Sciences, Moscow, Russia
⁹⁹ Institute for Theoretical and Experimental Physics (ITEP), Moscow, Russia
¹⁰⁰ National Research Nuclear University MEPhI, Moscow, Russia
¹⁰¹ D.V. Skobeltsyn Institute of Nuclear Physics, M.V. Lomonosov Moscow State University, Moscow, Russia
¹⁰² Fakultät für Physik, Ludwig-Maximilians-Universität München, München, Germany
¹⁰³ Max-Planck-Institut für Physik (Werner-Heisenberg-Institut), München, Germany
¹⁰⁴ Nagasaki Institute of Applied Science, Nagasaki, Japan

- ¹⁰⁵ Graduate School of Science and Kobayashi-Maskawa Institute, Nagoya University, Nagoya, Japan
¹⁰⁶ ^(a) INFN Sezione di Napoli; ^(b) Dipartimento di Fisica, Università di Napoli, Napoli, Italy
¹⁰⁷ Department of Physics and Astronomy, University of New Mexico, Albuquerque NM, United States of America
¹⁰⁸ Institute for Mathematics, Astrophysics and Particle Physics, Radboud University Nijmegen/Nikhef, Nijmegen, Netherlands
¹⁰⁹ Nikhef National Institute for Subatomic Physics and University of Amsterdam, Amsterdam, Netherlands
¹¹⁰ Department of Physics, Northern Illinois University, DeKalb IL, United States of America
¹¹¹ Budker Institute of Nuclear Physics, SB RAS, Novosibirsk, Russia
¹¹² Department of Physics, New York University, New York NY, United States of America
¹¹³ Ohio State University, Columbus OH, United States of America
¹¹⁴ Faculty of Science, Okayama University, Okayama, Japan
¹¹⁵ Homer L. Dodge Department of Physics and Astronomy, University of Oklahoma, Norman OK, United States of America
¹¹⁶ Department of Physics, Oklahoma State University, Stillwater OK, United States of America
¹¹⁷ Palacký University, RCPTM, Olomouc, Czech Republic
¹¹⁸ Center for High Energy Physics, University of Oregon, Eugene OR, United States of America
¹¹⁹ LAL, Univ. Paris-Sud, CNRS/IN2P3, Université Paris-Saclay, Orsay, France
¹²⁰ Graduate School of Science, Osaka University, Osaka, Japan
¹²¹ Department of Physics, University of Oslo, Oslo, Norway
¹²² Department of Physics, Oxford University, Oxford, United Kingdom
¹²³ ^(a) INFN Sezione di Pavia; ^(b) Dipartimento di Fisica, Università di Pavia, Pavia, Italy
¹²⁴ Department of Physics, University of Pennsylvania, Philadelphia PA, United States of America
¹²⁵ National Research Centre "Kurchatov Institute" B.P.Konstantinov Petersburg Nuclear Physics Institute, St. Petersburg, Russia
¹²⁶ ^(a) INFN Sezione di Pisa; ^(b) Dipartimento di Fisica E. Fermi, Università di Pisa, Pisa, Italy
¹²⁷ Department of Physics and Astronomy, University of Pittsburgh, Pittsburgh PA, United States of America
¹²⁸ ^(a) Laboratório de Instrumentação e Física Experimental de Partículas - LIP, Lisboa; ^(b) Faculdade de Ciências, Universidade de Lisboa, Lisboa; ^(c) Department of Physics, University of Coimbra, Coimbra; ^(d) Centro de Física Nuclear da Universidade de Lisboa, Lisboa; ^(e) Departamento de Física, Universidade do Minho, Braga; ^(f) Departamento de Física Teórica y del Cosmos, Universidad de Granada, Granada; ^(g) Dep Física and CEFITEC of Faculdade de Ciencias e Tecnologia, Universidade Nova de Lisboa, Caparica, Portugal
¹²⁹ Institute of Physics, Academy of Sciences of the Czech Republic, Praha, Czech Republic
¹³⁰ Czech Technical University in Prague, Praha, Czech Republic
¹³¹ Charles University, Faculty of Mathematics and Physics, Prague, Czech Republic
¹³² State Research Center Institute for High Energy Physics (Protvino), NRC KI, Russia
¹³³ Particle Physics Department, Rutherford Appleton Laboratory, Didcot, United Kingdom
¹³⁴ ^(a) INFN Sezione di Roma; ^(b) Dipartimento di Fisica, Sapienza Università di Roma, Roma, Italy
¹³⁵ ^(a) INFN Sezione di Roma Tor Vergata; ^(b) Dipartimento di Fisica, Università di Roma Tor Vergata, Roma, Italy
¹³⁶ ^(a) INFN Sezione di Roma Tre; ^(b) Dipartimento di Matematica e Fisica, Università Roma Tre, Roma, Italy
¹³⁷ ^(a) Faculté des Sciences Ain Chock, Réseau Universitaire de Physique des Hautes Energies - Université Hassan II, Casablanca; ^(b) Centre National de l'Energie des Sciences Techniques Nucléaires,

Rabat; ^(c) Faculté des Sciences Semlalia, Université Cadi Ayyad, LPHEA-Marrakech; ^(d) Faculté des Sciences, Université Mohamed Premier and LPTPM, Oujda; ^(e) Faculté des sciences, Université Mohammed V, Rabat, Morocco

¹³⁸ DSM/IRFU (Institut de Recherches sur les Lois Fondamentales de l'Univers), CEA Saclay (Commissariat à l'Energie Atomique et aux Energies Alternatives), Gif-sur-Yvette, France

¹³⁹ Santa Cruz Institute for Particle Physics, University of California Santa Cruz, Santa Cruz CA, United States of America

¹⁴⁰ Department of Physics, University of Washington, Seattle WA, United States of America

¹⁴¹ Department of Physics and Astronomy, University of Sheffield, Sheffield, United Kingdom

¹⁴² Department of Physics, Shinshu University, Nagano, Japan

¹⁴³ Department Physik, Universität Siegen, Siegen, Germany

¹⁴⁴ Department of Physics, Simon Fraser University, Burnaby BC, Canada

¹⁴⁵ SLAC National Accelerator Laboratory, Stanford CA, United States of America

¹⁴⁶ ^(a) Faculty of Mathematics, Physics & Informatics, Comenius University, Bratislava; ^(b) Department of Subnuclear Physics, Institute of Experimental Physics of the Slovak Academy of Sciences, Kosice, Slovak Republic

¹⁴⁷ ^(a) Department of Physics, University of Cape Town, Cape Town; ^(b) Department of Physics, University of Johannesburg, Johannesburg; ^(c) School of Physics, University of the Witwatersrand, Johannesburg, South Africa

¹⁴⁸ ^(a) Department of Physics, Stockholm University; ^(b) The Oskar Klein Centre, Stockholm, Sweden

¹⁴⁹ Physics Department, Royal Institute of Technology, Stockholm, Sweden

¹⁵⁰ Departments of Physics & Astronomy and Chemistry, Stony Brook University, Stony Brook NY, United States of America

¹⁵¹ Department of Physics and Astronomy, University of Sussex, Brighton, United Kingdom

¹⁵² School of Physics, University of Sydney, Sydney, Australia

¹⁵³ Institute of Physics, Academia Sinica, Taipei, Taiwan

¹⁵⁴ Department of Physics, Technion: Israel Institute of Technology, Haifa, Israel

¹⁵⁵ Raymond and Beverly Sackler School of Physics and Astronomy, Tel Aviv University, Tel Aviv, Israel

¹⁵⁶ Department of Physics, Aristotle University of Thessaloniki, Thessaloniki, Greece

¹⁵⁷ International Center for Elementary Particle Physics and Department of Physics, The University of Tokyo, Tokyo, Japan

¹⁵⁸ Graduate School of Science and Technology, Tokyo Metropolitan University, Tokyo, Japan

¹⁵⁹ Department of Physics, Tokyo Institute of Technology, Tokyo, Japan

¹⁶⁰ Tomsk State University, Tomsk, Russia

¹⁶¹ Department of Physics, University of Toronto, Toronto ON, Canada

¹⁶² ^(a) INFN-TIFPA; ^(b) University of Trento, Trento, Italy

¹⁶³ ^(a) TRIUMF, Vancouver BC; ^(b) Department of Physics and Astronomy, York University, Toronto ON, Canada

¹⁶⁴ Faculty of Pure and Applied Sciences, and Center for Integrated Research in Fundamental Science and Engineering, University of Tsukuba, Tsukuba, Japan

¹⁶⁵ Department of Physics and Astronomy, Tufts University, Medford MA, United States of America

¹⁶⁶ Department of Physics and Astronomy, University of California Irvine, Irvine CA, United States of America

¹⁶⁷ ^(a) INFN Gruppo Collegato di Udine, Sezione di Trieste, Udine; ^(b) ICTP, Trieste; ^(c) Dipartimento di Chimica, Fisica e Ambiente, Università di Udine, Udine, Italy

¹⁶⁸ Department of Physics and Astronomy, University of Uppsala, Uppsala, Sweden

- ¹⁶⁹ Department of Physics, University of Illinois, Urbana IL, United States of America
¹⁷⁰ Instituto de Fisica Corpuscular (IFIC), Centro Mixto Universidad de Valencia - CSIC, Spain
¹⁷¹ Department of Physics, University of British Columbia, Vancouver BC, Canada
¹⁷² Department of Physics and Astronomy, University of Victoria, Victoria BC, Canada
¹⁷³ Department of Physics, University of Warwick, Coventry, United Kingdom
¹⁷⁴ Waseda University, Tokyo, Japan
¹⁷⁵ Department of Particle Physics, The Weizmann Institute of Science, Rehovot, Israel
¹⁷⁶ Department of Physics, University of Wisconsin, Madison WI, United States of America
¹⁷⁷ Fakultät für Physik und Astronomie, Julius-Maximilians-Universität, Würzburg, Germany
¹⁷⁸ Fakultät für Mathematik und Naturwissenschaften, Fachgruppe Physik, Bergische Universität Wuppertal, Wuppertal, Germany
¹⁷⁹ Department of Physics, Yale University, New Haven CT, United States of America
¹⁸⁰ Yerevan Physics Institute, Yerevan, Armenia
¹⁸¹ Centre de Calcul de l’Institut National de Physique Nucléaire et de Physique des Particules (IN2P3), Villeurbanne, France
¹⁸² Academia Sinica Grid Computing, Institute of Physics, Academia Sinica, Taipei, Taiwan
^a Also at Department of Physics, King’s College London, London, United Kingdom
^b Also at Institute of Physics, Azerbaijan Academy of Sciences, Baku, Azerbaijan
^c Also at Novosibirsk State University, Novosibirsk, Russia
^d Also at TRIUMF, Vancouver BC, Canada
^e Also at Department of Physics & Astronomy, University of Louisville, Louisville, KY, United States of America
^f Also at Physics Department, An-Najah National University, Nablus, Palestine
^g Also at Department of Physics, California State University, Fresno CA, United States of America
^h Also at Department of Physics, University of Fribourg, Fribourg, Switzerland
ⁱ Also at II Physikalisches Institut, Georg-August-Universität, Göttingen, Germany
^j Also at Departament de Fisica de la Universitat Autonoma de Barcelona, Barcelona, Spain
^k Also at Departamento de Fisica e Astronomia, Faculdade de Ciencias, Universidade do Porto, Portugal
^l Also at Tomsk State University, Tomsk, and Moscow Institute of Physics and Technology State University, Dolgoprudny, Russia
^m Also at The Collaborative Innovation Center of Quantum Matter (CICQM), Beijing, China
ⁿ Also at Universita di Napoli Parthenope, Napoli, Italy
^o Also at Institute of Particle Physics (IPP), Canada
^p Also at Horia Hulubei National Institute of Physics and Nuclear Engineering, Bucharest, Romania
^q Also at Department of Physics, St. Petersburg State Polytechnical University, St. Petersburg, Russia
^r Also at Borough of Manhattan Community College, City University of New York, New York City, United States of America
^s Also at Department of Financial and Management Engineering, University of the Aegean, Chios, Greece
^t Also at Centre for High Performance Computing, CSIR Campus, Rosebank, Cape Town, South Africa
^u Also at Louisiana Tech University, Ruston LA, United States of America
^v Also at Institucio Catalana de Recerca i Estudis Avancats, ICREA, Barcelona, Spain
^w Also at Department of Physics, The University of Michigan, Ann Arbor MI, United States of America
^x Also at Graduate School of Science, Osaka University, Osaka, Japan
^y Also at Fakultät für Mathematik und Physik, Albert-Ludwigs-Universität, Freiburg, Germany
^z Also at Institute for Mathematics, Astrophysics and Particle Physics, Radboud University Nijmegen/Nikhef, Nijmegen, Netherlands

aa Also at Department of Physics, The University of Texas at Austin, Austin TX, United States of America

ab Also at Institute of Theoretical Physics, Ilia State University, Tbilisi, Georgia

ac Also at CERN, Geneva, Switzerland

ad Also at Georgian Technical University (GTU), Tbilisi, Georgia

ae Also at Ochadai Academic Production, Ochanomizu University, Tokyo, Japan

af Also at Manhattan College, New York NY, United States of America

ag Also at Departamento de Física, Pontificia Universidad Católica de Chile, Santiago, Chile

ah Also at The City College of New York, New York NY, United States of America

ai Also at Departamento de Física Teórica y del Cosmos, Universidad de Granada, Granada, Portugal

aj Also at Department of Physics, California State University, Sacramento CA, United States of America

ak Also at Moscow Institute of Physics and Technology State University, Dolgoprudny, Russia

al Also at Département de Physique Nucléaire et Corpusculaire, Université de Genève, Geneva, Switzerland

am Also at Institut de Física d'Altes Energies (IFAE), The Barcelona Institute of Science and Technology, Barcelona, Spain

an Also at School of Physics, Sun Yat-sen University, Guangzhou, China

ao Also at Institute for Nuclear Research and Nuclear Energy (INRNE) of the Bulgarian Academy of Sciences, Sofia, Bulgaria

ap Also at Faculty of Physics, M.V.Lomonosov Moscow State University, Moscow, Russia

aq Also at National Research Nuclear University MEPhI, Moscow, Russia

ar Also at Department of Physics, Stanford University, Stanford CA, United States of America

as Also at Institute for Particle and Nuclear Physics, Wigner Research Centre for Physics, Budapest, Hungary

at Also at Giresun University, Faculty of Engineering, Turkey

au Also at CPPM, Aix-Marseille Université and CNRS/IN2P3, Marseille, France

av Also at Department of Physics, Nanjing University, Jiangsu, China

aw Also at Institute of Physics, Academia Sinica, Taipei, Taiwan

ax Also at University of Malaya, Department of Physics, Kuala Lumpur, Malaysia

ay Also at LAL, Univ. Paris-Sud, CNRS/IN2P3, Université Paris-Saclay, Orsay, France

* Deceased